Cinnamoyl-CoA Reductase 1 (CCR1) and CCR2 Function Divergently in Tissue Lignification, Flux Control and Cross-talk with Glucosinolate Pathway in *Brassica napus*

Nengwen Yin,[a,b,1] Bo Li,[a,c,1] Xue Liu,[a] Ying Liang,[a,b] Jianping Lian,[a] Yufei Xue,[a] Cunming Qu,[a,b] Kun Lu,[a,b] Lijuan Wei,[a,b] Rui Wang,[a,b] Jiana Li,[a,b,2] and Yourong Chai[a,b,2]

[a] Chongqing Engineering Research Center for Rapeseed, College of Agronomy and Biotechnology, Southwest University, Chongqing 400715, China

[b] Engineering Research Center of South Upland Agriculture of Ministry of Education, Academy of Agricultural Sciences, Southwest University, Chongqing 400715, China

[c] Current address: Criminal Police Corps of Chongqing Public Security Bureau，Chongqing 400021, China

[1]These authors contributed equally to this work.

[2] Address correspondence to ljn1950@swu.edu.cn and chaiyourong@163.com.

The authors responsible for distribution of materials integral to the findings presented in this article in accordance with the policy described in the Instructions for Authors (www.plantcell.org) are Jiana Li (ljn1950@swu.edu.cn) and Yourong Chai (chaiyourong@163.com).

ORCID IDs: 0000-0002-9055-2030 (N.Y.); 0000-0002-9078-961X (B.L.); 0000-0002-3877-885X (X.L.); 0000-0001-9651-4564 (Y.L.); 0000-0003-2453-2266 (J.L.); 0000-0001-7041-5517(Y.X.); 0000-0003-2413-2350 (C.Q.); 0000-0003-1370-8633 (K.L.); 0000-0001-6405-0240 (L.W.); 0000-0002-7440-9197 (R.W.);

0000-0002-1605-8528 (J.L.); 0000-0001-6611-624X (Y.C.)

Short title: Divergent functions of *CCR1* and *CCR2* in *Brassica*

One sentence summary: *Brassica napus CCR1* and *CCR2* play divergent roles in lignin monomers biosynthesis, tissue lignification, flux control, crosstalk with glucosinolate pathway and trait modifications when overexpressed.

Abstract

Cinnamoyl-CoA reductase (CCR) is the entry point of lignin pathway and a crucial locus in dissection and manipulation of associated traits. *Brassica* crops have worldwide importance, but their CCR-related metabolisms and traits are largely uncharacterized. Here, 16 *CCR* genes are identified from *B. napus* and its parental species *B. rapa* and *B. oleracea*. They are divided into *CCR1* subfamily and *CCR2* subfamily, which differ from each other in organ-specificity, participation in yellow-seed trait and responses to various stresses. *BnCCR1* is preferentially involved in biosynthesis of G and H lignins and development of vascular system, while *BnCCR2* is preferentially involved in biosynthesis of S lignin and development of interfascicular fibers. *BnCCR1* has stronger effects on lignification-related development, lodging resistance, flux control and seed color, whereas *BnCCR2* has stronger effect on sinapates biosynthesis. *BnCCR1* overexpressing plants show a delay in bolting and flowering, while *BnCCR2* overexpressing plants have less developed vascular system in leaf due to suppressed G lignin accumulation. Unexpectedly, both *BnCCR1* and *BnCCR2* overexpressors show no improvement in resistance to UV-B and *S. sclerotiorum*. Besides, their glucosinolate profiles are greatly and almost oppositely remodeled through pathway crosstalk. These results provide systemic dissection on *Brassica CCR*s and *CCR1-CCR2* divergence in Brassicaceae.

Key Words: *Brassica*, Cinnamoyl-CoA reductase (CCR), Lignin, Flavonoids, Glucosinolates.

INTRODUCTION

The diverse phenylpropanoid compounds ranging from simple phenolic esters to complex polymers play important roles during plant growth and development, conferring plants with adaptability to the changing environment. Phenylpropanoid-based polymers, such as lignins, flavonoids, lignans, hydroxycinnamic acids, hydroxycinnamic acid esters, salicylic acid, suberin, coumarins and stilbenes confer mechanical strength, pollen viability, pest deterrence, disease resistance, UV protection and abiotic stresses-tolerance to plants (Vogt, 2010; Fraser and Chapple, 2011). Lignins constitute one important phenylpropanoid metabolites, are aromatic heteropolymers, are predominantly deposited in secondarily thickened plant cell walls, and are the second most abundant biopolymers on the planet (Huang et al., 2010; Vanholme et al., 2010). Lignin monomers are covalently linked to hemicellulose and thereby cross-linked with plant polysaccharides. They perform many functions in plants, providing structural support, giving rigidity and strength to stems for plants to stand upright, and enabling xylems to withstand the negative pressure generated during water transport (Escamilla-Treviño et al., 2010; Labeeuw et al., 2015). In addition, lignins have been suggested to be induced upon various biotic and abiotic stresses, such as pathogen infection, insect feeding, drought, heat, wounding and perturbations in cell wall structure (Baucher et al., 1998; Caño-Delgado et al., 2003; Vanholme et al., 2010; Weng and Chapple, 2010; Chantreau et al., 2014).

Lignin polymers are generally comprised of three major types of aromatic hydroxycinnamyl alcohols, i.e. *p*-hydroxyphenyl (H), guaiacyl (G) and syringyl

(S) units, whose dehydrogenative polymerization products are called *p*-coumaryl, coniferyl and sinapyl monolignols respectively (Boerjan et al., 2003; Do et al., 2007; Weng et al., 2011). The major monolignol type in gymnosperms (softwood) is G unit, while in angiosperms both G and S units are dominant. H-type monolignol is of minor proportion in seed plants, with much higher proportion in monocots (especially grasses) than in dicots (hardwood) (Boerjan et al., 2003; Vanholme et al., 2010; Labeeuw et al., 2015).

The lignin biosynthetic pathway has been extensively studied in recent decades (Boerjan et al., 2003; Ralph et al., 2008; Vanholme et al., 2012; Vanholme et al., 2013; Anderson et al., 2015; Gui et al., 2019). Most of the enzymes involved in lignin biosynthesis have been identified and are well characterized (Fraser and Chapple, 2011; Vanholme et al., 2013; Anderson et al., 2015), mainly by mutants characterization or by downregulation of related genes. To date, engineering of lignins mainly pursues reduced lignin content or altered lignin composition to meet the demands of agro-industrial processes, such as chemical pulping, forage digestibility, and the bioethanol production from lignocellulosic biomass (Baucher et al., 2003; Ragauskas et al., 2006; Li et al., 2008; Weng et al., 2010; Ko et al., 2015; De Meester et al., 2020). However, sometimes when altering the expression of the genes involved in lignin biosynthetic pathway, the metabolic flux of its neighbor pathways would be changed correspondingly (Hoffmann et al., 2004; Besseau et al., 2007; Li et al., 2010; Thévenin et al., 2011). Furthermore, dramatic modification of lignin content or lignin composition may provoke deleterious effects on plant growth, such as dwarfism and collapsed xylem vessels, with concomitant loss of biomass and yield (Piquemal et al., 1998; Jones et al., 2001; Ruel et al., 2009; Berthet et al., 2011; De Meester et al., 2020). Besides the “expected” interaction among different phenylpropanoid branch pathways (especially between lignin and flavonoid pathways), the “unexpected” interaction between

phenylpropanoid pathway and other metabolic pathways was also reported recently. For example, manipulation of auxin-glucosinolate compound pathway will drastically influence phenylpropanoids deposition and gene expression linked by proteasome-dependent degradation of PAL (Hemm et al., 2003; Kim et al., 2015; Kim et al., 2020). However, there is no report on whether manipulation of phenylpropanoid pathway could influence auxin-glucosinolate compounds deposition and pathway gene expression.

Cinnamoyl-CoA reductase (CCR) is the entry point for the lignin-specific branch of the phenylpropanoid pathway and catalyzes the monolignol biosynthesis (Lacombe et al., 1997; Kawasaki et al., 2006). It catalyzes the NADPH-dependent conversion of hydroxycinnamoyl CoA esters into their corresponding hydroxycinnamaldehydes in monolignol biosynthesis (Ruel et al., 2009; Zhou et al., 2010). *CCR* genes have been studied in multiple species including *Arabidopsis thaliana* (Lauvergeat et al., 2001; Goujon et al., 2003; Anderson et al., 2015), rice (Kawasaki et al., 2006), poplar (Van Acker et al., 2014; Chao et al., 2017), tobacco (Dauwe et al., 2007; Prashant et al., 2011), switchgrass (Escamilla-Treviño et al., 2010), alfalfa (Zhou et al., 2010), sorghum (Li et al., 2016), and so on. *A. thaliana* possesses 11 annotated *CCR* homologs (Costa and Dolan, 2003), but only *AtCCR1* and *AtCCR2* encode true CCR enzyme (Lauvergeat et al., 2001). *AtCCR1* is preferentially expressed in tissues undergoing lignification, while *AtCCR2* is poorly expressed during development but is strongly and transiently induced by *Xanthomonas campestris*, suggesting that *AtCCR1* is involved in constitutive lignification whereas *AtCCR2* is involved in resistance (Lauvergeat et al., 2001). In monocot grasses, *CCR1* expression can be detected in various organs with a relatively high transcription level in stem (Tu et al., 2010; Giordano et al., 2014), thus is thought to be involved in constitutive lignification. In poplar and switchgrass, *CCR2* is expressed at very low levels in most organs, but can be significantly induced by biotic and abiotic stresses (Fan et

al., 2006; Escamilla-Treviño et al., 2010).

In addition to a key role in the formation of monolignol precursors, CCR was reported to act as an important regulator in defense responses (Kawasaki et al., 2006), photorespiration and photo-oxidative stress (Dauwe et al., 2007), and to mediate cell proliferation exit for leaf development (Xue et al., 2015). Manipulation of *CCR* (mainly through downregulation) typically results in a significant variation of lignin content and composition (Goujon et al., 2003; Zhou et al., 2010; Wagner et al., 2013; Zhang et al., 2015). Moreover, plants with dramatically downregulated *CCR* genes usually showed a stunted growth and delayed development (van der Rest et al., 2006; Tamasloukht et al., 2011; Thévenin et al., 2011; De Meester et al., 2020), and the alternation of carbon flux between lignin and other metabolic pathways was also accompanied (van der Rest et al., 2006; Dauwe et al., 2007; Tu et al., 2010; Wagner et al., 2013). The *CCR*-downregulated tomato (van der Rest et al., 2006) and perennial ryegrass (Tu et al., 2010) plants accumulated higher levels of flavonoids and other phenolics. The redirection of the metabolic flux into flavonoids was achieved through chalcone synthase activity with enhanced availability of *p*-coumaroyl-CoA esters, which is situated at the junction point of the phenylpropanoid metabolic network leading to flavonoids or to other phenolics (Thévenin et al., 2011). CCR deficiency would also cause changes in starch metabolism and photorespiration in *N. tabacum* (Dauwe et al., 2007), or repression of hemicellulose and pectin biosynthesis (Leplé et al., 2007).

Lodging and diseases (e.g. stem/white rot of rapeseed and sunflower, cotton verticillium wilt, rice blast, potato late blight, etc.) are fatal problems in field production of most crops. Reducing the plant height has proven to be a useful strategy for improving lodging resistance, but dwarfness will reduce canopy photosynthetic capacity and yield (Zhang et al., 2001; Tongyan et al., 2002; Acreche and Slafer, 2011; Peng et al., 2014). Therefore, other strategies are needed for further improvement in lodging resistance (Peng et al., 2014). Stem strength, particularly of the basal internodes, is important for stem

lodging resistance of crops (Zuber et al., 1999). Increasing stem strength would be a very promising strategy for breeding crops with high lodging resistance and yield (Ma, 2009). Moreover, Lignin is a physical barrier which can restrict pathogens to the infection site and confer disease resistance in plants (Lee et al., 2019). It has long been proposed that the accumulation of lignin might be related to stem strength and plant defense against pathogens, however, there is few reports at the molecular level to address how the regulation of lignin biosynthesis affects crop lodging and pathogen resistance via gene manipulation. In wheat, accumulation of lignin is closely related to lodging resistance, and wheat culms with higher lignin content could have a better lodging resistance (Peng et al., 2014). Regarding defense, the lignin biosynthesis related genes can be significantly upregulated when plants are suffering from various stresses, and increased lignin accumulation would appear subsequently (Moura et al., 2010). In rice, *Snl6*, a member of the *CCR*-like gene family, is required for NH1-mediated resistance to bacterial pathogen *Xanthomonas oryzae* pv. *Oryzae* (Bart et al., 2010). As an effector of *OsRac1*, *OsCCR1* is involved in *OsRac1*-stimulated lignin synthesis during defense responses in rice (Kawasaki et al., 2006). However, there is few reports on overexpressing *CCR* in enhancing lodging or disease resistance with molecular breeding values of crops.

Brassica, a relative genus of model plant *A. thaliana*, is of great importance since it contains various important oilseed, vegetable and ornamental crops. Among them, rapeseed (*Brassica napus* L., AACC, 2n=38) and its parental species *B. rapa* (AA, 2n=20) and *B. oleracea* (CC, 2n=18) have been attracting special attention in both crop science and plant evolutionary study. As the world's third-largest oilseed crop, rapeseed is widely grown for both high quality edible oil and meal/cake for feed (Friedt and Snowdon, 2009; Lomascolo et al., 2012; Liu et al., 2015). Unfortunately, *Brassica* crops especially rapeseed frequently suffer from some detrimental stresses such as lodging (Liu et al., 2010; Acreche and Slafer, 2011; Berry and Spink, 2012; Peng et al., 2014) and stem rot disease caused by *Sclerotinia sclerotiorum* with serious yield penalty and quality deterioration (del Río et al.,

2007; Koch et al., 2007; Ding et al., 2015). In rapeseed, lodging, including stem lodging and root lodging, could lead to 20%–46% yield loss and about 4 percent points of oil content reduction, and limits the efficiency of mechanical harvest (Pan et al., 2012; Kendall et al., 2017; Berry, 2018). There is little knowledge at present concerning the functional genes involved in lignin biosynthesis pathway in rapeseed or even in *Brassica* species. Comprehensive characterization of the lignin biosynthesis in rapeseed will enable us to manipulate the lignin content or composition through genetic engineering, and to strengthen the capacity for lodging and pathogen resistance.

In the present study, the *CCR1* and *CCR2* subfamily members from *B. napus* and its two parental species, *B. rapa* and *B. oleracea*, were isolated, their expression patterns in different organs and under various stresses were investigated, and overexpression manipulation of *BnCCR1* and *BnCCR2* was performed for deciphering their biological functions. Our results demonstrated that *BnCCR1* was mainly involved in the biosynthesis of H and G units, while *BnCCR2* showed a preference in the biosynthesis of S units and in plant defense. A dramatic shift of carbon flux in phenylpropanoid pathway and an obvious crosstalk between phenylpropanoid pathway and glucosinolate pathway was found in both *BnCCR1*- and *BnCCR2*-transgenic plants, especially for *BnCCR1* manipulation. Besides, *BnCCR1* and *BnCCR2* showed distinctly differential association with flux regulation and development control, which accounted for distinct phenotypic modification in vascular anatomy, lodging resistance, seed color, flowering time and glucosinolate profiles in corresponding overexpressors. Surprisingly and unexpectedly, both *BnCCR1*- and *BnCCR2*-overexpressors did not show increased resistance to *S. sclerotiorum* and UV-B light, implying complicated association of CCR and lignin pathway with disease resistance.

RESULTS

Isolation and Characterisation of *CCR* Genes from *Brassica* species

CCR genes were isolated from *B. napus* and its parental species *B. rapa* and *B. oleracea* using RACE strategy. Full-length cDNAs and corresponding gDNA sequences of 3, 4 and 6 *CCR1*-subfamily gene sequences were isolated from *B. rapa* (*BrCCR1-1* and *BrCCR1-2, BrCCR1-2'*), *B. oleracea* (*BoCCR1-1, BoCCR1-1'* and *BoCCR1-2, BoCCR1-2'*) and *B. napus* (*BnCCR1-1*, *BnCCR1-2, BnCCR1-2'*, *BnCCR1-3, BnCCR1-3'* and *BnCCR1-4*), while 3, 3 and 4 *CCR2*-subfamily gene sequences were isolated from *B. rapa* (*BrCCR2-1A*, *BrCCR2-1B*, *BrCCR2-2*), *B. oleracea* (*BoCCR2-1A*, *BoCCR2-1B*, *BoCCR2-2*) and *B. napus* (*BnCCR2-1*, *BnCCR2-2*, *BnCCR2-3*, *BnCCR2-4*), respectively. Besides, 1 *CCR2* pseudogene from each parental species and 2 *CCR2* pseudogenes from *B. napus* were also isolated (Supplemental Table 1). To determine the copy number of the *BnCCR1*, *BoCCR1*, *BrCCR1*, *BnCCR2*, *BoCCR2* and *BrCCR2* genes, Southern hybridization analysis with the probes designed according to the coding region was performed (Supplemental Figure 1). 4 clear bands and 3 to 6 weak bands were revealed for *BnCCR1* with the digestion of *Dra*I, *Eco*RI, *Eco*RV, *Hin*dIII, *Xba*I. 2 or 3 clear bands and 1 or 2 weak bands for *BrCCR1*, 2 clear bands and 0 or 3 weak bands for *BoCCR1* (Supplemental Figure 1A), with the digestion of same restriction enzymes. For *BnCCR2*, 5 or 6 specific bands were obtained, and 3 or 4 specific bands were successfully blotted for *BrCCR2* and *BoCCR2*, respectively (Supplemental Figure 1B). The numbers of the clear bands obtained from Southern hybridization are well correlated with the cloned gene sequence numbers. After our cloning work of *Brassica CCR* family, whole genome sequencing and annotation data of *B. rapa*, *B. oleracea* and *B. napus* were available in GenBank, then we performed *in-silico* cloning of all *CCR1* and *CCR2* subfamily genes, which indicated that each parental species contains only 2 *CCR1* genes and 2 *CCR2* genes together with 1 *CCR2* pseudogene while *B. napus* has the total sets of both parental species (Supplemental Table 1).

Considering high full-length sequence identities (96.0%-99.0%) within each pair of *BrCCR1-2*/*BrCCR1-2'*, *BoCCR1-1/BoCCR1-1'*, *BoCCR1-2/BoCCR1-2'*, *BnCCR1-2/BnCCR1-2'*, *BnCCR1-3/BnCCR1-3'*, *BrCCR2-1A*/*BrCCR2-1B* and *BoCCR2-1A/BoCCR2-1B*, it is clear that the *CCR1* and *CCR2* gene/pseudogene numbers are only those revealed by *in-silico* cloning, and the above sequence pairs are cloned from two heterozygous alleles of each gene. Supplemental Table 1 shows all identity parameters of *CCR1*-subfamily and *CCR2*-subfamily genes/pseudogenes from *B. napus* and its parental species *B. oleracea* and *B. rapa* in terms of our cloning work and 3 genome datasets (NCBI GenBank, Genoscope and BRAD).

The basic features of the cDNA and gDNA sequences are displayed in Supplemental Table 2, and the deduced protein features are depicted in Supplemental Table 3. Multiple alignments of these *Brassica* CCRs and CCRs from other 3 dicots species showed that the conserved NADP binding domain and the CCR-featured traditional motif (KNWYCYGK, which was believed as the catalytic site) and novel motif $H_{202}K_{205}R_{253}$ (CCR-SBM or CCR substrate binding motif) were conserved in all *Brassica* CCRs (Supplemental Figure 2, Lacombe et al., 1997; Chao et al., 2019) . Therefore, it is speculated that these *Brassica* CCRs have catalytic activities. A phylogenetic tree was constructed to reveal the relationships of *Brassica* CCR1 and CCR2 proteins with CCRs from all whole-genome-sequenced species of other Brassicales species and other malvids orders (Figure 1). Firstly, it is clear that an early intrafamily duplication event generated the CCR1 and CCR2 groups within Brassicaceae, i.e. AtCCR1 and AtCCR2 have respective CCR1 and CCR2 orthologs only within Brassicaceae family. Secondly, the Brassicaceae CCR1 group is much more conserved than the Brassicaceae CCR2 group, which could be reflected by the great difference in branch lengths. Thirdly, outside the Brassicaceae family, other Brassicales families (e.g. Cleomaceae and Caricaceae) and other malvids orders (e.g. Malvales, Myrtales and Sapindales) have similar trends in

CCR evolution (gene duplication and unequal divergence of paralogs) as revealed in Brassicaceae. However, paralog numbers (duplication event numbers) vary distinctly among relative families and orders, and the single-copy CCR from Brassicales species *Carica papaya* is nearer to non-Brassicales CCRs than to other Brassicales CCRs.

Divergence of Organ-specificity Among *Brassica CCR* Family Members

Both real-time quantitative and semi-quantitative RT-PCR detections were adopted to detect the overall expression and member-specific expression of the *CCR1* subfamily and *CCR2* subfamily from the 3 *Brassica* species. The results of the two methods conformed to each other. Both *CCR1* subfamily and *CCR2* subfamily were expressed in all detected organs in the 3 species, but organ-specificity was also distinct. In all the 3 species the highest *CCR1* subfamily expression was detected in silique pericarp, while the highest *CCR2* subfamily expression varied among species (bud in *B. napus*, silique pericarp in *B. rapa*, and root in *B. oleracea*), implying faster divergence of organ-specificity in *CCR2* than in *CCR1* among species. Within each species, divergence of organ-specificity and expression intensity among *CCR* paralogs were distinct, and generally stronger divergence of organ-specificity among *CCR2* paralogs could be observed than among *CCR1* paralogs. For *CCR1* subfamily, *BnCCR1-2*, *BrCCR1-2* and *BoCCR1-1* were the dominant paralog within respective species. For *CCR2* subfamily, *BnCCR2-4*, *BrCCR2-1A* and *BoCCR2-2* were the dominant paralog within respective species (Figure 2, Supplemental Figures 3, 4 and 5).

Differential Involvement Between *CCR1* and *CCR2* During Yellow-seed Coat Development of *Brassica*

Expression of *CCR1* subfamily and *CCR2* subfamily in reproductive organs of yellow-seed stocks of the 3 species was detected in comparison with that of the black-seed stocks. The results revealed interesting rules. In all the 3 species, *CCR1* subfamily overall expression was distinctly lower in developing seeds especially in late-stage seeds of yellow-seed stocks (09L587 of *B. napus*, 09L600 of *B. rapa* and 09L599 of *B. oleracea*) than in black-seed

stocks (5B of *B. napus*, 09L597 of *B. rapa* and 09L598 of *B. oleracea*). However, in all the 3 species, *CCR2* subfamily overall expression was distinctly higher in reproductive organs especially in developing seeds of yellow-seed stocks than in black-seed stocks. Within each subfamily, different paralogs were involved differentially in contributing to expression difference between yellow-seed stocks and black-seed stocks (Figure 2, Supplemental Figures 3, 4 and 5). As black-seed stocks should have a higher intensity of seed coat lignification than yellow-seed stocks, it could be speculated that downregulated expression of *CCR1* subfamily in developing seeds especially in late-stage seeds is a contribution factor of decrease in lignification and lignin content of *Brassica* yellow seeds, while upregulated expression of *CCR2* subfamily in developing seeds could hardly compensate this effect.

Differential Responsiveness to Various Stresses between *BnCCR1* and *BnCCR2* Subfamilies

B. napus seedlings were treated with fungal pathogen *S. sclerotiorum*, insect pest *Pieris rapae*, and various abiotic stresses such as NaCl, Na_2CO_3, drought & high temperature, and UV-B. Real-time quantitative and semi-quantitative RT-PCR methods were simultaneously implemented to detect the responsive dynamics of overall and member-specific expression of *BnCCR1* and *BnCCR2* subfamilies (Figure 3; Supplemental Figure 6). For *BnCCR1*, its overall expression showed limited upregulations by NaCl (5.53 folds in stems at 48 h), drought & high temperature (2.68 folds in leaves at 48 h) and UV-B treatment (6.89, 5.50 and 3.95 folds in leaves, stems and roots, respectively, at 80 min), while kept almost constant when treated with other stresses (Figure 3). Under the same stresses, both the overall and the member-specific expression of *BnCCR2* subfamily were dramatically upregulated. Its overall expression in leaves was upregulated by 400.3 folds at 48 h after *S. sclerotiorum* inoculation, by 49.59 folds at 80 min after UV-B treatment, by 10.75 folds at 48 h after *P. rapae* inoculation, and with slow and slight increase after high temperature & drought treatment (Figure 3). However, after salts treatments, the expression of *BnCCR2* showed elevation-declining or declining-recovery trends depending on different salts and organs. Moreover, all *BnCCR2* subfamily members could be triggered by these

stresses, and *BnCCR2-4* had a relatively higher expression than other members facing those treatments (Supplemental Figure 6). Although both *BnCCR1* and *BnCCR2* subfamilies can be distinctly regulated by multiple stresses, *BnCCR1* only mildly responds to abiotic stresses, while *BnCCR2* responds sharply and intensively to both biotic and abiotic stresses, i.e. *BnCCR2* is speculated to play more important roles than *BnCCR1* in coping with various stresses in *B. napus*.

BnCCR* Over-expression Dramatically Influenced Plant Morphology, but Did Not Increase Resistance to UV-B and *S. sclerotiorum

To further uncover the function of *Brassica CCR* genes, overexpression transgenic plants were generated. *BnCCR1-2* and *BnCCR2-4* were selected for transgenic study as they are the dominant member within *BnCCR1* subfamily and *BnCCR2* subfamily respectively. The transgenic lines were coded as *BnCCR1-2ox* or ox1 lines for *BnCCR1-2* overexpression, and *BnCCR2-4ox* or ox2 lines for *BnCCR2-4* overexpression, in the following analysis. The transgenic lines were screened along with non-transgenic controls and WT by GUS staining, Basta resistance and PCR detection with specific primers (Supplemental Figure 7). Six *BnCCR1-2ox* lines and 7 *BnCCR2-4ox* lines with triple-positive detection were obtained, with different extents of over-expression levels revealed by qRT-PCR detection (Supplemental Figure 8). T2 or T3 generations of ox1-5, ox1-8, ox1-12, ox1-14, ox2-4, ox2-11, ox2-16 and ox2-25 were selected for further analysis on the basis of a strongly upregulated *BnCCR1* or *BnCCR2* expression in comparison to WT.

For agronomic traits investigation, more than 5 individual representative transgenic plants of T2 generation were assayed. All *BnCCRox* plants showed a stronger morphological development than WT throughout the whole plant life (Figure 4). Compared with WT, both *BnCCR1-2ox* and *BnCCR2-4ox* had larger and longer leaves, higher leaf chlorophyll content, larger stem diameter, wider silique, better developed root system, higher breaking-resistant stem strength, better lodging resistance and more siliques per plant, with distinctly stronger effects in *BnCCR1-2ox* lines than in *BnCCR2-4ox* lines (Figure 4;

Supplemental Figures 9 and 10). Phytohormone detection showed that abscisic acid (ABA) increased significantly in the leaves of *BnCCRox* lines compared with WT (Supplemental Figure 11). The leaves of *BnCCR1-2ox* had more obvious wrinkles and less leaf margin serrates than WT (Figures 4C; Supplemental Figures 10E, 10G and 10I). *BnCCR2-4ox* plants had a looser morphology with larger leaf angles (Figures 4B and 4J), and their leaves were more easily to show bending and rollover phenomenon than WT when under strong sunlight and high temperature conditions (Supplemental Figure 10D). On the other hand, upper stems of *BnCCR1-2ox* plants at late bolting stage were more easily to appear bending phenomenon, but this phenomenon would disappear after flowering (Figures 4F to 4I; Supplemental Figure 10A). Moreover, *BnCCR1-2ox* lines flowered 7 to 10 days later than WT on average, and this phenomenon varied among years and environments. However, *BnCCR2-4ox* plants had no significant difference in the flowering time when compared with WT. Interesting phenomenon was observed on petiole-vein system, which was distinctly larger in transgenic plants than WT, but phloroglucinol-HCl staining showed that petiole-vein lignification was strengthened only in *BnCCR1-2ox* plants while weakened in *BnCCR2-4ox* plants (Figure 4D; Supplemental Figures 10F, 10H and 10J). Seed yield per plant of *BnCCR1-2ox* had little difference compared with WT, but *BnCCR2-4ox* had slightly decreased seed yield (Supplemental Figure 9L).

To investigate the resistance of the transgenic plants to *S. sclerotiorum*, the 4th and 5th detached leaves during 9-12 true-leaf stage and the middle part of the stem during early flowering stage were inoculated with *S. sclerotiorum* mycelia plugs (Supplemental Figure 12). The results showed that both *BnCCR1-2ox* and *BnCCR2-4ox* plants exhibited no better resistance when compared with WT, even some transgenic lines had a little reduction in resistance in leaf identification (*BnCCR1-2ox* [10.01 cm^2] and *BnCCR2-4ox* [11.35 cm^2] vs WT [9.31 cm^2] in average lesion areas, Supplemental Figure 12A, 12B and 12E). Furthermore, UV-B treatment assay of seedlings also showed no improvement in UV-B resistance for *BnCCRox* lines than WT (Supplemental Figure 12H).

Yellow-seed Traits Generated in *BnCCRox* Lines

In addition to the dramatic changes of the plant phenotypes, the seed color of *BnCCRox* lines also had an obvious alteration compared with WT. As displayed in Figure 5A, the seed color of both *BnCCR1-2ox* and *BnCCR2-4ox* turned lighter compared with WT, from dark to yellow, and *BnCCR1-2ox* showed a stronger effect than *BnCCR2-4ox*. Microscopic investigation of the frozen sections of seed coat (Figure 5B) and R value obtained through NIRS assay (Figure 5E) further proved this effect. However, the thickness of the seed coat had no significant difference between *BnCCRox* and WT, which was different from traditionally bred yellow-seeded cultivars which usually had thinner seed coat than black-seeded cultivars (Qu et al., 2013; Zhang et al., 2013). In order to explore the causes for the seed color perturbation, the condensed tannin content of seed coat was measured using butanol-HCl method. As expected, the *BnCCR1-2ox* seed coat had an apparent reduction of the condensed tannin compared with WT, e.g. ox1-5, ox1-8, ox1-12 and ox1-14 had a decrease of 69%, 29%, 40% and 57% respectively (Figures 5C and 5G). But unexpectedly, a significant increase was found for *BnCCR2-4ox* seed coat when compared with WT, e.g. ox2-4, ox2-11, ox2-16 and ox2-25 showed an increase of 88%, 300%, 158% and 83% respectively (Figures 5C and 5G), implying looser condensation of the tannin structure caused by unknown mechanisms. Furthermore, all *BnCCRox* lines had a significant reduction of the thousand-seed weight, with *BnCCR1-2ox* lines reduced by 10%-20%, and *BnCCR2-4ox* lines reduced by 15%-30% (Figure 5D). Intriguingly, the NIRS detection results showed that the total glucosinolates content of *BnCCR1-2ox* lines had a considerable increase compared with WT, but it displayed a decline in *BnCCR2-4ox* lines (Figure 5F).

***BnCCR* Over-expression Greatly Changed Lignification Phenotypes**

Because the transgenic plant stems, roots and silique pericarps had varied phenotypes compared with WT and they were also the main lignified organs of *B. napus*, we performed microscopic investigation on their freehand sections or frozen sections. The frozen cross sections of stem middle part at early flowering stage and stem middle-lower part at maturing stage were investigated (Figures 6A to 6C), which displayed that both *BnCCR1-2ox* and

BnCCR2-4ox stems had an changed shape with more concave and convex and a wider xylem parts with deeper histochemical staining, and some extreme *BnCCR1-2ox* lines appeared an ectopic lignin deposition as shown in Figure 6C. Observed with higher amplification folds of the sections, *BnCCR1-2ox* showed a better developed xylem part, had more number and more concentrated vessels with deeper brown color (indicate more G lignin unit) stained by Mäule staining in which G- and S-type lignin units could be stained brown and red respectively (Figures 6F and 6G, early flowering stage), with brighter red phloroglucinol-HCl staining (Figure 6H, mature stage) and brighter blue fluorescence (Figures 6I and 6J, early flowering stage) as compared with WT. These indicated that *BnCCR1-2ox* stems contained higher level of lignin content compared with WT. *BnCCR2-4ox* stem sections also displayed a better developed xylem part and interfascicular fiber part. Although its vessel number and size were no obviously different from WT, there was a significant deeper red color (indicating the S lignin unit) stained by both Mäule staining (Figures 6F and 6G) and phloroglucinol-HCl staining (Figure 6H), especially to the interfascicular fiber cells wall, and brighter blue florescence under UV light (Figures 6I and 6J) compared with WT. This result indicated that *BnCCR2-4ox* stems had higher proportion of S lignin units besides with higher total lignin content. Similar enhancement trends of the lignification pattern were also found in detection results of siliques (Figures 6K to 6N).

Through investigation, we found that there were two types of roots for rapeseed. Type I had higher proportion of interfascicular fibers (Figure 6D), while type II had higher proportion of vessels (Figure 6E). In *BnCCR1-2ox* and *BnCCR2-4ox* lines, both type I and type II roots displayed a better developed xylem tissues with bigger size and more concentrated vessels, and had a deeper staining by phloroglucinol-HCl method compared with WT (Figures 6D and 6E). Besides, type II roots of *BnCCR1-2ox* showed a significantly better vessel development (Figure 6E) than WT and *BnCCR2-4ox*. Through

comparison of the above-mentioned histochemical staining assay or fluorescence excitation assay of stems and roots, *BnCCR1-2ox* had better developed vascular bundles, while *BnCCR2-4ox* had better developed interfascicular fibers, than WT (Figures 6D, 6G, 6H and 6J).

To detect the difference of leaf traits between *BnCCRox* lines and WT, the frozen section investigation of the middle part of petiole was carried out. Compared with WT (Figures 6O to 6Q), the transverse section of *BnCCR1-2ox* petioles tends to be more circular with more and better developed vascular bundles (Figures 6O and 6Q). But for *BnCCR2-4ox* lines, it was smaller than WT and developed asymmetrically with fewer and less developed vascular bundles (Figure 6O and 6Q), maybe this was one reason that caused *BnCCR2-4ox* leaves much easier to bend and rollover than WT when under strong sunlight and high temperature conditions. Moreover, *BnCCR1-2ox* lines had a deeper brown color staining with Mäule staining and had a brighter blue fluorescence under UV light than WT (Figures 6P and 6Q), which indicated that *BnCCR1-2ox* petiole xylem contained higher lignin content as well as higher G-lignin proportion. The *BnCCR2-4ox* petiole sections displayed no better Mäule staining, and the blue fluorescence was significant weaker than WT (Figure 6Q), which indicated that *BnCCR2-4ox* petiole xylem contained less lignin content which was consistent with phloroglucinol-HCl staining of leaves (Supplemental Figure 10J).

Notable Changes in Content and Structure of Lignins in *BnCCR* Over-expression Lines

To determine whether the lignin biosynthesis and composition of the *BnCCR*-manipulated transgenic plants were changed as displayed in histochemical assay, the mature stems and roots together with seed coats of corresponding plants at harvesting stage were sampled for biochemical analysis. The results showed that the acetyl-bromide soluble lignin content of both *BnCCR1-2ox* and *BnCCR2-4ox* was significantly increased compared to WT (Table 1). The lignin content of stems of *BnCCR1-2ox* lines ox1-5, ox1-8,

ox1-12 and ox1-14 increased by 24%, 34%, 23% and 15%, respectively (Table 1). For *BnCCR2-4ox* lines ox2-4, ox2-11, ox2-16 and ox2-25, their stem lignin content increased by 40%, 25%, 31% and 51%, respectively (Table 1). In roots, the lignin content of ox1-5, ox1-8, ox1-12, ox1-14, ox2-4, ox2-11, ox2-16 and ox2-25 increased by 0.4%, 18%, 15%, 5%, 18%, 25%, 12% and 23% compared with WT, respectively (Table 1). In seed coat, the lignin content of the *BnCCR1-2ox* lines ox1-5, ox1-8, ox1-12 and ox1-14 increased by 64%, 18%, 27% and 1% compared with WT (Table 1), respectively. Unexpectedly, the seed coat lignin content of the *BnCCR2-4ox* lines ox2-4, ox2-11, ox2-16 and ox2-25 increased by 128%, 112%, 130% and 92%, respectively (Table 1). These results reminiscent the condensed tannin detection result of *BnCCR2-4ox* which also had an unexpected significant increase.

For characterizing the lignin structure, the lignin composition of the transgenic plants and WT was investigated by thioacidolysis. Thioacidolysis selectively cleaves the labile β–O–4-ether bonds in lignin polymer, and the released lignin fraction is referred as non-condensed lignin units (Lapierre et al., 1995; Leplé et al., 2007). The sum of H, G and S lignin units can suggest the total thioacidolysis yield, thus, the condensation degree of the lignin polymer. The results showed an obvious altered lignin structure in both types of transgenic plants (Table 2). In stem samples, the thioacidolysis yield of ox1-5, ox1-12, ox2-4 and ox2-16 increased by 14.4%, 16.5%, 22% and 28% compared with WT, respectively, which was in consistent with the lignin content analysis result. In root samples, the thioacidolysis yield of ox2-16 increased by 67.6% compared to WT, while no big difference was detected between ox1-5 and WT, which was in consistent with the change of its root lignin content, and this diminished difference may be caused by the increase in the proportion of condensation bonds in lignin due to the increased G units in ox1-5 (Table 2).

S/G ratio, which was typically used to characterize the lignin structure, also changed significantly in both stems and roots of *BnCCRox* lines. In the stems of both *BnCCR2-4ox* and WT, their lignin had higher content of S units than G units. In the stem, the S/G ratio was increased by 20.2% and 22.5% of ox2-4 and ox2-16 compared with WT (Table 2), which was mainly attributed to their greater proportion of S lignin content (Table 2; Supplemental Figure 13),

and was in consistent with the Mäule staining results. However, in the case of the stems of *BnCCR1-2ox* lines, the G units, other than S units, served as the main lignin units, so it was contrary to *BnCCR2-4ox* and WT. Due to increased G units proportion, the S/G ratio in the stems of ox1-5 and ox1-12 decreased by 47.3% and 24.0%, respectively, compared to WT (Table 2; Supplemental Figure 13). In roots, the alteration tendency of S/G ratio of ox1-5 and ox2-16 was similar to that in stems, decreased to 0.22 and increased to 0.78, respectively as compared with WT (0.49) (Table 2).

Another striking change was H lignin proportion, which generally had trace amount in dicotyledonous stems (usually no more than 1%). The H lignin content of ox1-5 and ox1-12 (3.29% and 2.78% in the stem respectively) was about 4 and 3 folds of the WT respectively (Table 2; Supplemental Figure 13). The H lignin content in the stem of ox2-4 and ox2-16 increased by 59.0% and 45.7% compared with WT, respectively, though not as distinct as ox1-5 and ox1-12. In the root of ox1-5, the H lignin content also had an obvious increase, reaching about two folds of WT amount (7.43% of WT VS 15.59% of ox1-5) (Table 2; Supplemental Figure 13). In conclusion, the lignin structure of *B. rapus* was undoubtedly modified after the manipulation of *BnCCR* genes.

There were several studies reporting that manipulation of lignin biosynthesis pathway was often accompanied by biosynthesis perturbation of cellulose or hemicellulose (Leplé et al., 2007; Prashant et al., 2011; Huang et al., 2012; Vanholme et al., 2012). Through NIRS assay, however, the results indicated that both cellulose and hemicellulose contents of both *BnCCR1-2ox* and *BnCCR2-4ox* lines had no significant difference when compared with WT (Supplemental Figure 14), except that cellulose content of ox1-5 had a small decrease by 14.12%.

Metabolic Remodeling of Phenylpropanoid and Glucosinolate Pathways by Over-expressing *BnCCR1* and *BnCCR2*

The drastic alteration of seed color, seed coat condensed tannin content, lignin structure and plant phenotypes all indicated flux change within and outside the lignin biosynthetic network. To dissect the underlying metabolic

shift, the methanolic extracts of stems, leaves, petioles and 30DAP seeds of wild-type and representative transgenic lines (ox1-5 and ox2-16) were analyzed using UPLC-HESI-MS/MS. The metabolites were identified based on accurate mass and MS^n fragmentation data in fitting with published mass spectra data (Tohge et al., 2005; Rochfort et al., 2006; Tu et al., 2010; Lin et al., 2011; Shao et al., 2014).

The secondary metabolites of the phenylpropanoid-lignin/flavonoid compound pathway showed distinct remodeling (Figure 7; Supplemental Data Set 1). Conforming to prediction, most phenolic compounds synthesized at the downstream of CCR were apparently increased in the stems of ox1-5 and ox2-16 lines, including sinapoylhexose, sinapic acid, sinapoyl malate, ferulic acid, feruloyl malate, *p*-coumaraldehyde and 1,2-disinapoylglucoside, with an increase of about 1 to 10 folds, and ox2-16 displayed stronger effects than ox1-5 (Figure 7; Supplemental Data Set 1). The common phenylpropanoid pathway compounds 5-O-caffeoylshikimic acid and *p*-coumaric acid showed slight reduction. However, flavonoids in ox1-5 stems were reduced to 3%-71% of WT, including km-3-O-sophoroside-7-O-glucoside, rutin, is-3-sophoroside-7-glucoside, km-3-O-sinapoylsophoroside-7-O-glucoside, qn-3-O-sophoroside, qn-3-O-glucoside, km-3-O-glucoside, is-3-O-glucoside; and ox2-16 showed the same trend as ox1-5 but with a less extent. Leaf extracts of ox1-5 and ox2-16 lines had similar variation tendency as in stems, but some compounds were undetectable in leaves or had an opposite change (Supplemental Data Set 1). In leaves of ox1-5 and ox2-16, compared with WT, the CCR-downstream compounds sinapic acid, sinapoyl malate, ferulic acid and feruloyl malate in lignin-related pathway were upregulated by tens of folds or even more than one hundred folds (greater effect than in stems), while the flavonoids is-3-O-glucoside-7-O-glucoside, qn-3-O-glucoside and is-3-O-glucoside were distinctly downregulated with an exception of km-3-O-sophoroside-7-O-glucoside and km-3-O-glucoside-7-O-glucoside

which were upregulated unexpectedly. Metabolites profiling was also performed on 30 DAP seeds, because the soluble compounds of secondary metabolites reached maximum levels at this stage (Auger et al., 2010). As expected, the CCR-downstream compounds sinapic acid and disinapoylgentiobiose were significantly increased both in ox1-5 and ox2-16 lines (Supplemental Data Set 2). The contents of the most compounds of epicatechin, procyanidin and the oligomers of epicatechin with different degrees of polymerization, and other important flavonoids were significantly reduced (by even more than 90% for some flavonoids) in ox1-5 compared with wild type, and ox2-16 showed the same trend as ox1-5 but with a less extent (Supplemental Data Set 2), but the kaempferol derivatives km-3-O-diglucoside and km-3-O-sophoroside were exceptionally increased.

In metabolic profiling, glucosinolates were unexpectedly found to be drastically changed by *BnCCR* overexpression. A variety of aliphatic glucosinolates were distinctly differentially deposited between *BnCCRox* lines and WT plants. For example, 2(R)-2-hydroxy-3-butenyl glucosinolate, 1-S-[(3S)-3-Hydroxy-N-(sulfooxy)-5-hexenimidoyl]-1-thio-beta-D-glucopyranose, 3-butenylglucosinolate, isobutyl glucosinolate, 4-pentenyl glucosinolate, 5-methylsulfinylpentyl glucosinolate and 5-methylthiopentyl glucosinolate were upregulated to hundreds of folds or even more than 1000 folds in ox1-5 stems as compared with WT, while in ox2-16 stems they were just slightly upregulated or even downregulated (Supplemental Data Set 1). In addition, although 1-S-[(3S)-3-Hydroxy-N-(sulfooxy)-5-hexenimidoyl]-1-thio-beta-D-glucopyranos, 4-methylthiobutyl glucosinolate and 6-methylthiohexyl glucosinolate were non-detectable in WT, 1-S-[(3S)-3-Hydroxy-N-(sulfooxy)-5-hexenimidoyl]-1-thio-beta-D-glucopyranos was obviously accumulated in both types of transgenic plants, and 4-methylthiobutyl glucosinolate and 6-methylthiohexyl glucosinolate were

obviously accumulated in ox1-5 stems (not in ox2-16 stems).

According to the quantitative results, glucosinolates had larger amounts of accumulation in leaves than in stems (in WT, some aliphatic glucosinolates in leaves was tens to thousands folds higher than in stems, Supplemental Data Set 1), and most of them were several folds higher in ox1-5 than in WT. However, most of them were downregulated by hundreds of folds in the leaves of ox2-16 in comparison with WT. 2(R)-2-Hydroxy-3-butenyl glucosinolate, 1-S-[(3S)-3-Hydroxy-N-(sulfooxy)-5-hexenimidoyl]-1-thio-beta-D-glucopyranose and 5-methylthiopentyl glucosinolate were even not detectable in the leaves of ox2-16 (Supplemental Data Set 1). In seed coat, there was a similar trend for glucosinolates accumulation in ox1-5 and ox2-16 as in leaves, and 2-Hydroxy-2-methylpropyl glucosinolate and 6-methylthiohexyl glucosinolate were detected only in ox1-5 but not in ox2-16 and WT (Supplemental Data Set 2).

We also did the same analysis on the secondary metabolites in petioles, and similar results were obtained as those in stems (Supplemental Data Set 3).

Taken together, these results suggested that the change in lignification in *BnCCRox* lines was associated with a flux redirection within and outside the phenylpropanoid pathway. Over-expression of *BnCCR* genes led to enhancement of lignin pathway and its derivative pathways, but the flavonoid pathway was significantly suppressed. Unexpectedly, the accumulation of glucosinolates was also greatly affected after *BnCCR* upregulation, and *BnCCR1* subfamily and *BnCCR2* subfamily showed distinct or even opposite effects on glucosinolate profiles.

Differential Redirection of Gene Expression in Lignin, Flavonoid and Glucosinolate Pathways in *BnCCR1* and *BnCCR2* Over-expressors

To further reveal the molecular mechanism underlying the shift of the

metabolism in *BnCCRox* lines, the expression of dozens of key genes involved in lignin, flavonoid and glucosinolate biosynthesis were quantified by qRT-PCR.

The overall expression of *BnCCR1* and *BnCCR2* subfamilies in various organs of both *BnCCR1-2ox* and *BnCCR2-4ox* lines was detected (Supplemental Figure 15). In *BnCCR1-2ox* lines as compared with WT, *BnCCR1* subfamily itself was upregulated by about 10 folds in stems, leaves and petioles and about 2-3 folds in seeds, and *BnCCR2* subfamily showed no significant upregulation. In *BnCCR2-4ox* lines as compared with WT, the *BnCCR2* subfamily itself was greatly upregulated in in stems (8-30 folds), leaves (70-250 folds), petioles (25-30 folds) and seeds (4-15 folds), and *BnCCR1* subfamily was also significantly upregulated (1-3 folds) in the stems, petioles and 30DAP seeds but significantly downregulated by 70% in the leaves. These results indicated that over-expression of *BnCCR1* subfamily had little impact on the expression of *BnCCR2* subfamily, but over-expression of *BnCCR2* subfamily could significantly upregulate or downregulate the expression of *BnCCR1* subfamily depending on different organs.

Subsequently, ox1-5, ox1-12, ox2-4 and ox2-16 were chosen to further determine the expression patterns of lignin, flavonoid and glucosinolate biosynthesis pathways. In the stems of both *BnCCR1-2ox* and *BnCCR2-4ox* lines as compared with WT, the common phenylpropanoid pathway loci *C4H* and *4CL* and the lignin-pathway early-step loci *C3H*, *HCT* and *CCoAOMT* were mildly upregulated (Figure 8A), and *CCR*-downstream loci *CAD* and *F5H* were slightly upregulated. *COMT* was specific, apparently upregulated in the stems of *BnCCR1-2ox*, but downregulated to less than 10% in the stems of *BnCCR2-4ox* as compared with WT.

On the other hand, the expression of the flavonoid biosynthesis pathway was significantly downregulated in *BnCCRox* lines. Regulatory genes *TT1*, *TT2*, *TT16*, *TTG1* and *TTG2*, and structural genes *CHS*, *CHI*, *F3H*, *F3'H*, *FLS*,

ANR, *TT19*, *GSTF11* and *TT12* were all suppressed to certain extent in 30DAP seeds of both *BnCCR1-2ox* and *BnCCR2-4ox* (Figure 8B), with less extent in *BnCCR2-4ox* than in *BnCCR1-2ox*. *CHS*, *CHI*, *F3H*, *ANR* and *TT19* were downregulated to less than 20% in the 30DAP seeds of ox1-5 when compared with WT (Figure 8B). The structural genes *AHA10* and *TT10* and the regulatory genes *TT8* and *MYB111* were significantly downregulated in 30DAP seeds of *BnCCR2-4ox*, but were unexpectedly significantly upregulated in the 30DAP seeds of *BnCCR1-2ox* lines (Figure 8B). The overall downregulation of the whole flavonoid pathway could account for the reduction of the flavonoids in *BnCCRox* lines.

The expression of the genes involved in glucosinolate biosynthesis was detected in leaf samples since leaf was the main organ for glucosinolate biosynthesis (Figure 8C). Most of the genes associated with the aliphatic glucosinolate biosynthesis, such as *MYB28*, *MYB29*, *CYP79F1*, *CYP83A1*, *AOP2* and *GSL*, were significantly upregulated in *BnCCR1ox* lines (Figure 8C). Especially, the expression of *MYB29*, *CYP79F1* and *GSL* could hardly be detected in WT and *BnCCR2ox* lines, but was considerably expressed in *BnCCR1ox* lines. *AOP2* was a specific locus, which showed considerable downregulation in *BnCCR2ox*, a trend opposite to that in *BnCCR1ox* (Figure 8C). These results coincided with the results of metabolic assay that the aliphatic glucosinolates had a significant accumulation in *BnCCR1ox* lines but a dramatic decrease in *BnCCR2ox* lines. The expression of most genes involved in indole glucosinolate biosynthesis, such as *MYB122*, *CYP79B2*, *ST5a* and *IGMT1*, was dramatically decreased in both *BnCCR1ox* and *BnCCR2ox* lines, except that *MYB34* was significantly upregulated in both *BnCCR1ox* and *BnCCR2ox* lines (Figure 8C). *MYB51* was significantly upregulated in *BnCCR1ox* lines but extremely downregulated in *BnCCR2ox* lines, implying that *MYB51* may also be involved in aliphatic glucosinolate biosynthesis in *B. napus*.

DISCUSSION

Both *BnCCR1* and *BnCCR2* are Crucial for Lignification Associated with Different Monolignols and Cellular Types

As one of the most important components of plant cell wall, lignin is closely correlated to plant mechanical strength and adversity resistance. Lodging and *S. sclerotiorum* attack are the main factors restricting rapeseed production. Understanding the mechanism of the lignin biosynthesis in rapeseed would facilitate to resolve these problems.

Plants with downregulated CCR activities often displayed various degrees of reduction in lignin content and alteration in lignin structure depending on different species (Goujon et al., 2003; van der Rest et al., 2006; Leplé et al., 2007; Zhou et al., 2010; Prashant et al., 2011). The lignin content had a great decrease in *Arabidopsis CCR1* mutant *irx4* (Jones et al., 2001) and *CCR*-suppressed transgenic *Arabidopsis* (Goujon et al., 2003), tobacco (Piquemal et al., 1998), poplar (Leplé et al., 2007), *Medicago truncatula* (Zhou et al., 2010) and perennial ryegrass (Tu et al., 2010). When *CCR1* in *Betula platyphylla* (Zhang et al., 2015) was overexpressed and suppressed, lignin accumulation was upregulated by 14.6% and downregulated by 6.3%, respectively.

In this study, anatomical observation and histochemical staining both indicated significant improvement of lignification in stems and roots in both *BnCCR1* and *BnCCR2* over-expressors, and *BnCCR1* over-expressor showed stronger effect on development of vessels and vascular bundles in xylem while *BnCCR2* over-expressor showed stronger effect on interfascicular fibers. In biochemical detection, lignin content in the mature stems, roots and seed coat was significantly increased in transgenic lines of both *BnCCR1-2ox* and *BnCCR2-4ox*, suggesting that both *BnCCR1* subfamily and *BnCCR2* subfamily play a pivotal role in lignin biosynthesis in *B. napus*. Interestingly, although

BnCCR1-2ox lines had better lignification pattern than *BnCCR2-4ox* lines in morphological and microscopic observation, the measured lignin content of *BnCCR2-4ox* lines was obviously higher than *BnCCR1-2ox* lines in all three organs, especially in seeds coat. The lignin content in seed coat of *BnCCR2-4ox* lines was about two folds of *BnCCR1-2ox* lines, similar to the trend of condensed tannin assay result in seed coat. This contradictory phenomenon might be caused by lowered polymerization or loosened structure of lignins in association with other cell wall components in *BnCCR2-4ox*, which facilitated digestion and enhanced detection value, or by interference from non-targeted but structure-similar macromolecules when undergone measurement (Voelker et al., 2010).

In addition to variation of lignin content, substantial alterations of lignin structure both in stems and roots of *BnCCRox* lines were evidenced by thioacidolysis assay. The proportions of H, G and S lignin units were dramatically changed with the over-expression of *BnCCR* genes. The S/G ratio was significantly reduced in *BnCCR1-2ox*, mainly due to the stronger increase of G lignin units which was in accordance with the Mäule staining results. In contrast, the S/G ratio in *BnCCR2-4ox* was significantly increased, mainly attributed to stronger increase of S lignin units. The alteration of S/G ratio caused by *CCR* manipulation always had different trends in different species. In the previous reports, a lower S/G ratio, mainly caused by relatively stronger effect of *CCR* downregulation on S units, was observed on *Arabidopsis irx4* mutants (Patten et al., 2005), *CCR*-downregulated poplar (Leplé et al., 2007) and *ccr1*-knockout *M. truncatula* mutants (Zhou et al., 2010). A higher S/G ratio, mainly caused by relatively stronger effect of *CCR* downregulation on G units, was found in *CCR*-downregulated tobacco (Piquemal et al., 1998; Chabannes et al., 2001), maize (Tamasloukht et al., 2011), dallisgrass (Giordano et al., 2014) and *CCR2*-knockout *M. truncatula* mutants (Zhou et al., 2010). No obvious change of S/G ratio was recorded in poplar (Leplé et al., 2007) and

perennial ryegrass with *CCR* manipulation (Tu et al., 2010).

Moreover, there was another dramatic difference concerning the H lignin units. In general, H lignin units have trace amount presented in angiosperms. The H lignin units percentage in the stems of *BnCCR1-2ox* (3.29% in ox1-5) was 2-3 folds higher than WT (0.83%), and also more than one fold higher in roots (7.43% in WT and 15.59% in ox1-5). Metabolic and qRT-PCR assay displayed that the accumulation of *p*-coumaraldehyde and the transcript level of *F5H* and *COMT* also had a significant increase in *BnCCR1-2* over-expressor. Reasonably, *p*-coumaroyl-CoA and caffeoyl-CoA might serve as the primary substrates for BnCCR1 (as suggested in Figure 9). The caffeoyl aldehyde could be derived from the *p*-coumaraldehyde, and could also form coniferaldehyde through F5H and COMT catalysis (these two enzymes could mediate the hydroxylation and methylation of the C3 on the aromatic ring, Figure 9). In *CCR1*-downregulated perennial ryegrass (Tu et al., 2010) and Mu-insertion maize mutant *Zmccr1*$^{-}$ (Tamasloukht et al., 2011), the H subunit level was reduced by about 50% and 31% respectively, suggesting that the optimal substrate of CCR1 of perennial ryegrass and maize was *p*-coumaroyl-CoA. On the other hand, reduced H subunit accumulation was reported in the *CCR*-downregulated *A. thaliana* (Goujon et al., 2003), Norway spruce (Wadenback et al., 2008) and alfalfa (Nakashima et al., 2008). On the other hand, BnCCR2 might prefer feruloyl-CoA as its major substrate, because of higher accumulation of S units and its downstream derivatives sinapate esters, and higher increase in transcript level of *F5H* in *BnCCR2ox* as compared with *BnCCR1ox* (Figure 9). Interestingly, qRT-PCR results indicated that *BnCCR1* expression was significantly co-upregulated in *BnCCR2ox* lines, while *BnCCR2* expression had no obvious co-upregulation in *BnCCR1ox* lines. Thus, the increase of H lignin units in *BnCCR2-4ox* lines might be mainly caused by co-upregulation of *BnCCR1* (Supplemental Figure 15). CCR1 and CCR2 in *M. truncatula* (Zhou et al., 2010) and switchgrass (Escamilla-Treviño et al., 2010) also had preference on different hydroxycinnamoyl-CoA substrates, CCR1 preferring feruloyl CoA while CCR2 preferring caffeoyl-and *p*-coumaroyl-CoAs.

Conclusively, *CCR1* subfamily in *B. napus* is mainly involved in the

biosynthesis of H and G type lignin units and mainly contributes to lignification of vessels and vascular bundles in xylem, while *CCR2* subfamily in *B. napus* is mainly involved in the biosynthesis of S type lignin units and mainly contributes to lignification of interfascicular fibers in xylem.

Upregulation of *BnCCR* Genes Enhanced Lodging Resistance, Modified Morphology, but Did Not Improve Disease and UV-B Resistance

The expression perturbation of the genes located at the lignin biosynthetic pathway often accompanied with moderate to severe defects in plant growth and development depending on which gene was targeted. Generally, genetic suppression of the upstream loci, including *4CL*, *HCT*, *C3H*, *C4H* and *CCR*, can most possibly cause obvious abnormal phenotypes (Franke et al., 2002; Hoffmann et al., 2004; Derikvand et al., 2008; Schilmiller et al., 2009; Tian et al., 2013). However, when downstream loci, such as *F5H*, *COMT* and *CAD*, were suppressed, there was generally no significant deleterious effects to the plants growth (Sibout et al., 2005; Tu et al., 2010; Weng et al., 2010). For the severely silenced *CCR* plants, phenotypic abnormalities with irregular vessels usually arise, including plant size reduction, delayed flowering, delayed senescence, retarded seed development, biomass yield reduction and compromised pathogen defense (Jones et al., 2001; van der Rest et al., 2006; Leplé et al., 2007; Zhou et al., 2010; Vanholme et al., 2012; Van Acker et al., 2014; Xue et al., 2015; De Meester et al., 2018; De Meester et al., 2020). Opposite to suppression strategy in most studies, this study carried out over-expression of both *CCR1*- and *CCR2*-type genes in *B. napus* and systemically characterized its molecular breeding effects.

Firstly, *BnCCR* over-expression improved lodging resistance compared with WT, especially for *BnCCR1-2ox* (Figure 4, Supplemental Figure 10). The stems and roots of both *BnCCR1-2ox* and *BnCCR2-4ox* lines were obviously stronger with increased diameters and more lateral roots. The vascular bundles of the stems and roots of *BnCCR1-2ox* developed much better than WT, with bigger size and more vessel numbers. When *CCR1* was reintroduced into *A. thaliana ccr1* mutants under the control of the ProSNBE promoter, specific expression of *CCR1* in the protoxylem and metaxylem vessel cells

showed a full recovery in vascular integrity (De Meester et al., 2018). Due to more accumulation of S units, the interfascicular fibers of the stems and roots of *BnCCR2-4ox* lines developed much better than WT and *BnCCR1-2ox*. Correspondingly, breaking-resistance of both *BnCCR1-2ox* and *BnCCR2-4ox* plants was greatly enhanced in comparison with WT, with larger effect in *BnCCR1-2ox* lines than in *BnCCR2-4ox* lines. These results imply an improved lodging resistance of *BnCCRox* lines due to better development and growth in both morphology and lignification of roots and stems, which provides significant potential in molecular breeding of rapeseed with enhanced lodging resistance through over-expressing *BnCCR* genes.

Secondly, *BnCCR* over-expression also modified leaf morphology. *BnCCRox* leaves were larger and longer with more smooth edge compared with WT. The *BnCCR1-2ox* plants had spoon shaped leaves with clearer and better developed leaf veins, and its petioles had more vascular bundles (Figure 4C; Supplemental Figure 10E). Mäule staining results indicated that petiole xylem was exclusively composed of vascular bundles without interfascicular fibers, which could account for better development of leaf veins in *BnCCR1-2ox* plants, since vascular bundles contained higher proportion of G lignin units and *BnCCR1-2* was mainly involved in the biosynthesis of G and H lignin. In *Arabidopsis*, *CCR1* also mediated cell proliferation exit for leaf development, and *ccr1-4* mutant had a significantly reduced leaf and plant size compared with WT (Xue et al., 2015). However, *BnCCR2-4ox* plants showed less lignification in leaf veins, and its petioles had a less developed and asymmetric distribution of vascular bundle system (Figure 6O; Supplemental Figure 10J), which could be one reason that its leaf was easier to emerge rollover phenomenon (Figure 4G; Supplemental Figure 10D). Weaker leaf vein lignification in *BnCCR2-4ox* plants possibly resulted from two reasons: weakened G units synthesis (since *BnCCR2-4* overexpression mainly forced S units synthesis), and downregulated *BnCCR1* expression in leaves of *BnCCR2-4ox* plants (Supplemental Figure 15B). Enhanced levels of ABA might also play a role in the alteration of leaf phenotypes of *BnCCRox* plants (Supplemental Figure 11), as ABA plays important roles in plant growth and development (Cutler et al., 2010).

Thirdly, resistance of *BnCCRox* plants to *S. sclerotiorum* and UV-B was not improved, conflicting with traditional notion and our original expectation. There are many factors involved in plant disease resistance, such as the epidermal wax layer, trichomes, lignified cell walls, phenolics, phytoalexins and pathogenesis-related proteins (Zhao et al., 2007a). In the present study, although the lignin content was increased through *BnCCR* over-expression, the other important factors correlated to the plant resistance were not enhanced or even suppressed by flux competition between lignin pathway and flavonoid and other pathways, which could be reflected by the changes of flavonoid and glucosinolate metabolic profiles. Besides, decrease of epidermal wax layer was observed on leaves of *BnCCR1-2ox* plants compared with *BnCCR2-4ox* and WT (Supplemental Figure 17). According to this study, sole over-expression of *CCR* genes in *B. napus* could not enhance resistance to *S. sclerotiorum* and UV-B, although *BnCCR2* subfamily could be sharply and intensively induced by *S. sclerotiorum* infection and UV-B irradiation. In *A. thaliana*, previous reports assumed that *AtCCR1* might be mainly involved in constitutive biosynthesis of structural lignins for morphological development, while *AtCCR2* might be mainly involved in defense mechanism (Lauvergeat et al., 2001). However, to date there is no functional verification of this assumption through over-expression transgenic study in *A. thaliana*. Through over-expression study of *Brassica CCR1* and *CCR2* genes, our results indicate that the functional divergence between Brassicaceae *CCR1* and *CCR2* is not as simple as this assumption. *BnCCR2* genes were similar to *AtCCR2* in terms of responsiveness to various stresses, but *BnCCR2* over-expression caused distinct tissue lignification other than enhancement in resistance to *S. sclerotiorum* and UV-B. The most possible explanation of this unexpected phenomenon might be that Brassicaceae *CCR2* is a necessary factor for plant defense, but a successful defense achievement needs the involvement of other necessary factors.

***BnCCR1* and *BnCCR2* Differentially Affect Plant Development Progress**

During the progress of the growth and development of *BnCCRox* plants, the upper stem of *BnCCR1-2ox* plants at bolting stage was more easily to

bend, but *BnCCR2-4ox* plants had no such case (Figure 4F; Supplemental Figure 10A). As reported, S lignin percentage in stems would gradually increase with the plants growth and development process, reaching the highest percentage at mature stage (Tu et al., 2010; Giordano et al., 2014). Mäule staining of stem cross sections in this study revealed similar trend (Supplemental Figure 16), suggesting that S lignin might play an important role for maturation and mechanical strength of stems. (Kaur et al., 2012) found that the stem of *CAD*-downregulated *Nicotiana* plants (ir-CAD) presented a rubbery phenomenon, and the S/G ratio was significantly reduced. Here the S/G ratio was also significantly decreased in *BnCCR1-2ox* plants (1.29 in WT, 0.68 in ox1-5, and 0.98 in ox1-12). Moreover, our results showed that in WT the S/G ratio in stem (1.29) was significantly higher than in root (0.49), which might be one factor contributing the more flexible texture of roots compared with stems, although total lignin content was higher in root than in stem (Table 1). Lower percentage of S units (or higher percentage of G and H units) might contribute to a lower level of stiffness of the stem, together with the lower lignin content in the upper stem, which might be one reason of the bending phenomenon of *BnCCR1-2ox* at bolting stage. However, when *BnCCR1-2ox* plants entered flowering stage, the bending phenomenon disappeared, which might be due to increase in total lignin content and S lignin percentage in stems (Supplemental Figure 16). After flowering, the upper portion of rapeseed plants would gradually become more and more heavy, then the stems should accumulate enough total lignin with higher S lignin proportion to afford enough mechanical strength. Relationship between S/G ratio and the texture of the plant stems was summarized in the Supplemental Table 4. These results suggest that higher S/G ratio contributes to stronger stiffness in plant stems, which is manifested during reproductive growth.

In this study, *BnCCR1-2ox* plants flowered distinctly later than WT and *BnCCR2-4ox* plants, implying that the function of Brassicaceae *CCR1* is also

associated with plant development progress. (Vermerris et al., 2002) reported that there was an evolutionarily conserved mechanism between cell wall biosynthesis and production of flowers. The delayed increase of S lignin proportion, lowered stem stiffness and delayed stem maturation at bolting stage were reflections of delayed development progress and flowering in *BnCCR1-2ox* plants. Moreover, cross-talk between the networks controlling flowering and glucosinolate profiles was proved in previous reports (Jensen et al., 2015; Mohammadin et al., 2017), and *AOP2* played an important role (Jensen et al., 2015). In this study, the accumulation of aliphatic glucosinolates was greatly increased and *AOP2* expression level was upregulated by tens to hundreds of folds in *BnCCR1-2ox* plants, suggesting that cross-talk effect between glucosinolates and flowering network might be one reason of flowering delay.

BnCCR1 and _BnCCR2_ Exert Different Flux Control on Flavonoid Pathway and Lignin-derivative Pathways in _B. napus_

In metabolic engineering, products, precursor steps as well as associated neighbor pathways would be affected via metabolic flux redirection. In lignin engineering, for example, significantly higher amounts of vanillin, ferulic acid, *p*-coumaric acid, coniferaldehyde and syringaldehyde were released from the cell wall samples of *MtCAD1* mutants than the wild-type (Zhao et al., 2013). In the *C3'H* (Abdulrazzak et al., 2006) or *HCT* (Besseau et al., 2007) defect *Arabidopsis*, *C3H1*-downregulated maize (Fornalé et al., 2015), *CCR*-silenced tomato (van der Rest et al., 2006) and perennial ryegrass (Tu et al., 2010), the accumulation of flavonoids was significantly increased. In *CCR*-downregulated *N. tabacum*, cellulose content was reduced (Leplé et al., 2007), and starch metabolism and photorespiration was changed (Dauwe et al., 2007).

Besides enhancement of lignin monomers, our results also showed that both *BnCCR1-2* and *BnCCR2-4* over-expressors had significantly increased levels of various CCR-downstream pathway products when compared with WT, especially for sinapate esters (Supplemental Data Set 1; Figure 9), which could be caused by the enhanced expression levels of corresponding genes

965 *CCR*, *F5H*, *COMT* and *CAD*. Moreover, *BnCCR2-4ox* plants had a stronger
966 effect on the accumulation of sinapate esters in stems than *BnCCR1-2ox*
967 plants, implying that the metabolic route related to BnCCR2 catabolism (mainly
968 S units synthesis) might be closer to sinapate ester pathway than BnCCR1
969 (Figure 9). On the contrary, those intermediates located at the up-stream of
970 CCR, such as the 5-O-caffeoylshikimic acid and *p*-coumaric acid, were mildly
971 downregulated in *BnCCR1-2ox* plants.

972 More strikingly, many compounds synthesized in flavonoid pathway, such
973 as kaempferol, quercetin, isorhamnetin, cyanidin and other derivatives, were
974 significantly reduced in *BnCCRox* plants compared with WT. The defect of the
975 flavonoid accumulation could be observed on the lightening of seed coat color
976 in *BnCCRox* seeds. The dramatic reduction in flavonoids was theoretically
977 caused by the reduced availability of *p*-coumaroyl-CoA precursor for CHS as
978 *BnCCR* overexpression attracted more of this common precursor into lignin
979 pathway (Figure 9). This kind of flux shift could be further evidenced on
980 molecular level (Figure 8). qRT-PCR results showed that some key genes of
981 flavonoid pathway, like *CHS* (*TT4*), *CHI* (*TT5*), *ANR* (*Ban*) and *MYB123* (*TT2*),
982 etc., were significantly downregulated. Seed color degree, metabolic profile
983 and gene expression profile all indicated that suppression impact on flavonoid
984 pathway was greater in *BnCCR1-2ox* plants than in *BnCCR2-4ox* plants
985 (Figure 5). Higher flux control effect on flavonoid pathway by BnCCR1 than by
986 BnCCR2 could result from the fact that the metabolic routes of BnCCR1
987 catabolism (mainly H and G units synthesis) were closer to flavonoid pathway
988 than that of BnCCR2 (mainly S units synthesis) as suggested in Figure 9.

989 *Brassica* yellow-seed cultivars are superior to traditional black-seed
990 cultivars in both seed oil content, oil quality and meal quality, featured by
991 thinner seed coat, little seed coat pigments (proanthocyanidins/condensed
992 tannins) and lower crude fibers (lignin, cellulose, etc.) (Qu et al., 2013; Zhang
993 et al., 2013). In natural yellow-seed cultivars of all the 3 *Brassica* species, the
994 expression of *CCR1* subfamily was distinctly lower in developing seeds
995 especially in late-stage seeds than in black-seed stocks, but the expression of
996 *CCR2* subfamily was distinctly upregulated (Figure 2, Supplemental Figures 3,
997 4 and 5). This means that downregulation of *CCR1* subfamily is a contribution

factor of the decrease in lignification and lignin content of natural *Brassica* yellow seeds, while upregulation of *CCR2* subfamily could hardly compensate this effect. When *BnCCR1* and *BnCCR2* were overexpressed, the seeds of transgenic plants also showed a yellow-seed phenotype and the seed coat pigments in these artificial yellow-seed lines were largely decreased (Figure 5). However, opposite to natural yellow seeds, the thickness of transgenic seed coat was not decreased (Figure 5), and lignin content in the transgenic seed coat was increased (Table 1). These results imply that *CCR1* and *CCR2* in *Brassica* are differently associated with natural yellow-seed trait, and overexpression of *CCR1* and *CCR2* will generate "yellow seeds" with less pigments but more lignins.

BnCCR1 and _BnCCR2_ Play Different Roles in Crosstalk between Phenylpropanoid Pathway and Glucosinolate Pathway

In this study, the accumulation of glucosinolates also changed dramatically in *BnCCRox* plants, besides great variation in compounds of phenylpropanoid compound pathway. There were a few reports on crosstalk effect of glucosinolate pathway on phenylpropanoid pathway (Hemm et al., 2003; Kim et al., 2015; Kim et al., 2020). In *Arabidopsis*, (Kim et al., 2015) found that the accumulation of phenylpropanoids were significantly suppressed in *ref5-1* mutant, and *REF5* was proved to encode CYP83B1 which was involved in biosynthesis of indole glucosinolates. Defect of phenylpropanoids deposition was also detected in *Arabidopsis ref2* mutant, as *REF2* encoded CYP83A1 which played a role in aliphatic glucosinolate pathway (Hemm et al., 2003). In low-lignin *c4h*, *4cl1*, *ccoaomt1* and *ccr1* mutants of *Arabidopsis*, transcripts of some glucosinolate biosynthesis genes were more abundant (Vanholme et al., 2012). However, to date there is no systemic study on crosstalk effect of phenylpropanoid pathway on glucosinolate pathway.

In present study, the aliphatic glucosinolates were significantly increased in leaves, petioles, stems and seeds of ox1-5, some of which were upregulated by more than 1000 folds in stems, as compared with WT (Supplemental Data Set 1). The increased aliphatic glucosinolates in *BnCCR1-2ox* could result

from upregulated expression of *MYB28*, *MYB29*, *CYP79F1*, *CYP83A1*, *AOP2* and *GSL* in the leaves of transgenic plants (Figure 8). Among them, the expression of *MYB29*, *CYP79F1* and *GSL* could almost only be detected in *BnCCR1-2ox*, not in WT. On the contrary, the contents of most glucosinolate components were drastically decreased in the ox2-16 leaves, petioles, stems and 30DAP seeds, some of which were lowered to less than one hundredth or even non-detectable, with only very few glucosinolate components showing mild increase or little change in ox2-16 organs. The undetectable *MYB29* expression and extremely lower expression of *MYB51*, *MYB122*, *AOP2*, *CYP79B2*, *ST5a* and *IGMT1* in *BnCCR2-4ox* plants could be responsible for the decrease of glucosinolate content. Because the WT material ZS10 of this study was a “double-low” (low erucic acid, low glucosinolates) commercial cultivar, the low proportion of indole and aromatic glucosinolates in WT and the limited change of indole and aromatic glucosinolates in *BnCCR*-overexpressing plants might be caused by breeding impairment of respective biosynthesis pathways of these two types of glucosinolates. If a “double-high” stock was used as WT for *BnCCR* transformation, the effect on indole and aromatic glucosinolates deposition might not be so mild. Taken together, both *BnCCR1-2* and *BnCCR2-4* distinctly affect glucosinolate biosynthesis, but have divergent or almost opposite effects.

In conclusion, the genetic manipulation of *CCR* expression in *B. napus* substantially gives rise to a redirection of the metabolic flux within, or even beyond, the phenylpropanoids biosynthetic pathway. *CCR* manipulation in *B. napus* not only affects lignin, sinapate ester and flavonoid profiles, but also remodels glucosinolates profile in various organs of transgenic plants (Figure 9).

Crosstalk between glucosinolate biosynthesis and phenylpropanoid biosynthesis could be linked through PAL degradation that mediated by Med5-KFBs-dependent manner (Kim et al., 2020). On the other hand, what mechanism is involved in change of glucosinolate biosynthesis by manipulating phenylpropanoid genes, such as *CCR*, needs to be clarified. Our qRT-PCR results indicate that at least transcription regulation is involved, but whether mediator-mediated protein degradation is also involved deserves

future study.

METHODS

Plant Materials

B. napus: black-seed varieties 5B and ZS10, yellow-seed variety 09L587. *B. rapa*: black-seed variety 09L597 and yellow-seed variety 09L600. *B. oleracea*: black seed variety 09L598 and yellow-seed variety 09L599. T1 transgenic lines together with non-transgenic wild-type (WT) ZS10 plants were grown in artificial growth room (25°C, 16-h photoperiod/20°C, 8-h dark period). Later generations of transgenic lines and all other materials were planted in field cages, with common plantation conditions. Samples were immediately frozen in liquid nitrogen and stored at -80°C for gene expression analysis, biochemical and histochemical assay, gas chromatography–mass spectrometry (GC-MS) detection and UPLC-HESI-MS/MS analysis. Mature seeds, stems and roots (about 65 DAP) were harvested for agronomic traits investigation and biochemical analysis.

Stress treatments

***S. sclerotiorum* infection and resistance investigation.** The *S. sclerotiorum* strain was kindly provided by Prof. Wei Qian (Southwest University, China), and the inoculation on *B. napus* was performed as described previously (Mei et al., 2011). The 4th or 5th fully expanded leaves at the 9- to 12-leaf stage and stem segments at early flowering stage were sampled for resistance assay in the laboratory. Moist towels were placed at the bottom of an appropriate container. Filter papers were placed over the towels, and the detached leaves and stem segments were placed on the filter papers. Two plugs (6 mm in diameter) punched from the growing margin of 3-day-old culture of *S. sclerotiorum* on PDA medium were placed separately on two sides of the midrib of leaf and the stem segment. The container was sealed with plastic film to keep humidity, with temperature maintained at 21°C in laboratory. The lesion size (S) was calculated with the formula $S=\pi\times a\times b/4$, where a and b represent the long and the short diameters of the ellipse-like lesion which was measured 2 days after leaf inoculation or 3 days after stem inoculation. Leaf

discs of 2-3 cm in diameter around the infection site were sampled after 0, 6, 12, 24 and 48 h of inoculation.

***P. rapae* inoculation treatment.** Leaves of the same position of normal-growth *B. napus* seedlings in pots were inoculated with *P. rapae* worms of similar size, which were laid on *B. napus* plants in preparation. Each leaf was inoculated with 4 worms, and each inoculated plant was covered with a plastic net to prevent worm escaping. Leaves, stems and roots were sampled after 0, 6, 12, 24 and 48 h of inoculation.

Treatment with high temperature & drought. Normal-growth *B. napus* seedlings in pots were put into a growth chamber which was kept at 37°C with no watering. Leaves, stems and roots were sampled after 0, 6, 12, 24 and 48 h of treatment.

Salt treatment. Normal-growth *B. napus* seedlings in pots were watered with 500 mL NaCl or Na_2CO_3 (0.3 mol/L), and the leaves, stems and roots were collected after 0, 6, 12, 24 and 48 treatment.

UV-B Treatment. Normal-growth *B. napus* seedlings in pots were irradiated with UV-B light from 4 UV-B lamps (2.4 mW/cm^2), and leaves, stems and roots were collected after 0, 20, 40, 60 and 80 min of treatment.

Isolation of *Brassica CCR* cDNA and Genomic sequences

All samples were frozen in liquid nitrogen and stored at -80°C. Total RNA was extracted from roots, stems, leaves, flowers and developing seeds of the 3 *Brassica* species using EASYspin Kit (Biomed, China) and RNAprep pure plant kit (TIANGEN, China). Equal 1 µg RNA from each organ were pooled for total cDNA synthesis for 5'-RACE and 3'-RACE using GeneRacer^{TM} Kit (Invitrogen, USA). Based on *in-silico* cloning and multi-alignment of *Brassica* genomic and cDNA tags from NCBI GenBank nr/nd, GSS and EST databases, RACE (rapid amplification of cDNA ends) primers were designed according to conservative sites of *CCR* genes (Supplemental Data Set 4).

5’-RACE primary and nested amplifications of *Brassica CCR1* genes were performed using primer pairs 5’P+RCCR1 and 5’NP+RCCR1-1N / 5’NP+RCCR1-2N, while 3’-RACE primary and nested amplifications of *Brassica CCR1* genes were performed using primer pairs 3’P+FCCR1C1 and 3’NP+FCCR1C2, respectively. 5’-RACE primary and nested amplifications of *Brassica CCR2* genes were performed using primer pairs 5’P+RCCR2-51 and 5’NP+RCCR2-52, while 3’-RACE primary and nested amplifications of *Brassica CCR2* genes were performed using primer pairs 3’P+FCCR2-31 and 3’NP+FCCR2-32, respectively. All reactions were performed using standard Taq-PCR, annealed at 52°C, with extension time of 1 min.

The full-length cDNAs of *Brassica CCR* genes were PCR-amplified from the 3’-RACE total cDNA template using Taq plus enzyme (a mixture of Pfu proofreading and Taq DNA polymerases). The primers are listed in Supplemental Data Set 4. Forward primers FCCR1-1, FCCR1-2, FBCR1-13 and FBCR1-24 were paired with reverse primers RCCR1-1, RCCR1-2, RBCR1-3, RBCR1-1 and RBCR1-24 to form 20 primer combinations to amplify full-length cDNAs of *CCR1* subfamily genes from *B. napus*, *B. rapa* and *B. oleracea*. For amplification of *CCR2* subfamily genes from the 3 *Brassica* species, forward primers FBNCR210, FBRCR221, FBOCR2E1 and FBOCR2G5 were paired with reverse primers RBNCR22, RBNCR28, RBOCR22 and RBOCR2G9 to form 16 primer combinations. Gradient annealing temperature of 52-60°C was adopted for each PCR, with an extension time of 2 min. All successful primer pairs were used to amplify the corresponding gDNA sequences by replacing the total cDNA template with total gDNA of respective species. *Brassica CCR2* pseudogenes were directly amplified without RACE information using corresponding primers listed in Supplemental Data Set 4. PCRs for gDNA and pseudogenes had an annealing temperature of 55°C and an extension time of 3 min.

Agarose gel electrophoresis, gel recovery, TA-cloning with pMD 19-T

vector (TaKaRa Dalian, China), *Escherichia coli* transformation, colony identification and Sanger's sequencing were performed with regular molecular methods.

Bioinformatic Methods for this Study

Open reading frame (ORF) finding and translation, parameter calculation and sequence alignment of genes and proteins were performed on Vector NTI Advance 11.53 (Invitrogen, USA). Structural and functional predictions of proteins were performed on Expasy website (http://www.expasy.org).

After our cloning work of *Brassica CCR* family, whole genome sequencing and annotation data of *B. rapa*, *B. oleracea* and *B. napus* were available in GenBank, then we performed *in-silico* cloning of all *CCR1* and *CCR2* subfamily genes from these 3 species. Using the cloned *Brassica CCR* sequences as queries (E-probes), BLASTn and BLASTp were performed against the nr/nt, nr refseq_rna, refseq_protein, refseq_genomes, wgs, est and tsa databases of *Brassica* (taxid:3705) on NCBI (https://blast.ncbi.nlm.nih.gov/Blast.cgi), Genoscope (http://www.genoscope.cns.fr/brassicanapus/) and BRAD (http://39.100.233.196/#/), sequences of all *CCR1* and *CCR2* genes and proteins from *Brassica* were *in-silico* cloned and multi-aligned with the actually cloned sequences in this study.

For phylogenetic analysis, all true-CCR protein sequences from representative whole-genome-sequenced species of Brassicales and other malvids orders were *in-silico* cloned into a fasta file, which was sent to Seaview 4.0 to perform clustalo multi-alignment and construct a Squared-type phylogenetic tree using the Distance-BioNJ-Poisson mode. The reliability of the tree was measured by bootstrap analysis with 1,000 replicates.

Southern hybridization analysis

Total genomic DNA was extracted from leaves of the 3 *Brassica* species using a standard cetyltrimethylammonium bromide protocol (Porebski et al., 1997). It was digested with restriction enzymes *Dra*I, *Eco*RI, *Eco*RV, *Hin*dIII and *Xba*I (70 µg for each enzyme) respectively, and separated on a 0.8% (w/v)

agarose gel. Following electrophoresis, DNA was transferred to a positively charged nylon membranes (Roche, Switzerland) using established protocols. The *Brassica CCR1*- and *CCR2*-specific probes were amplified by PCR with primer pairs FCCR1C1+RCCR1 and FBCCR2I+RBCCR2I respectively, and labelled using digoxigenin (DIG) Probe Synthesis Kit (Roche, Switzerland), with an annealing temperature of 61°C and extension time of 1 min. Sequences of all primers are provided in Supplemental Data Set 4. Hybridizations with the probes were performed at 43°C overnight, with chemiluminescent detection using DIG Luminescent Detection Kit (Roche, Switzerland).

Detection of Transcription Levels

Total RNA of each sample was extracted using EASYspin Kit (Biomed, China) and RNAprep pure plant kit (TIANGEN, China), and treated with DNase I to eliminate contaminated gDNA. Equal quantities of RNA (1μg) were adopted for the synthesis of total cDNA using the PrimeScript™ RT reagent kit with gDNA Eraser (TaKaRa Dalian, China). The transcript levels of *CCR1*, *CCR2* and other target genes were detected using both quantitative real-time PCR (qRT-PCR) and semi-quantitative RT-PCR (sRT-PCR) as described previously (Zhao et al., 2007b). The *25SrRNA* primer pair was used as an internal control in qRT-PCR. A 25-fold dilution series of original reverse-transcription products was used for qRT-PCR using SsoAdvaned™ Universal SYBR Green Supermix (BioRad, USA) on CFX96™ Real-Time System (BioRad, USA). Conditions for qRT-PCR were as follows: 95°C for 2 min; 40 cycles of amplification with 95°C for 30 s and 62°C for 30 s. A melting curve was obtained after amplification by heating products from 60 to 95°C. Transcript levels were determined based on changes in Cq values relative to the internal control. Results were analyzed using the CFX Manager™ 3.0 software (Bio-Rad, USA). Conditions for sRT-PCR on Veriti Thermal Cycler (ABI, USA) were as follows: 94°C for 2 min; 31 cycles of amplification with 94°C for 0.5 min, 60-64°C for 0.5 min and 72°C for 1 min; followed by 72°C for 10 min. The *26SrRNA* primer pair was used as an external control in sRT-PCR. Sequences of all primers for qRT-PCR and sRT-PCR are listed in Supplemental Data Set 4.

Construction of Overexpression Vectors

The *BnCCR1-2* and *BnCCR2-4* full-length cDNAs harbored on the sequenced recombinant pMD 19-T vectors were subcloned into platform vector pC2301M1DPB using *Bam*HI+*Sac*I double digestion and *Xba*I single digestion, under the control of a double CaMV35S promoter (P_{D35S}) and the nopaline synthase terminator (T-nos) (Fu et al., 2017), to generate plant overexpression vectors pCD-*BnCCR1-2ox* and pCD-*BnCCR2-4ox*, respectively. The overexpression vectors were transformed into *Agrobacterium tumefaciens* (LBA4404) through a freeze–thaw method (Chen et al., 1994), and engineering strains were obtained after Taq-PCR verification (annealed at 55°C, extension for 1.5 min) with primer pairs F35S3N+RCCR1-2 and FCCR1-2+RNOS5N for pCD-*BnCCR1-2ox* and primer pairs F35S3N+RBNCR22 and FBNCR210+RNOS5N for pCD-*BnCCR2-4ox*.

Rapeseed Genetic Transformation and Screening

A modified *Agrobacterium*-mediated transformation protocol according to (Cardoza and Stewart, 2003) was used to transform “double low” (low erucic acid and low glucosinolates) rapeseed commercial cultivar Zhongshuang 10 (ZS10) with overexpression vectors pCD-*BnCCR1-2ox* and pCD-*BnCCR2-4ox*, using hypocotyl segments as explants (Fu et al., 2017). The regenerated plants were identified first by leaf β-glucuronidase (GUS) staining and leaf Basta-resistance test (200 ppm), then by Taq-PCR detection of target genes (as those for engineering strains verification) and the selectable and screenable marker gene *BAR* (primer pair FBar+RBar, annealed at 58°C, extension for 30 s). The T1 transgenic plants were grown in artificial growth room and were selfed. Representative T2 and T3 transgenic lines and WT were grown in field cages, and positive plants of above identifications were subjected to traits investigation and further studies.

Agronomic Traits Investigation

The area and length of the 4th or the 5th leaves which was fully expanded were surveyed during vegetative stage, and the length and width of the petioles of these leaves were measured at the same time. The primary branch numbers, middle stem diameter and stem strength at reproductive stage, and the plant traits at harvest stage, were recorded and measured. The weight of 1000 seeds and yield per plant were measured after the harvested seeds were dry. Stem strength determination: Freshly collected middle stem segments were placed horizontally, and the force exerted to break the stem was recorded with a universal force testing device (model DC-KZ300, Sichuan, China) to determine the stems rigidity, which was normalized with the stem's length and diameter.

Measurement of Leaf SPAD Readings

A SPAD-502 chlorophyll meter (Minolta, Osaka, Japan) was used to obtain SPAD values (SPAD units) from the 4th or the 5th fully expanded leaves of five representative transgenic plants of each line. Three average distributed points SPAD readings were obtained per leaf, and averaged as the mean SPAD reading of the leaves (Yang et al., 2014).

Quantification of Insoluble Condensed Tannins of Seed Coat

The modified method for quantification of insoluble condensed tannins was according to (Auger et al., 2010) and (Naczk et al., 2000). The oven-dried seed coat was milled to fine powder using a microball mill, and extracted with hexane for 12 h using a Soxhlet apparatus and then dried at room temperature. 10 mg sample of seed coat powder was extracted with the extraction solution of three milliliters of butanol-HCl (95:5; v/v), 300 μL methanol and 100 μL of 2% ferric ammonium sulfate (w/v) in 2 N HCl. The tubes were heated for 3 h at 95°C in a water bath, centrifuged after cooling, and extracted again with the same extraction solution for 1 h. The absorbance of the pooled supernatant was measured at 550 nm against a reagent-only blank using UV-VIS

spectrophotometer (UV-5100B, Shanghai, China). A calibration curve was prepared using procyanidin with amounts ranging from 0 to 200 μg/mL.

Near-infrared Reflectance Spectroscopy (NIRS) Measurements

Measurements for cellulose and hemicellulose of the stem, seed color, oil content, fatty acid profile, total glucosinolates and fibre components of the seeds were obtained using an NIR System 6500 with WinISI II software (FOSS GmbH, Rellingen, Germany) according to (Liu et al., 2012). The dried harvested stems were ground with a universal mill to pass a 40-mesh screen. The calibrations which were developed by our laboratory specifically for the measurement of these traits for *B. napus* seeds and stems, were used to detect the phenotype values for seed colour (visual light absorbance), acid detergent lignin (ADL, % dry weight), acid detergent fibre content (ADF, % dry weight) and neutral detergent fibre content (NDF, % dry weight) from NIRS spectra. NIRS-derived estimates for each trait and genotype were averaged over two technical repetitions. Cellulose concentrations were calculated as the difference between NDF (predominantly phenylpropanoid compounds, cellulose and hemicellulose) and ADF (predominantly phenylpropanoid compounds and hemicellulose), and hemicellulose concentration as the difference between ADF and ADL (phenylpropanoids).

Histochemical Staining, Autofluorescence and Anatomical Studies

Cross sections were obtained by using a frozen section machine (Leica CM1850, Germany). Fresh petioles at vegetative stage, fresh stems and roots of the plants at reproductive stage, fresh mature silique coat and dry mature seeds coat were cut into slices of 60, 60, 60, 60 and 5 μm thick, respectively. Phloroglucinol-HCl staining and Mäule staining of those plant organ sections were performed as previously described (Chapple et al., 1992; Chen et al., 2002). Stained sections were observed on a stereoscopic microscope (Nikon C-BD230, Japan; OLYMPUS SZX2-FOA, Japan) and a fluorescence

microscope (Nikon ECLIPSE E600W, Japan).

Determination of Lignin Content and Composition

Lignin content was quantified using a modified acetyl bromide soluble lignin method (Fukushima and Hatfield, 2001; Chang et al., 2008), and lignin composition was determined with a modified thioacidolysis method according to previous reports (Lapierre et al., 1995; Yosef and Ben-Ghedalia, 1999; Robinson and Mansfield, 2009).

Cell Wall Isolation

Harvested stems were dried in a 70°C forced air oven for 72 h, and then were ground with a Wiley mill to pass a 40-mesh screen or with a microball mill to pass an 80-mesh screen using to meet the requirements of the subsequent extraction method. 60-70 mg samples were added into a 2 mL Sarstedt screw cap tube, adding with 1.5 mL of 80% aqueous ethanol to the dispensed ground material, and vortex thoroughly (10 min). This step was repeated for a total of three cycles, followed by centrifugation at 10,000 rpm for 10 min, and the supernatant was decanted. Add 1.5 mL of chloroform/methanol (2:1 v/v) solution to the residue, and shake the tube thoroughly to resuspend the pellet. Centrifuge at 10,000 rpm for 10 min, and decant the supernatant. Resuspend the pellet in 500 μL of acetone, and evaporate the solvent with a stream of air at 35°C until dry (If needed, dried samples can be stored at room-temperature until further processing). To initiate the removal of starch from the sample, resuspend the pellet in 1.5 mL of a 0.1 M sodium acetate buffer pH 5.0, cap the Sarstedt tubes, and heat for 30 min at 80°C in a heating block. Cool the suspension on ice, and add the following agents to the pellet: 35 μL of 0.01% sodium azide (NaN_3), 35 μL amylase (from Bacillus species, 50 μg/mL in H_2O, Sigma); 3.56 μL pullulanase (from Bacillus acidopullulyticus, 17.8 units, Sigma). Cap the tube, and vortex thoroughly. The suspension is incubated over night at 37°C in the shaker (Orienting the tubes horizontally aides

improved mixing). After enzyme digestion, the suspension was heated at 100°C for 10 min in a heating block to terminate digestion. Centrifuge at 10,000 rpm for 10 min, and discard the supernatant containing solubilized starch. The remaining pellet was washed three times by adding 1.5 mL water, vortexing, centrifuging, and decanting of the washing water. For removing the water, 1.5 mL anhydrous ethanol was added to resuspend the pellet, followed by vortexing, centrifuging, decanting of the supernatant, and resuspending the pellet with 500 μL of acetone. Finally, evaporate the solvent with a stream of air at 35°C until dry. It may be necessary to break the material in the tube with a spatula for better drying. If needed, the dried samples can be stored at room-temperature until further processing.

Spectrophotometer Test of Lignin Content

2 mg of prepared cell wall material was interacted with 200 μL of freshly made acetyl bromide solution (25% v/v acetyl bromide in glacial acetic acid) in a culture tube under 50°C for 3 h with shaking at 30 min intervals during first 2 h and with vortex every 15 min during the last 1 h, and the reaction was stopped on ice for 5 min. Add 800 μL of 2 M sodium hydroxide and 140 μL of freshly prepared 0.5 M hydroxylamine hydrochloride, and vortex the tubes. Transfer the reaction solution to a 15 mL graduated test tube with stopper, and the tubes were rinsed with glacial acetic acid to complete the transfer. Fill up the tubes exactly to the 15.0 mL mark with glacial acetic acid, cap, and invert several times to mix. The absorbance of the solutions was read at 280 nm on a Varian Cary 50 spectrophotometer. A blank was included to correct for background absorbance by the reagents. Determine the percentage of acetyl bromide soluble lignin (%ABSL) using the coefficient (23.35) with the following formula: % ABSL Calc: $\frac{\text{abs}}{(\text{Coeff}\times 1\text{cm})}\times\frac{(15\text{ml}\times 100\%)}{\text{weight(mg)}}$, 1 cm represents the pathlength, multiplication of %ABSL with 10 results in the ug/mg cell wall unit.

GC-MS Test of Lignin Composition

Transfer approximately 5 mg of cell wall material into a screw-capped glass tube for thioacidolysis. Add 1 mL freshly made thioacidolysis reagent consisting of 2.5% boron trifluoride diethyl etherate (BF3) and 10% ethanethiol (EtSH) in dioxane solution, purge vial headspace with nitrogen gas (N_2), and cap immediately. After 4 h reaction at 100°C with gentle mixing every hour, the reaction was stopped by cooling on ice for 5 min. The pH of the reaction was adjusted to 3-4 by adding 300 μL of 0.4 M sodium bicarbonate. Add 2 mL water, 200 μL tetracosane (0.5 mg/ml ethyl acetate) and 0.8 mL of ethyl acetate, and vortex. Transfer 300 μL of the ethyl acetate layer into a 2 mL Sarstedt tube (make sure no water is transferred), and evaporate the solvent with N_2. To remove excess water, 200 μL acetone was added and evaporated twice. The finally obtained oily residue was redissolved in 500 μL of ethyl acetate, and 100 μL of resuspended sample was added with 20 μL of pyridine, and 100 μL of N, O-bis(trimethylsilyl) acetamide for the TMS derivatization, and incubated for 2 h at 25°C. The GC-MS test was performed to identify and quantify the lignin monomer trimethylsilylated derivatives, as 1 μL injecion volume sample was separated with a Restek Rxi-5ms column (30 m X 0.25 mm X 0.25 μm film thickness) under split mode, and the injector and detector temperatures were set to 250°C. Helium was the carrier gas. The following temperature gradient was used with a 30 min solvent delay and a 1.1 mL/min flow rate: Initial hold at 130°C for 3 min, a 3°C/min ramp to a 250°C whish was hold for 5 min, and then equilibration to the initial temperature of 130°C. Quantitation of the main lignin-derived monomers was performed after an appropriate calibration relative to the Tetracosane internal standard, and the characteristic mass spectrum ions of 299 m/z, 269 m/z and 239 m/z were representative for S, G and H trimethylsilylated derivatives respectively.

Phenolic Profiling by UPLC-HESI-MS/MS

Extraction of Soluble Metabolites

Samples of stems, leaves, petioles and seeds (30 DAP) were ground

under liquid nitrogen in a mortar and pestle, and freeze-dried by using a vacuum freeze drier (SCANVAC, Coolsafe 110 – 4, Denmark). 30 mg ground lyophilized stems, leaves and petiole material were extracted twice by sonication with 1.0 mL of 50% methanol plus 1.5% acetic acid for 1 h at 4°C, clarified at 15,000×g for 10 min. The supernatants were combined and concentrated by using a vacuum concentration (SCANVAC, scan speed 32, Denmark), and redissolved in 0.5 mL of 50% methanol, filtered through a 0.22 µm nylon syringe filter. 50 mg ground lyophilized seed material was extracted as previously described (Auger et al., 2010) with a little modification. One ml of a methanol/acetone/water/TFA mixture (40:32:28:0.05, v/v/v/v) was added to the seed samples, and sonicated for 1 h at 4°C. After centrifugation (15,000 ×g, 5 min), the pellet was extracted further with 1 mL methanol/acetone/water/TFA mixture overnight at 4°C under agitation (200 rpm), while the supernatant was stored at -80°C. Supernatants were pooled and clarified at 15,000 ×g for 10 min, then concentrated. To further remove the water, 200 µL methanol was added to the extracts two times during evaporation. The dried extracts were redissolved in 1 mL of 1% acetic acid in methanol and filtered through a 0.22 µm nylon syringe filter, then stored at -80°C before analysis.

UPLC-HESI-MS/MS Analysis

UPLC was performed on Dionex Ultimate-3000 UHPLC System (Thermo Fisher Scientific, Tacoma, Washington, USA), as 5 µL samples were separated on a Waters ACQUITY UPLC BEH C18 column (1.7 µm, 2.1 mm ×150 mm). The flow rate was 0.2 mL/min, and the oven temperature was 30°C. Eluent A was 0.1% formic acid in water, and eluent B was 0.1% formic acid in acetonitrile. The following gradient was applied for stems, leaves and petiole extracts elution: 5% B for 5 min, 5% B to 95% B for 20 min, 95% B for 5 min, followed by column wash and re-equilibration. For seed metabolites elution, gradient conditions were as follows: 5% to 9% B for 5 min, 9% B to 16% B for 10 min, 16% B to 50% B for 25 min, 50% B to 95% B for 15 min, 95% B for 5

min, followed by column wash and re-equilibration. Mass analyses were carried out with the mass spectrometer Thermo Scientific™ Q Exactive™ (Thermo Fisher Scientific, Tacoma, Washington, USA) equipped with a HESI source used in the negative ion mode. Source parameters were as following: spray voltage of 3.0 kV, sheath gas flow rate at 35 arbitrary units, auxiliary gas flow rate at 10, capillary temperature at 350°C, and aux gas heater temperature at 300°C. Nitrogen gas was used as sheath gas and auxiliary gas. Full MS/dd-MS2 were acquired from m/z 100 to m/z 1500. Thermo Xcalibur software version 3.0.63 (Thermo Fisher Scientific) was used for data collection and processing. Contents of the metabolites were expressed relative to the calibration curves of available standards. Standard compounds, namely *p*-coumaric acid, caffeic acid, ferulic acid, epicatechin, quercetin, kaempferol and isorhamnetin (from PureChem-Standard Co., Ltd, Chengdu, China) as well as sinigrin, sinapic acid, coniferyl aldehyde and abscisic acid (from Sigma-Aldrich, USA) were analyzed under the same conditions described above.

Statistical Issues

Except for non-necessary cases and specially indicated situation, all experiments in this study were carried out with 3 replications, and all experimental results were statistically analyzed. Statistical significance was calculated by two-tailed Student's t test (*$P < 0.05$, **$P < 0.01$), and error bars indicate SD. One-way ANOVA followed by Duncan's multiple comparisons test was used to determine the differences. Values of $P < 0.05$ were considered to be statistically significant. The results of statistical analyses are shown in Supplemental Data Set 5.

Accession Numbers

Sequence data of the genes and proteins involved in this article can be found in the NCBI (http://www.ncbi.nlm.nih.gov/) databases under the accession numbers indicated in Supplemental Table 1 and Figure 1.

Supplemental data

Supplemental Figure 1. Southern blot detection of *CCR* subfamily genes in *B. napus*, *B. rapa* and *B. oleracea*.

Supplemental Figure 2. Multi-alignment indicates that *Brassica* CCRs contain complete structural features as those in model plants *A. thaliana* and popular.

Supplemental Figure 3. Expression patterns of *CCR1*-genes and *CCR2*-genes show distinct organ-specificity and difference between black and yellow seeds in *B. napus*.

Supplemental Figure 4. Expression patterns of *CCR1*-genes and *CCR2*-genes show distinct organ-specificity and difference between black and yellow seeds in *B. rapa*.

Supplemental Figure 5. Expression patterns of *CCR1*-genes and *CCR2*-genes show distinct organ-specificity and difference between black and yellow seeds in *B. oleracea.*

Supplemental Figure 6. *BnCCR1*-genes and *BnCCR2*-genes distinctly respond to various stresses in *B. napus* seedlings.

Supplemental Figure 7. Basta-resistance, GUS-staining and PCR determination of transgenic lines.

Supplemental Figure 8. qRT-PCR shows distinct upregulation of the target genes in respective T2 lines of *BnCCR1-2ox* and *BnCCR2-4ox*.

Supplemental Figure 9. Multiple agronomic traits are significantly modified in *BnCCR1-2ox* and *BnCCR2-4ox* lines.

Supplemental Figure 10. *BnCCR1-2ox* and *BnCCR2-4ox* lines show different

growth behaviors and leaf vein strengths.

Supplemental Figure 11. ABA content is upregulated in leaves of *BnCCR1-2ox* and *BnCCR2-4ox* lines.

Supplemental Figure 12. Plants of both *BnCCR1-2ox* and *BnCCR2-4ox* do not show enhanced resistance to *S. sclerotiorum* and UV-B.

Supplemental Figure 13. GC-MS chromatograms show different changes of monolignol proportions in *BnCCR1-2ox* and *BnCCR2-4ox* lines.

Supplemental Figure 14. Contents of cellulose and hemicellulose in the stems of *BnCCR1-2ox* and *BnCCR2-4ox* lines are not changed based on NIRS detection.

Supplemental Figure 15. *BnCCR1* expression is obviously altered in *BnCCR2-4ox* lines, whereas *BnCCR2* expression has little change in *BnCCR1-2ox* lines.

Supplemental Figure 16. Mäule staining of stem sections indicates a trend of increase of S-type lignins during developmental process in *B. napus*.

Supplemental Figure 17. Leaf surfaces of *BnCCR1-2ox* and *BnCCR2-4ox* plants are less flat with decreased wax deposition than WT.

Supplemental Table 1. Identity parameters of *CCR1*-subfamily and *CCR2*-subfamily genes from *B. napus* and its parental species *B. oleracea* and *B. rapa*.

Supplemental Table 2. cDNA and gDNA basic parameters of *Brassica CCR1* and *CCR2* subfamily genes cloned in this study.

Supplemental Table 3. Basic parameters and important features of *Brassica*

CCR1 and CCR2 proteins.

Supplemental Table 4. S/G value of stem lignin, stem stiffness, and plant phenotype of different angiosperm species.

Supplemental Data Set 1. Contents of major soluble secondary metabolites differentially accumulated in stems and leaves of ox1-5 and ox2-16 compared with WT as revealed by UPLC-HESI-MS/MS.

Supplemental Data Set 2. Contents of major soluble secondary metabolites differentially accumulated in 30DAP seeds of ox1-5 and ox2-16 compared with WT as revealed by UPLC-HESI-MS/MS.

Supplemental Data Set 3. Contents of major soluble secondary metabolites differentially accumulated in petioles of ox1-5 and ox2-16 compared with WT as revealed by UPLC-HESI-MS/MS.

Supplemental Data Set 4. Primers used in this study.

Supplemental Data Set 5. Data of statistical analysis in this study (Student's *t*-test and ANOVA).

AUTHOR CONTRIBUTIONS

Y.C., J.L. and N.Y. designed the study; N.Y., B.L., X.L. and Y.X. performed the experiments; Y.C. did molecular and bioinformatic analysis, N.Y., J.L., M.C., K.L., L.W. and Y.L. analyzed or evaluated the results; J.L. and R.W. provided some *Brassica* materials. N.Y. and Y.C. performed final analysis and wrote the article.

ACKNOWLEDGEMENTS

We thank Prof Xuekuan Zhang for providing Zhongshuang 10 seeds, Prof Wei Qian for providing the *S. sclerotiorum* source strain, Prof Ningjia He, Dr.

Guangyu Ding and Dr. Shiyao Liu for assistance on GC-MS measurements. This research was supported by Natural Science Foundation of China (31871549, 32001579, 31830067 and 31171177), National Key R&D Program of China (2016YFD0100506), Special financial aid to post-doctor research fellow of Chongqing (XmT2018057), 111 Project (B12006), and Young Eagles Program of Chongqing Municipal Commission of Education (CY200215).

FIGURE LEGENDS

Figure 1. Phylogenetic analysis of CCR refseq_proteins from representative whole-genome-sequenced Malvids species including *B. napus, B. rapa* and *B. oleracea*.

Latin name, refseq_protein name and accession number are provided for each sequence. Names of cloned genes in this study are given after the accession numbers. Vertical bars on the right indicate corresponding order or order-family names.

Figure 2. Overall expression patterns of *CCR1*-subfamily and *CCR2*-subfamily show distinct organ-specificity and difference between black and yellow seeds in *B. napus*, *B. rapa* and *B. oleracea*.

5B, 09L597 and 09L598 are black-seed stocks, while 09L587, 09L600 and 09L599 are yellow-seed stocks, of *B. napus*, *B. rapa* and *B. oleracea*, respectively. The value (SEM in brackets) above the sRT-PCR band represents the relative expression level of qRT-PCR result. The expression level in root is set as 1.000 for quantification of other organs. Ro, roots; Hy, Hypocotyl; YS, young stems; OS, old stems; Co, cotyledons; Le, leaves; SP, silique pericarp; Fl, flowers; Bu, buds; 15D-55D, seeds of the corresponding days after pollination.

Figure 3. Overall expression of *BnCCR1*-subfamily and *BnCCR2*-subfamily distinctly respond to various stresses in *B. napus* seedlings.

The value (SEM in brackets) above the sRT-PCR band represents the relative expression level of qRT-PCR result. The expression level in the first sample is

set as 1.000 for quantification of other samples. m, minutes; D&HT, drought & high temperature.

Figure 4. Different phenotypic modifications in *BnCCR1-2ox* and *BnCCR2-4ox* plants.

(A) to **(M)** Plant phenotypes of different stages. Vegetative stage (**[A]** to **[D]**), middle-later bolting stage (**[E]** to **[G]**), flowering stage (**[H]** to **[J]**), harvest stage (**[K]** to **[M]**). Bending phenomenon of the upper stem of *BnCCR1-2ox* plants at late bolting stage **(F)** will disappear after flowering **(I)**.

(N) and **(O)** Root system at mature stage.

(P) and **(Q)** Root system of one-week old seedlings, and the investigated values with statistical significance. Data represent means ± SD of at least 5 biological replicates. Asterisks indicate that means differed significantly from WT values (*P < 0.05; **P < 0.01, Student's *t* tests).

(R) Siliques at mature stage, indicating the wider siliques of *BnCCR1-2ox* and *BnCCRR2-4ox* compared with WT. Bar = 1cm.

Figure 5. Yellow seeds from T3 plants of *BnCCR1-2ox* and *BnCCR2-4ox* in contrast with black seeds from WT plants.

(A) and **(B)** Seeds and seed coat cross-sections, highlighting the yellow-seed trait caused by seed color lightening by *CCR* overexpression. Bar = 50μm.

(C) Extractable insoluble condensed tannins from seed coat, showing deeper color of *BnCCR2-4ox* as compared with *BnCCR1-2ox* and WT which implies easier extraction.

(D) 1000 seeds weight; **(E)** seeds R value (higher value means deeper yellow color of the seeds coat); **(F)** glucosinolates content (μmol/g); **(G)** insoluble condensed tannins content of the seed coat. Data represent means ± SD of at least three biological replicates. Values are means ± SD of three biological replicates. Different letters behind the SD indicate statistically significant differences (one-way ANOVA, P < 0.05, Duncan's test).

Figure 6. *BnCCR1-2ox* and *BnCCR2-4ox* plants show differently fortified lignification patterns in various organs.

(A) to **(C)** Whole cross frozen stem-sections at early flowering stage (**[A]** and **[B]**), and whole cross free hand stem-section at harvesting stage **(C)**. **(A)** Mäule staning; **(B)** and **(C)** phloroglucinol-HCl staining. Bar = 2mm.

(D) to **(E)** Cross-sections at mature stage of roots with more interfascicular fibers **(D)** and less interfascicular fibers **(E)**, stained with phloroglucinol-HCl method. Bar = 500μm.

(F) to **(J)** Cross-sections of different parts of the stem at different developing stages. Middle-lower part of the stem at early flowering stage using Mäule staining with different amplification folds (**[F]** and **[G]**). Middle-lower part of the stem at mature stage with phloroglucinol-HCl staining **(H).** Autofluorescence of the middle stem at early flowering stage under UV light with different amplification folds (**[I]** and **[J]**)**.** if, interfascicular fiber; ph, phloem; pi, pith; xy, xylem. **(F)** and **(I)**, bar = 200μm; **(G)**, **(H)** and **(J)**, bar = 80μm.

(K) to **(N)** Silique wall cross-sections at mature stage. Whole sections **(K)**; Local sections (**[L]** to **[N]**)**. (K)** to **(L)** Phloroglucinol-HCl staining; **(M)** and **(N)** Autofluorescence viewed under UV light. **(K)**, bar = 500μm; **(L)** and **(M)**, bar = 100μm; **(N)**, bar = 50μm.

(O) to **(Q)** Cross sections of the middle petiole with different methods. The whole cross-sections without any treatment **(I)**; The vascular bundle with Mäule staining **(P)**; The autofluorescence of the vascular bundle under UV light **(Q)**; bar = 50μm. **(I)**, bar = 1000μm; **(P)**, bar = 100μm; **(Q)**, bar = 50μm.

Figure 7. Secondary metabolites are distinctly modified in stems of *BnCCR1-2ox* and *BnCCR2-4ox* plants.

Secondary metabolites were determined by UPLC-HESI-MS/MS. 1, 1-S-[(3S)-3-Hydroxy-N-(sulfooxy)-5-hexenimidoyl]-1-thio-beta-D-glucopyranose; 2, 3-butenyl glucosinolate; 3, 4-pentenyl glucosinolate-1; 4, 4-pentenyl glucosinolate-2; 5, km-3-O-sophoroside-7-O-glucoside; 6, 3-O-caffeoylquinic

acid; 7, qn-3-O-sophoroside; 8, sinapoylhexose; 9, sinapoyl malate.

Figure 8. Gene expression patterns of lignin, flavonoid and glucosinolate pathways are tremendously and differentially influenced in *BnCCR1-2ox* and *BnCCR2-4ox* plants.

(A) Transcript levels of the genes related to lignin biosynthesis in stems.

(B) Transcript levels of the genes related to flavonoid biosynthesis in seeds.

(C) Transcript levels of the genes related to glucosinolate biosynthesis in leaves. The *MYB29*, *CYP79F1* and *GSL* have no expression in WT, hence their expression level in *BnCCRox* is set relative to zero. The expression levels of other genes are set relative to WT. The yellow frame marks the genes involved in the synthesis of aliphatic glucosinolates. The red frame marks the genes involved in the synthesis of indole glucosinolates.

Figure 9. BnCCR1 and BnCCR2 play different roles in phenylpropanoid pathway.

The metabolic flux shifts in *BnCCR1-2ox* and *BnCCR2-4ox* plants are displayed in this map. The main route, which is conserved in angiosperms, is marked with the big background arrows (the general phenylpropanoid pathway is marked in light blue, while lignin-specific pathway is marked in brown). The blue arrows and names represent flux enhancement related to *BnCCR1-2ox*. Metabolites accumulation and related gene expression are increased in the stem of *BnCCR1-2ox*, indicating that overexpression of *BnCCR1* subfamily will significantly promote the biosynthesis of G and H lignin units. The purple arrows and names represent flux enhancement related to *BnCCR2-4ox*. Metabolites accumulation and related genes expression are increased in the stem of *BnCCR2-4ox*, indicating that overexpression of *BnCCR2* subfamily will significantly promote the biosynthesis of S lignin unit. The metabolites and the enzymes downregulated in both *BnCCR1-2ox* and *BnCCR2-4ox* plants are marked in green, whereas those with upregulation are in red. Unexpectedly,

glucosinolates deposition and pathway gene expression are significantly and differently remodeled in *BnCCR1-2ox* and *BnCCR2-4ox* plants. Dashed arrows represent unknown or unauthenticated routes. Arrows with a question mark are suggested pathways in this study. Two successive arrows represent two or more metabolic conversions.

The enzymes and their abbreviations are as follows: ANR, anthocyanidin reductase; ANS, anthocyanidin synthase; CAD, cinnamyl alcohol dehydrogenase; 4CL, 4-coumarate:CoA ligase; C3H, *p*-coumarate 3-hydroxylase; C4H, cinnamate 4-hydroxylase; CCoAOMT, caffeoyl-CoA O-methyltransferase; CCR, cinnamoyl-CoA reductase; CHI, chalcone isomerase; CHS, chalcone synthase; COMT, caffeic acid *O*-methyltransferase; CSE, caffeoyl shikimate esterase; DFR, dihydroflavonol 4-reductase; F3H, flavanone 3-hydroxylase; F3'H, flavonoid 3'-hydroxylase; F5H, ferulate 5-hydroxylase; FLS, flavonol synthase; HCALDH, hydroxycinnamaldehyde dehydrogenase; HCT, hydroxycinnamoyl-CoA:shikimate/quinic hydroxycinnamoyl transferase; LAC, laccase; LDOX, leucoanthocyanidin dioxygenase; Med: mediator; PAL, phenylalanine ammonia-lyase; PER, peroxidase; SGT, sinapate 1-glucosyltransferase; SMT, sinapoylglucose:malate sinapoyltransferase; SST, sinapoylglucose:sinapoylglucose sinapoylglucosetransferase; UGT, uridine diphosphate glycosyltransferase.

Table 1. Total lignin content of the main lignified organs of T2 generation plants.

Table 2. Lignin monomer compositions measurement of the T2 generation *BnCCR* overexpression representative lines.

REFERENCES

Abdulrazzak, N., Pollet, B., Ehlting, J., Larsen, K., Asnaghi, C., Ronseau, S., Proux, C., Erhardt, M., Seltzer, V., Renou, J.P., Ullmann, P., Pauly, M., Lapierre, C., and

Werck-Reichhart, D. (2006). A *coumaroyl-ester-3-hydroxylase* insertion mutant reveals the existence of nonredundant meta-hydroxylation pathways and essential roles for phenolic precursors in cell expansion and plant growth. Plant Physiol. **140,** 30-48.

Acreche, M.M., and Slafer, G.A. (2011). Lodging yield penalties as affected by breeding in Mediterranean wheats. Field Crop Res. **122,** 40-48.

Anderson, N.A., Tobimatsu, Y., Ciesielski, P.N., Ximenes, E., Ralph, J., Donohoe, B.S., Ladisch, M., and Chapple, C. (2015). Manipulation of guaiacyl and syringyl monomer biosynthesis in an arabidopsis *cinnamyl alcohol dehydrogenase* mutant results in atypical lignin biosynthesis and modified cell wall structure. Plant Cell **27,** 2195-2209.

Auger, B., Marnet, N., Gautier, V., Maia-Grondard, A., Leprince, F., Renard, M., Guyot, S., Nesi, N., and Routaboul, J.M. (2010). A detailed survey of seed coat flavonoids in developing seeds of *Brassica napus* L. J. Agr. Food Chem. **58,** 6246-6256.

Bart, R.S., Chern, M., Vega-Sanchez, M.E., Canlas, P., and Ronald, P.C. (2010). Rice *Snl6*, a *cinnamoyl-CoA reductase-like* gene family member, is required for *nh1*-mediated immunity to *Xanthomonas oryzae pv. oryzae*. Plos Genet. **6**. e1001123.

Baucher, M., Monties, B., Van Montagu, M., and Boerjan, W. (1998). Biosynthesis and genetic engineering of lignin. Crit. Rev. Plant Sci. **17,** 125-197.

Baucher, M., Halpin, C., Petit-Conil, M., and Boerjan, W. (2003). Lignin: Genetic engineering and impact on pulping. Crit. Rev. Biochem. Mol. **38,** 305-350.

Berry, P.M. (2018). Lodging resistance in cereals. In: Meyers R. (eds) Encyclopedia of Sustainability Science and Technology. Springer **New York,** NY. https://doi.org/10.1007/1978-1001-4939-2493-1006_1228-1003.

Berry, P.M., and Spink, J. (2012). Predicting yield losses caused by lodging in wheat. Field Crop Res. **137,** 19-26.

Berthet, S., Demont-Caulet, N., Pollet, B., Bidzinski, P., Cezard, L., Le Bris, P., Borrega, N., Herve, J., Blondet, E., Balzergue, S., Lapierre, C., and Jouanin, L. (2011). Disruption of *laccase4* and *17* results in tissue-specific alterations to lignification of *Arabidopsis thaliana* stems. Plant Cell **23,** 1124-1137.

Besseau, S., Hoffmann, L., Geoffroy, P., Lapierre, C., Pollet, B., and Legrand, M. (2007). Flavonoid accumulation in *Arabidopsis* repressed in lignin synthesis affects auxin transport and plant growth. Plant Cell **19,** 148-162.

Boerjan, W., Ralph, J., and Baucher, M. (2003). Lignin biosynthesis. Annu. Rev. Plant Biol. **54,** 519-546.

Caño-Delgado, A., Penfield, S., Smith, C., Catley, M., and Bevan, M. (2003). Reduced cellulose synthesis invokes lignification and defense responses in *Arabidopsis thaliana*. Plant J. **34,** 351-362.

Cardoza, V., and Stewart, C.N. (2003). Increased agrobacterium-mediated transformation and rooting efficiencies in canola (*Brassica napus* L.) from hypocotyl segment explants. Plant Cell Rep. **21,** 599-604.

Chabannes, M., Barakate, A., Lapierre, C., Marita, J.M., Ralph, J., Pean, M., Danoun, S., Halpin, C., Grima-Pettenati, J., and Boudet, A.M. (2001). Strong decrease in lignin content without significant alteration of plant development is induced by simultaneous down-regulation of *cinnamoyl CoA reductase* (*CCR*) and *cinnamyl alcohol dehydrogenase* (*CAD*) in tobacco plants. Plant J. **28,** 257-270.

Chang, X.F., Chandra, R., Berleth, T., and Beatson, R.P. (2008). Rapid, microscale, acetyl bromide-based method for high-throughput determination of lignin content in *Arabidopsis thaliana*. J. Agr. Food Chem. **56,** 6825-6834.

Chantreau, M., Portelette, A., Dauwe, R., Kiyoto, S., Cronier, D., Morreel, K., Arribat, S., Neutelings, G., Chabi, M., Boerjan, W., Yoshinaga, A., Mesnard, F., Grec, S., Chabbert, B., and Hawkins, S. (2014). Ectopic lignification in the flax *lignified bast fiber1* mutant stem is associated with tissue-specific modifications in gene expression and cell wall composition. Plant Cell **26,** 4462-4482.

Chao, N., Jiang, W.T., Wang, X.C., Jiang, X.N., and Gai, Y. (2019). Novel motif is capable of determining CCR and CCR-like proteins based on the divergence of CCRs in plants. Tree Physiol. **39,** 2019-2026.

Chao, N., Li, N., Qi, Q., Li, S., Lv, T., Jiang, X.N., and Gai, Y. (2017). Characterization of the *cinnamoyl-CoA reductase* (*CCR*) gene family in *Populus tomentosa* reveals the enzymatic active sites and evolution of CCR. Planta **245,** 61-75.

Chapple, C.C.S., Vogt, T., Ellis, B.E., and Somerville, C.R. (1992). An *Arabidopsis* mutant defective in the general phenylpropanoid pathway. Plant Cell **4,** 1413-1424.

Chen, H., Nelson, R.S., and Sherwood, J.L. (1994). Enhanced recovery of transformants of agrobacterium-tumefaciens after freeze-thaw transformation and drug selection. Biotechniques **16,** 664-&.

Chen, L., Auh, C., Chen, F., Cheng, X.F., Aljoe, H., Dixon, R.A., and Wang, Z.Y. (2002). Lignin deposition and associated changes in anatomy, enzyme activity, gene expression, and ruminal degradability in stems of tall fescue at different developmental stages. J. Agr. Food Chem. **50,** 5558-5565.

Costa, S., and Dolan, L. (2003). Epidermal patterning genes are active during embryogenesis in *Arabidopsis*. Development **130,** 2893-2901.

Cutler, S.R., Rodriguez, P.L., Finkelstein, R.R., and Abrams, S.R. (2010). Abscisic acid: emergence of a core signaling network. Annu. Rev. Plant Biol., **61,** 651-679.

Dauwe, R., Morreel, K., Goeminne, G., Gielen, B., Rohde, A., Van Beeumen, J., Ralph, J., Boudet, A.M., Kopka, J., Rochange, S.F., Halpin, C., Messens, E., and Boerjan, W. (2007). Molecular phenotyping of lignin-modified tobacco reveals associated changes in cell-wall metabolism, primary metabolism, stress metabolism and photorespiration. Plant J. **52**, 263-285.

De Meester, B., Calderón, B.M., de Vries, L., Pollier, J., Goeminne, G., Van Doorsselaere, J., Chen, M., Ralph, J., Vanholme, R., and Boerjan, W. (2020). Tailoring poplar lignin without yield penalty by combining a null and haploinsufficient *CINNAMOYL-CoA REDUCTASE2* allele. Nat. Commun. **11,** 1-13.

De Meester, B., de Vries, L., Ozparpucu, M., Gierlinger, N., Corneillie, S., Pallidis, A., Goeminne, G., Morreel, K., De Bruyne, M., De Rycke, R., Vanholme, R., and Boerjan, W. (2018). Vessel-specific reintroduction of *CINNAMOYL-COA REDUCTASE1* (*CCR1*) in dwarfed *ccr1* mutants restores vessel and xylary fiber integrity and increases biomass. Plant Physiol. **176,** 611-633.

del Río, L.E., Bradley, C.A., Henson, R.A., Endres, G.J., Hanson, B.K., Mckay, K., Halvorson, M., Porter, P.M., Le Gare, D.G., and Lamey, H.A. (2007). Impact of *Sclerotinia* stem rot on yield of canola. Plant Dis. **91,** 191-194.

Derikvand, M.M., Sierra, J.B., Ruel, K., Pollet, B., Do, C.T., Thevenin, J., Buffard, D., Jouanin, L., and Lapierre, C. (2008). Redirection of the phenylpropanoid pathway to feruloyl malate in *Arabidopsis* mutants deficient for cinnamoyl-CoA reductase 1. Planta **227,** 943-956.

Ding, Y.J., Mei, J.Q., Liu, Y., Wang, L., Li, Y.H., Wan, H.F., Li, J.N., and Qian, W. (2015). Transfer of sclerotinia stem rot resistance from wild *Brassica oleracea* into *B. rapa*. Mol. Breeding **35**.

Do, C.T., Pollet, B., Thevenin, J., Sibout, R., Denoue, D., Barriere, Y., Lapierre, C., and Jouanin, L. (2007). Both caffeoyl Coenzyme A 3-O-methyltransferase 1 and caffeic acid O-methyltransferase 1 are involved in redundant functions for lignin, flavonoids and sinapoyl malate biosynthesis in *Arabidopsis*. Planta **226,** 1117-1129.

Escamilla-Treviño, L.L., Shen, H., Uppalapati, S.R., Ray, T., Tang, Y.H., Hernandez, T., Yin, Y.B., Xu, Y., and Dixon, R.A. (2010). Switchgrass (*Panicum virgatum*) possesses a divergent family of cinnamoyl CoA reductases with distinct biochemical properties. New Phytol. **185,** 143-155.

Fan, B., Hu, S., Lu, H., and Jiang, X. (2006). Soluble prokaryotic expression of *4-coumarate: coenzyme A ligase* from *Populus tomentosa* and enzyme activity of recombinant 4CL1. Journal-Beijing Forestry University-Chinese Edition- **28,** 1-8.

Fornalé, S., Rencoret, J., Garcia-Calvo, L., Capellades, M., Encina, A., Santiago, R., Rigau, J., Gutierrez, A., del Rio, J.C., and Caparros-Ruiz, D. (2015). Cell wall modifications triggered by the down-regulation of *Coumarate 3-hydroxylase-1* in maize. Plant Sci. **236,** 272-282.

Franke, R., Hemm, M.R., Denault, J.W., Ruegger, M.O., Humphreys, J.M., and Chapple, C. (2002). Changes in secondary metabolism and deposition of an unusual lignin in the *ref8* mutant of *Arabidopsis*. Plant J. **30,** 47-59.

Fraser, C.M., and Chapple, C. (2011). The phenylpropanoid pathway in *Arabidopsis*. The Arabidopsis book / American Society of Plant Biologists **9,** e0152.

Friedt, W., and Snowdon, R. (2009). Oilseed rape. In Oil crops (Springer), pp. 91-126.

Fu, C., Chai, Y.R., Ma, L.J., Wang, R., Hu, K., Wu, J.Y., Li, J.N., Liu, X., and Lu, J.X. (2017). Evening primrose (*Oenothera biennis*) Δ6 fatty acid desaturase gene family: cloning, characterization, and engineered GLA and SDA production in a staple oil crop. Mol Breeding **37**(6), 83.

Fukushima, R.S., and Hatfield, R.D. (2001). Extraction and isolation of lignin for utilization as a standard to determine lignin concentration using the acetyl bromide spectrophotometric method. J. Agr. Food Chem. **49,** 3133-3139.

Giordano, A., Liu, Z.Q., Panter, S.N., Dimech, A.M., Shang, Y.J., Wijesinghe, H., Fulgueras, K., Ran, Y.D., Mouradov, A., Rochfort, S., Patron, N.J., and Spangenberg, G.C. (2014). Reduced lignin content and altered lignin composition in the warm season forage grass *Paspalum dilatatum* by down-regulation of a *Cinnamoyl CoA Reductase* Gene. Transgenic Res. **23,** 503-517.

Goujon, T., Ferret, V., Mila, I., Pollet, B., Ruel, K., Burlat, V., Joseleau, J.P., Barriere, Y., Lapierre, C., and Jouanin, L. (2003). Down-regulation of the *AtCCR1* gene in *Arabidopsis thaliana*: effects on phenotype, lignins and cell wall degradability. Planta **217,** 218-228.

Gui, J.S., Luo, L.F., Zhong, Y., Sun, J.Y., Umezawa, T., and Li, L.G. (2019). Phosphorylation

of LTF1, an MYB transcription factor in *Populus*, acts as a sensory switch regulating lignin biosynthesis in wood cells. Mol. Plant **12,** 1325-1337.

Hemm, M.R., Ruegger, M.O., and Chapple, C. (2003). The *Arabidopsis ref2* mutant is defective in the gene encoding CYP83A1 and shows both phenylpropanoid and glucosinolate phenotypes. Plant Cell **15,** 179-194.

Hoffmann, L., Besseau, S., Geoffroy, P., Ritzenthaler, C., Meyer, D., Lapierre, C., Pollet, B., and Legrand, M. (2004). Silencing of hydroxycinnamoyl-coenzyme A shikimate/quinate hydroxycinnamoyltransferase affects phenylpropanoid biosynthesis. Plant Cell **16,** 1446-1465.

Huang, H.H., Xu, L.L., Tong, Z.K., Lin, E.P., Liu, Q.P., Cheng, L.J., and Zhu, M.Y. (2012). De novo characterization of the Chinese fir (*Cunninghamia lanceolata*) transcriptome and analysis of candidate genes involved in cellulose and lignin biosynthesis. BMC Genomics **13**, 648.

Huang, J.L., Gu, M., Lai, Z.B., Fan, B.F., Shi, K., Zhou, Y.H., Yu, J.Q., and Chen, Z.X. (2010). Functional analysis of the *Arabidopsis PAL* gene family in plant growth, development, and response to environmental stress. Plant Physiol. **153,** 1526-1538.

Jensen, L.M., Jepsen, H.S.K., Halkier, B.A., Kliebenstein, D.J., and Burow, M. (2015). Natural variation in cross-talk between glucosinolates and onset of flowering in Arabidopsis. Front Plant Sci **6**, 697.

Jones, L., Ennos, A.R., and Turner, S.R. (2001). Cloning and characterization of irregular xylem4 (*irx4*): a severely lignin-deficient mutant of Arabidopsis. Plant J. **26,** 205-216.

Kaur, H., Shaker, K., Heinzel, N., Ralph, J., Galis, I., and Baldwin, I.T. (2012). Environmental stresses of field growth allow cinnamyl alcohol dehydrogenase-deficient *Nicotiana attenuata* plants to compensate for their structural deficiencies. Plant Physiol. **159,** 1545-1570.

Kawasaki, T., Koita, H., Nakatsubo, T., Hasegawa, K., Wakabayashi, K., Takahashi, H., Urnemura, K., Urnezawa, T., and Shimamoto, K. (2006). Cinnamoyl-CoA reductase, a key enzyme in lignin biosynthesis, is an effector of small GTPase Rac in defense signaling in rice. P. Natl. Acad. Sci. USA **103,** 230-235.

Kendall, S.L., Holmes, H., White, C.A., Clarke, S.M., and Berry, P.M. (2017). Quantifying lodging-induced yield losses in oilseed rape. Field Crop Res. **211,** 106-113.

Kim, J.I., Dolan, W.L., Anderson, N.A., and Chapple, C. (2015). Indole glucosinolate biosynthesis limits phenylpropanoid accumulation in *Arabidopsis thaliana*. Plant Cell **27,** 1529-1546.

Kim, J.I., Zhang, X., Pascuzzi, P.E., Liu, C.J., and Chapple, C. (2020). Glucosinolate and phenylpropanoid biosynthesis are linked by proteasome-dependent degradation of PAL. New Phytol. **225,** 154-168.

Ko, J.K., Ximenes, E., Kim, Y., and Ladisch, M.R. (2015). Adsorption of enzyme onto lignins of liquid hot water pretreated hardwoods. Biotechnol Bioeng. **112,** 447-456.

Koch, S., Dunker, S., Kleinhenz, B., Rohrig, M., and von Tiedemann, A. (2007). Crop loss-related forecasting model for *Sclerotinia* stem rot in winter oilseed rape. Phytopathology **97,** 1186-1194.

Labeeuw, L., Martone, P.T., Boucher, Y., and Case, R.J. (2015). Ancient origin of the biosynthesis of lignin precursors. Biol. Direct **10**, 23.

Lacombe, E., Hawkins, S., VanDoorsselaere, J., Piquemal, J., Goffner, D., Poeydomenge, O., Boudet, A.M., and GrimaPettenati, J. (1997). Cinnamoyl CoA reductase, the first committed enzyme of the lignin branch biosynthetic pathway: Cloning, expression and phylogenetic relationships. Plant J. **11,** 429-441.

Lapierre, C., Pollet, B., and Rolando, C. (1995). New insights into the molecular architecture of hardwood lignins by chemical degradative methods. Res. Chem. Intermediat. **21,** 397-412.

Lauvergeat, V., Lacomme, C., Lacombe, E., Lasserre, E., Roby, D., and Grima-Pettenati, J. (2001). Two *cinnamoyl-CoA reductase* (*CCR*) genes from *Arabidopsis thaliana* are differentially expressed during development and in response to infection with pathogenic bacteria. Phytochemistry **57,** 1187-1195.

Lee, M.H., Jeon, H.S., Kim, S.H., Chung, J.H., Roppolo, D., Lee, H.J., Cho, H.J., Tobimatsu, Y., Ralph, J., and Park, O.K. (2019). Lignin-based barrier restricts pathogens to the infection site and confers resistance in plants. Embo J. **38**, e101948.

Leplé, J.C., Dauwe, R., Morreel, K., Storme, V., Lapierre, C., Pollet, B., Naumann, A., Kang, K.Y., Kim, H., Ruel, K., Lefebvre, A., Joseleau, J.P., Grima-Pettenati, J., De Rycke, R., Andersson-Gunneras, S., Erban, A., Fehrle, I., Petit-Conil, M., Kopka, J., Polle, A., Messens, E., Sundberg, B., Mansfield, S.D., Ralph, J., Pilate, G., and Boerjan, W. (2007). Downregulation of cinnamoyl-coenzyme a reductase in poplar: Multiple-level phenotyping reveals effects on cell wall polymer metabolism and structure. Plant Cell **19,** 3669-3691.

Li, J.Q., Fan, F.F., Wang, L.H., Zhan, Q.W., Wu, P.J., Du, J.L., Yang, X.C., and Liu, Y.L. (2016). Cloning and expression analysis of *cinnamoyl-CoA reductase* (*CCR*) genes in sorghum. PeerJ **4**, e2005.

Li, X., Weng, J.K., and Chapple, C. (2008). Improvement of biomass through lignin modification. Plant J. **54,** 569-581.

Li, X., Bonawitz, N.D., Weng, J.K., and Chapple, C. (2010). The growth reduction associated with repressed lignin biosynthesis in *Arabidopsis thaliana* is independent of flavonoids. Plant Cell **22,** 1620-1632.

Lin, L.Z., Sun, J.H., Chen, P., and Harnly, J. (2011). UHPLC-PDA-ESI/HRMS/MSn analysis of anthocyanins, flavonol glycosides, and hydroxycinnamic acid derivatives in red mustard greens (*Brassica juncea* Coss Variety). J. Agr. Food Chem. **59,** 12059-12072.

Liu, C., Wang, J.L., Huang, T.D., Wang, F., Yuan, F., Cheng, X.M., Zhang, Y., Shi, S.W., Wu, J.S., and Liu, K.D. (2010). A missense mutation in the VHYNP motif of a DELLA protein causes a semi-dwarf mutant phenotype in *Brassica napus*. Theor. Appl. Genet. **121,** 249-258.

Liu, H., Yang, Q.Y., Fan, C.C., Zhao, X.Q., Wang, X.M., and Zhou, Y.M. (2015). Transcriptomic basis of functional difference and coordination between seeds and the silique wall of *Brassica napus* during the seed-filling stage. Plant Sci. **233,** 186-199.

Liu, L.Z., Stein, A., Wittkop, B., Sarvari, P., Li, J.N., Yan, X.Y., Dreyer, F., Frauen, M., Friedt, W., and Snowdon, R.J. (2012). A knockout mutation in the lignin biosynthesis gene *CCR1* explains a major QTL for acid detergent lignin content in *Brassica napus* seeds. Theor. Appl. Genet. **124,** 1573-1586.

Lomascolo, A., Uzan-Boukhris, E., Sigoillot, J.C., and Fine, F. (2012). Rapeseed and

sunflower meal: a review on biotechnology status and challenges. Appl. Microbiol. Biot. **95,** 1105-1114.

Ma, Q.H. (2009). The expression of *caffeic acid 3-O-methyltransferase* in two wheat genotypes differing in lodging resistance. J. Exp. Bot. **60,** 2763-2771.

Mei, J., Qian, L., Disi, J.O., Yang, X., Li, Q., Li, J., Frauen, M., Cai, D., and Qian, W. (2011). Identification of resistant sources against *Sclerotinia sclerotiorum* in *Brassica* species with emphasis on *B. oleracea*. Euphytica **177,** 393-399.

Mohammadin, S., Nguyen, T.P., van Weij, M.S., Reichelt, M., and Schranz, M.E. (2017). Flowering locus C (FLC) is a potential major regulator of glucosinolate content across developmental stages of *Aethionema arabicum* (Brassicaceae). Front Plant Sci. **8**, 876.

Moura, J.C.M.S., Bonine, C.A.V., Viana, J.D.F., Dornelas, M.C., and Mazzafera, P. (2010). Abiotic and biotic stresses and changes in the lignin content and composition in plants. J. Integr. Plant Biol. **52,** 360-376.

Naczk, M., Amarowicz, R., Pink, D., and Shahidi, F. (2000). Insoluble condensed tannins of canola/rapeseed. J. Agr. Food Chem. **48,** 1758-1762.

Nakashima, J., Chen, F., Jackson, L., Shadle, G., and Dixon, R.A. (2008). Multi-site genetic modification of monolignol biosynthesis in alfalfa (*Medicago sativa*): effects on lignin composition in specific cell types. New Phytol. **179,** 738-750.

Pan, L.G., Assirelli, A., Suardi, A., Civitarese, V., Del Giudice, A., Costa, C., and Santangelo, E. (2012). The harvest of oilseed rape (*Brassica napus* L.): The effective yield losses at on-farm scale in the Italian area. Biomass Bioenerg. **46,** 453-458.

Patten, A.M., Cardenas, C.L., Cochrane, F.C., Laskar, D.D., Bedgar, D.L., Davin, L.B., and Lewis, N.G. (2005). Reassessment of effects on lignification and vascular development in the *irx4 Arabidopsis* mutant. Phytochemistry **66,** 2092-2107.

Peng, D.L., Chen, X.G., Yin, Y.P., Lu, K.L., Yang, W.B., Tang, Y.H., and Wang, Z.L. (2014). Lodging resistance of winter wheat (*Triticum aestivum* L.): Lignin accumulation and its related enzymes activities due to the application of paclobutrazol or gibberellin acid. Field Crop Res. **157,** 1-7.

Piquemal, J., Lapierre, C., Myton, K., O'Connell, A., Schuch, W., Grima-Pettenati, J., and Boudet, A.M. (1998). Down-regulation of *cinnamoyl-CoA reductase* induces significant changes of lignin profiles in transgenic tobacco plants. Plant J. **13,** 71-83.

Porebski, S., Bailey, L.G., and Baum, B.R. (1997). Modification of a CTAB DNA extraction protocol for plants containing high polysaccharide and polyphenol components. Plant Mol. Biol. Rep. **15,** 8-15.

Prashant, S., Sunita, M.S., Pramod, S., Gupta, R.K., Kumar, S.A., Karumanchi, S.R., Rawal, S.K., and Kishor, P.B.K. (2011). Down-regulation of *Leucaena leucocephala* cinnamoyl CoA reductase *(LlCCR*) gene induces significant changes in phenotype, soluble phenolic pools and lignin in transgenic tobacco. Plant Cell Rep. **30,** 2215-2231.

Qu, C.M., Fu, F.Y., Lu, K., Zhang, K., Wang, R., Xu, X.F., Wang, M., Lu, J.X., Wan, H.F., Tang, Z.L., and Li, J.N. (2013). Differential accumulation of phenolic compounds and expression of related genes in black- and yellow-seeded *Brassica napus*. J. Exp. Bot. **64,** 2885-2898.

Ragauskas, A.J., Williams, C.K., Davison, B.H., Britovsek, G., Cairney, J., Eckert, C.A., Frederick, W.J., Hallett, J.P., Leak, D.J., Liotta, C.L., Mielenz, J.R., Murphy, R., Templer,

R., and Tschaplinski, T. (2006). The path forward for biofuels and biomaterials. Science **311,** 484-489.

Ralph, J., Kim, H., Lu, F., Grabber, J.H., Leple, J.C., Berrio-Sierra, J., Derikvand, M.M., Jouanin, L., Boerjan, W., and Lapierre, C. (2008). Identification of the structure and origin of a thioacidolysis marker compound for ferulic acid incorporation into angiosperm lignins (and an indicator for cinnamoyl CoA reductase deficiency). Plant J. **53,** 368-379.

Robinson, A.R., and Mansfield, S.D. (2009). Rapid analysis of poplar lignin monomer composition by a streamlined thioacidolysis procedure and near-infrared reflectance-based prediction modeling. Plant J. **58,** 706-714.

Rochfort, S.J., Imsic, M., Jones, R., Trenerry, V.C., and Tomkins, B. (2006). Characterization of flavonol conjugates in immature leaves of pak choi [*Brassica rapa* L. ssp *chinensis* L. (Hanelt.)] by HPLC-DAD and LC-MS/MS. J. Agr. Food Chem. **54,** 4855-4860.

Ruel, K., Berrio-Sierra, J., Derikvand, M.M., Pollet, B., Thevenin, J., Lapierre, C., Jouanin, L., and Joseleau, J.P. (2009). Impact of *CCR1* silencing on the assembly of lignified secondary walls in *Arabidopsis thaliana*. New Phytol. **184,** 99-113.

Saghaimaroof, M.A., Soliman, K.M., Jorgensen, R.A., and Allard, R.W. (1984). Ribosomal DNA spacer-length polymorphisms in barley: Mendelian inheritance, chromosomal location, and population-dynamics. P. Natl. Acad. Sci-Biol. **81,** 8014-8018.

Schilmiller, A.L., Stout, J., Weng, J.K., Humphreys, J., Ruegger, M.O., and Chapple, C. (2009). Mutations in the cinnamate 4-hydroxylase gene impact metabolism, growth and development in *Arabidopsis*. Plant J. **60,** 771-782.

Shao, Y.L., Jiang, J.J., Ran, L.P., Lu, C.L., Wei, C.X., and Wang, Y.P. (2014). Analysis of flavonoids and hydroxycinnamic acid derivatives in rapeseeds (*Brassica napus* L. var. *napus*) by HPLC-PDA-ESI(-)-MSn/HRMS. J. Agr. Food Chem. **62,** 2935-2945.

Sibout, R., Eudes, A., Mouille, G., Pollet, B., Lapierre, C., Jouanin, L., and Seguin, A. (2005). *CINNAMYL ALCOHOL DEHYDROGENASE-C* and *-D* are the primary genes involved in lignin biosynthesis in the floral stem of *Arabidopsis*. Plant Cell **17,** 2059-2076.

Tamasloukht, B., Lam, M.S.J.W.Q., Martinez, Y., Tozo, K., Barbier, O., Jourda, C., Jauneau, A., Borderies, G., Balzergue, S., Renou, J.P., Huguet, S., Martinant, J.P., Tatout, C., Lapierre, C., Barriere, Y., Goffner, D., and Pichon, M. (2011). Characterization of a *cinnamoyl-CoA reductase 1* (*CCR1*) mutant in maize: effects on lignification, fibre development, and global gene expression. J. Exp. Bot. **62,** 3837-3848.

Thévenin, J., Pollet, B., Letarnec, B., Saulnier, L., Gissot, L., Maia-Grondard, A., Lapierre, C., and Jouanin, L. (2011). The simultaneous repression of CCR and CAD, two enzymes of the lignin biosynthetic pathway, results in sterility and dwarfism in *Arabidopsis thaliana*. Mol. Plant **4,** 70-82.

Tian, X.M., Xie, J., Zhao, Y.L., Lu, H., Liu, S.C., Qu, L., Li, J.M., Gai, Y., and Jiang, X.N. (2013). Sense-, antisense- and RNAi-*4CL1* regulate soluble phenolic acids, cell wall components and growth in transgenic *Populus tomentosa* Carr. Plant Physiol. Bioch. **65,** 111-119.

Tohge, T., Nishiyama, Y., Hirai, M.Y., Yano, M., Nakajima, J., Awazuhara, M., Inoue, E., Takahashi, H., Goodenowe, D.B., Kitayama, M., Noji, M., Yamazaki, M., and Saito, K. (2005). Functional genomics by integrated analysis of metabolome and transcriptome of *Arabidopsis* plants over-expressing an MYB transcription factor. Plant J. **42,** 218-235.

Tongyan, W., Lingqin, X., and Xueju, Y. (2002). Study on the correlations between the components of the plant height and the yield and other traits of wheat. Journal of Agricultural University of Hebei (China), **25**, 10-12,18.

Tu, Y., Rochfort, S., Liu, Z.Q., Ran, Y.D., Griffith, M., Badenhorst, P., Louie, G.V., Bowman, M.E., Smith, K.F., Noel, J.P., Mouradov, A., and Spangenberg, G. (2010). Functional analyses of *caffeic acid O-methyltransferase* and *cinnamoyl-CoA-reductase* genes from perennial ryegrass *(Lolium perenne*). Plant Cell **22,** 3357-3373.

Van Acker, R., Leple, J.C., Aerts, D., Storme, V., Goeminne, G., Ivens, B., Legee, F., Lapierre, C., Piens, K., Van Montagu, M.C.E., Santoro, N., Foster, C.E., Ralph, J., Soetaert, W., Pilate, G., and Boerjan, W. (2014). Improved saccharification and ethanol yield from field-grown transgenic poplar deficient in cinnamoyl-CoA reductase. P. Natl. Acad. Sci. USA **111,** 845-850.

van der Rest, B., Danoun, S., Boudet, A.M., and Rochange, S.F. (2006). Down-regulation of cinnamoyl-CoA reductase in tomato (*Solanum lycopersicum* L.) induces dramatic changes in soluble phenolic pools. J. Exp. Bot. **57,** 1399-1411.

Vanholme, R., Demedts, B., Morreel, K., Ralph, J., and Boerjan, W. (2010). Lignin biosynthesis and structure. Plant Physiol. **153,** 895-905.

Vanholme, R., Storme, V., Vanholme, B., Sundin, L., Christensen, J.H., Goeminne, G., Halpin, C., Rohde, A., Morreel, K., and Boerjan, W. (2012). A systems biology view of responses to lignin biosynthesis perturbations in *Arabidopsis*. Plant Cell **24,** 3506-3529.

Vanholme, R., Cesarino, I., Rataj, K., Xiao, Y.G., Sundin, L., Goeminne, G., Kim, H., Cross, J., Morreel, K., Araujo, P., Welsh, L., Haustraete, J., McClellan, C., Vanholme, B., Ralph, J., Simpson, G.G., Halpin, C., and Boerjan, W. (2013). Caffeoyl shikimate esterase (CSE) is an enzyme in the lignin biosynthetic pathway in *Arabidopsis*. Science **341,** 1103-1106.

Vermerris, W., Thompson, K.J., McIntyre, L.M., and Axtell, J.D. (2002). Evidence for an evolutionarily conserved interaction between cell wall biosynthesis and flowering in maize and sorghum. BMC Evol. Biol. **2**, 1-8.

Voelker, S.L., Lachenbruch, B., Meinzer, F.C., Jourdes, M., Ki, C.Y., Patten, A.M., Davin, L.B., Lewis, N.G., Tuskan, G.A., Gunter, L., Decker, S.R., Selig, M.J., Sykes, R., Himmel, M.E., Kitin, P., Shevchenko, O., and Strauss, S.H. (2010). Antisense down-regulation of *4CL* expression alters lignification, tree growth, and saccharification potential of field-grown poplar. Plant Physiol. **154,** 874-886.

Vogt, T. (2010). Phenylpropanoid biosynthesis. Mol. Plant **3,** 2-20.

Wagner, A., Tobimatsu, Y., Goeminne, G., Phillips, L., Flint, H., Steward, D., Torr, K., Donaldson, L., Boerjan, W., and Ralph, J. (2013). Suppression of *CCR* impacts metabolite profile and cell wall composition in *Pinus radiata* tracheary elements. Plant Mol. Biol. **81,** 105-117.

Weng, J.K., and Chapple, C. (2010). The origin and evolution of lignin biosynthesis. New Phytol. **187,** 273-285.

Weng, J.K., Mo, H.P., and Chapple, C. (2010). Over-expression of *F5H* in *COMT*-deficient *Arabidopsis* leads to enrichment of an unusual lignin and disruption of pollen wall formation. Plant J. **64,** 898-911.

Weng, J.K., Akiyama, T., Ralph, J., and Chapple, C. (2011). Independent recruitment of an O-methyltransferase for syringyl lignin biosynthesis in *Selaginella moellendorffii*. Plant Cell

23, 2708-2724.

Xue, J.S., Luo, D.X., Xu, D.Y., Zeng, M.H., Cui, X.F., Li, L.G., and Huang, H. (2015). CCR1, an enzyme required for lignin biosynthesis in *Arabidopsis*, mediates cell proliferation exit for leaf development. Plant J. **83,** 375-387.

Yang, H., Li, J.W., Yang, J.P., Wang, H., Zou, J.L., and He, J.J. (2014). Effects of nitrogen application rate and leaf age on the distribution pattern of leaf SPAD readings in the rice canopy. Plos One **9**, e88421.

Yosef, E., and Ben-Ghedalia, D. (1999). Changes in thioacidolysis products of lignin in wheat straw as affected by SO_2 treatment and passage through the gastro-intestine of sheep. Anim. Feed Sci. Tech. **80,** 55-65.

Zhang, G.P., Chen, J.X., and Bull, D.A. (2001). The effects of timing of N application and plant growth regulators on morphogenesis and yield formation in wheat. Plant Growth Regul. **35,** 239-245.

Zhang, K., Lu, K., Qu, C.M., Liang, Y., Wang, R., Chai, Y.R., and Li, J.N. (2013). Gene silencing of *BnTT10* family genes causes retarded pigmentation and lignin reduction in the seed coat of *Brassica napus*. Plos One **8**, e61247.

Zhang, W.B., Wei, R., Chen, S., Jiang, J., Li, H.Y., Huang, H.J., Yang, G., Wang, S., Wei, H.R., and Liu, G.F. (2015). Functional characterization of *CCR* in birch (*Betula platyphylla* x *Betula pendula*) through overexpression and suppression analysis. Physiol. Plantarum **154,** 283-296.

Zhao, J., Wang, J., An, L., Doerge, R., Chen, Z.J., Grau, C.R., Meng, J., and Osborn, T.C. (2007a). Analysis of gene expression profiles in response to *Sclerotinia sclerotiorum* in *Brassica napus*. Planta **227,** 13-24.

Zhao, Q., Tobimatsu, Y., Zhou, R., Pattathil, S., Gallego-Giraldo, L., Fu, C., Jackson, L.A., Hahn, M.G., Kim, H., Chen, F., Ralph, J., and Dixon, R.A. (2013). Loss of function of cinnamyl alcohol dehydrogenase 1 leads to unconventional lignin and a temperature-sensitive growth defect in *Medicago truncatula*. P. Natl. Acad. Sci. USA **110,** 13660-13665.

Zhao, X.Y., Yu, X.H., Foo, E., Symons, G.M., Lopez, J., Bendehakkalu, K.T., Xiang, J., Weller, J.L., Liu, X.M., Reid, J.B., and Lin, C.T. (2007b). A study of gibberellin homeostasis and cryptochrome-mediated blue light inhibition of hypocotyl elongation. Plant Physiol. **145,** 106-118.

Zhou, R., Jackson, L., Shadle, G., Nakashima, J., Temple, S., Chen, F., and Dixon, R.A. (2010). Distinct cinnamoyl CoA reductases involved in parallel routes to lignin in *Medicago truncatula*. P. Natl. Acad. Sci. USA **107,** 17803-17808.

Zuber, U., Winzeler, H., Messmer, M.M., Keller, M., Keller, B., Schmid, J.E., and Stamp, P. (1999). Morphological traits associated with lodging resistance of spring wheat (*Triticum aestivum* L.). J. Agron. Crop. Sci. **182,** 17-24.

Table 1. Total lignin content of the main lignified organs of T2 generation plants.

lines	AcBr lignin in stem (CWR%)	AcBr lignin in root (CWR%)	AcBr lignin in seed coat (CWR%)
WT	12.71 ± 1.24 f	15.68 ± 0.37 e	2.51 ± 0.17 f
ox1-5	15.75 ± 0.79 d	15.74 ± 0.89 e	3.97 ± 0.12 d
ox1-8	17.00 ± 0.33 bc	18.42 ± 1.54 abc	2.86 ± 0.20 e
ox1-12	15.65 ± 0.27 d	17.99 ± 0.67 bc	3.15 ± 0.12 e
ox1-14	14.61 ± 0.44 e	16.44 ± 0.52 de	2.33 ± 0.19 f
ox2-4	17.75 ± 0.46 b	18.49 ± 0.81 abc	5.60 ± 0.15 a
ox2-11	15.93 ± 0.90 d	19.54 ± 1.85 a	5.23 ± 0.19 b
ox2-16	16.68 ± 1.75 cd	17.52 ± 1.33 cd	5.63 ± 0.20 a
ox2-25	19.21 ± 0.31 a	19.35 ± 0.41 ab	4.77 ± 0.35 c

Lignin analysis was carried out by AcBr method. CWR, cell wall residue. Values are means ± SD of at least 3 biological replicates. Different letters behind the SD indicate statistically significant differences (one-way ANOVA, $P < 0.05$, Duncan's test).

Table 2. Lignin monomer compositions measurement of the T2 generation *BnCCR* overexpression representative lines.

Lines	H+G+S (μmol/g dry cell wall residues)	H%	G%	S%	S/G
WT stem	484.05 ± 90.4 a	0.83 ± 0.08 a	43.35 ± 0.25 b	55.82 ± 0.26 c	1.29 ± 0.01 c
ox1-5 stem	553.15 ± 37.27 a	3.29 ± 1.29 b	57.66 ± 2.84 d	39.05 ± 1.65 a	0.68 ± 0.06 a
ox1-12 stem	563.94 ± 16.49 a	2.78 ± 0.12 b	48.99 ± 0.43 c	48.23 ± 0.31 b	0.98 ± 0.01 b
ox2-4 stem	592.14 ± 87.53 a	1.32 ± 0.06 a	38.72 ± 0.64 a	59.97 ± 0.66 d	1.55 ± 0.04 d
ox2-16 stem	619.84 ± 35.11 a	1.21 ± 0.27 a	38.32 ± 0.92 a	60.47 ± 1.18 d	1.58 ±0.07 d
WT root	180.5 ± 8.22 a	7.43 ± 0.67 a	62.28 ± 2.68 b	30.29 ± 2.24 b	0.49 ± 0.06 b
ox1-5 root	170.84 ± 9.43 a	15.59 ± 0.42 b	69.34 ± 3.25 b	15.07 ± 2.83 a	0.22 ± 0.05 a
ox2-16 root	302.08 ± 25.64 b	6.71 ± 0.77 a	52.46 ± 3.19 a	40.83 ± 2.63 c	0.78 ± 0.10 c

Lignin monomer compositions were measured by thioacidolysis method. Values are means ± SD of at least 3 biological replicates. Different letters behind the SD indicate statistically significant differences (one-way ANOVA, $P < 0.05$, Tukey's test).

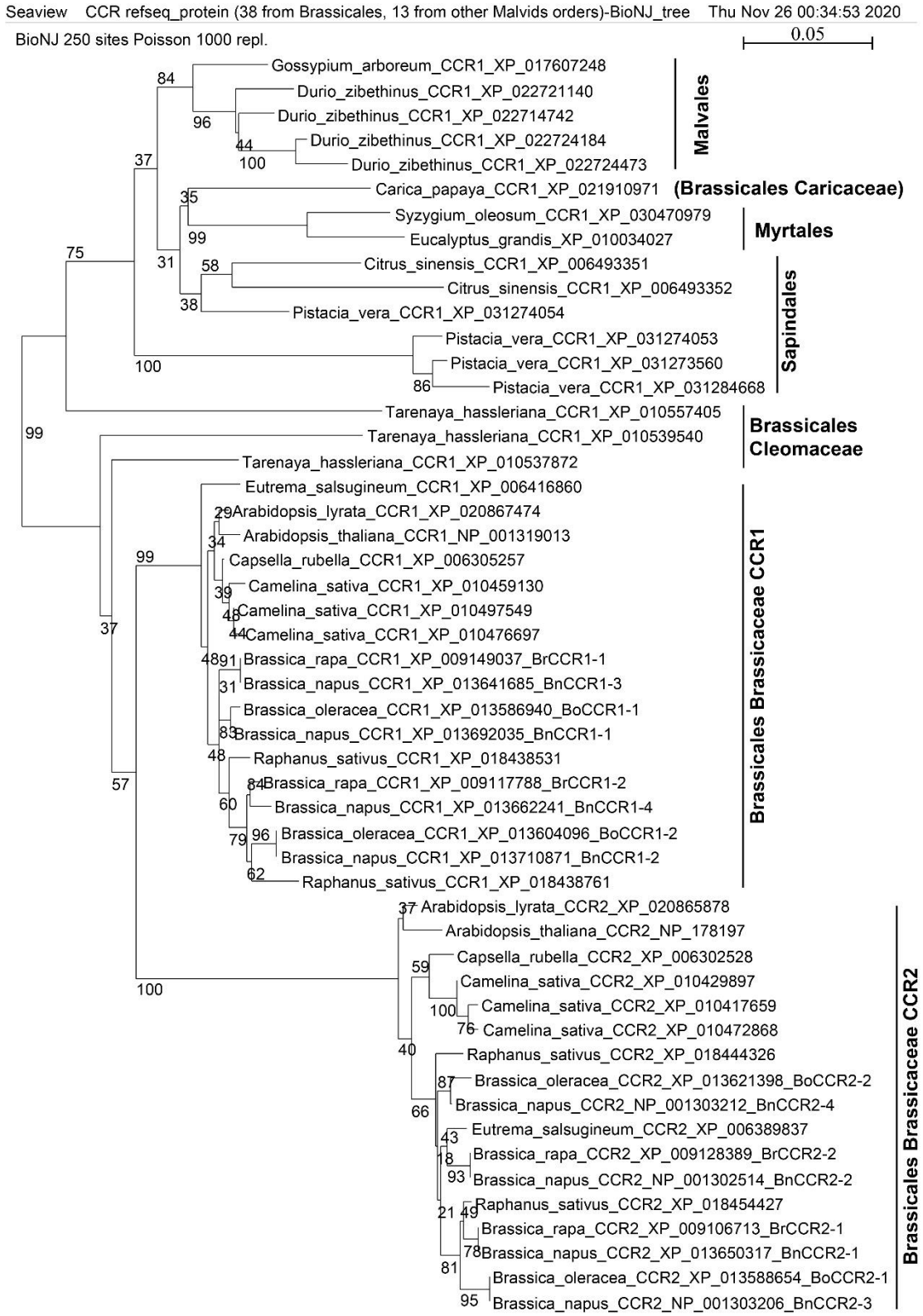

Figure 1. Phylogenetic analysis of CCR refseq_proteins from representative whole-genome-sequenced Malvids species including *B. napus, B. rapa* and *B. oleracea*.

Latin name, refseq_protein name and accession number are provided for each sequence. Names of cloned genes in this study are given after the accession numbers. Vertical bars on the right indicate corresponding order or order-family names.

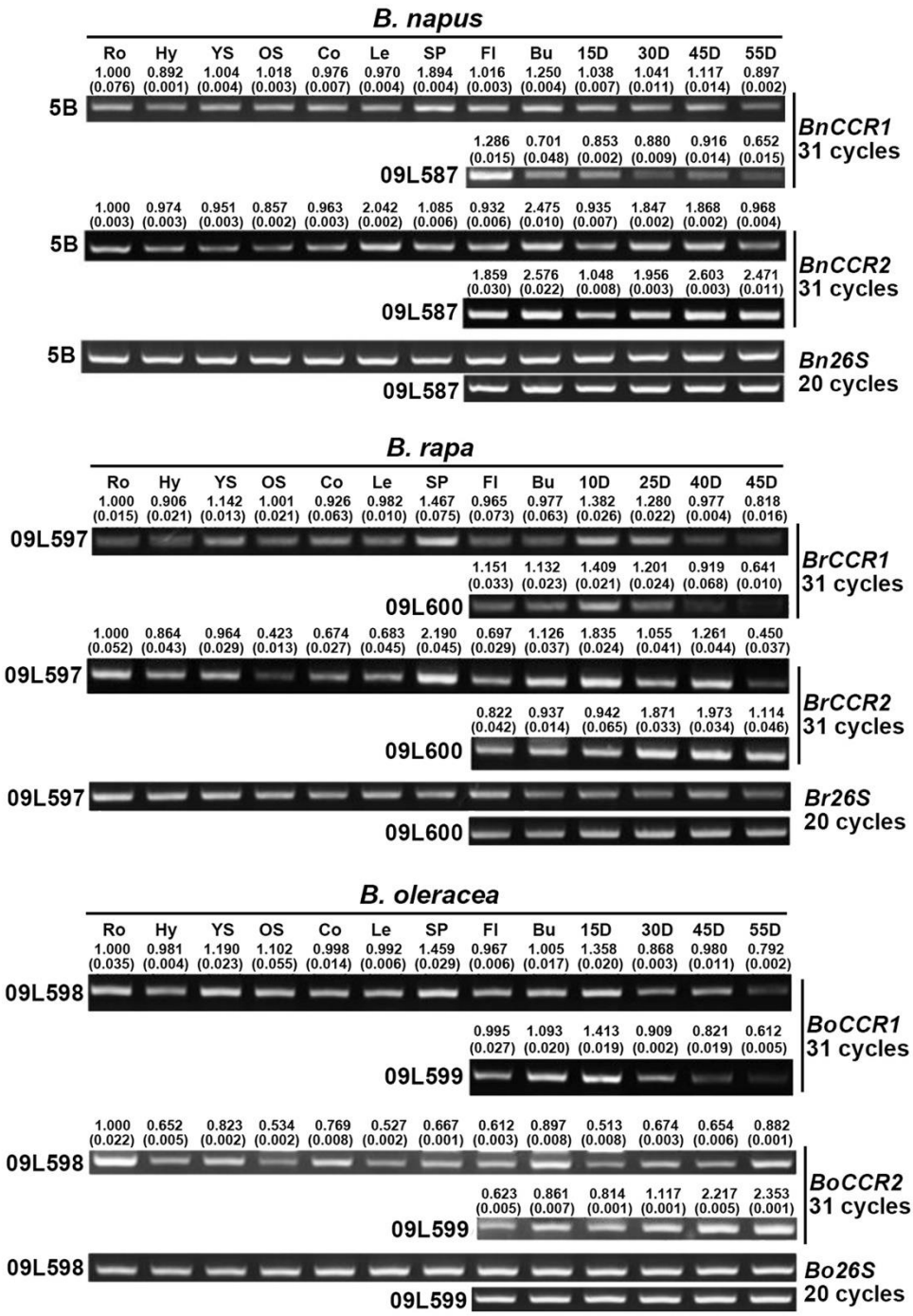

Figure 2. Overall expression patterns of *CCR1*-subfamily and *CCR2*-subfamily show distinct organ-specificity and difference between black and yellow seeds in *B. napus*, *B. rapa* and *B. oleracea*.

5B, 09L597 and 09L598 are black-seed stocks, while 09L587, 09L600 and 09L599 are yellow-seed stocks, of *B. napus*, *B. rapa* and *B. oleracea*, respectively. The value (SEM in brackets) above the sRT-PCR band represents the relative expression level of qRT-PCR result. The expression level in root is set as 1.000 for quantification of other organs. Ro, roots; Hy, Hypocotyl; YS, young stems; OS, old stems; Co, cotyledons; Le, leaves; SP, silique pericarp; Fl, flowers; Bu, buds; 15D-55D, seeds of the corresponding days after pollination.

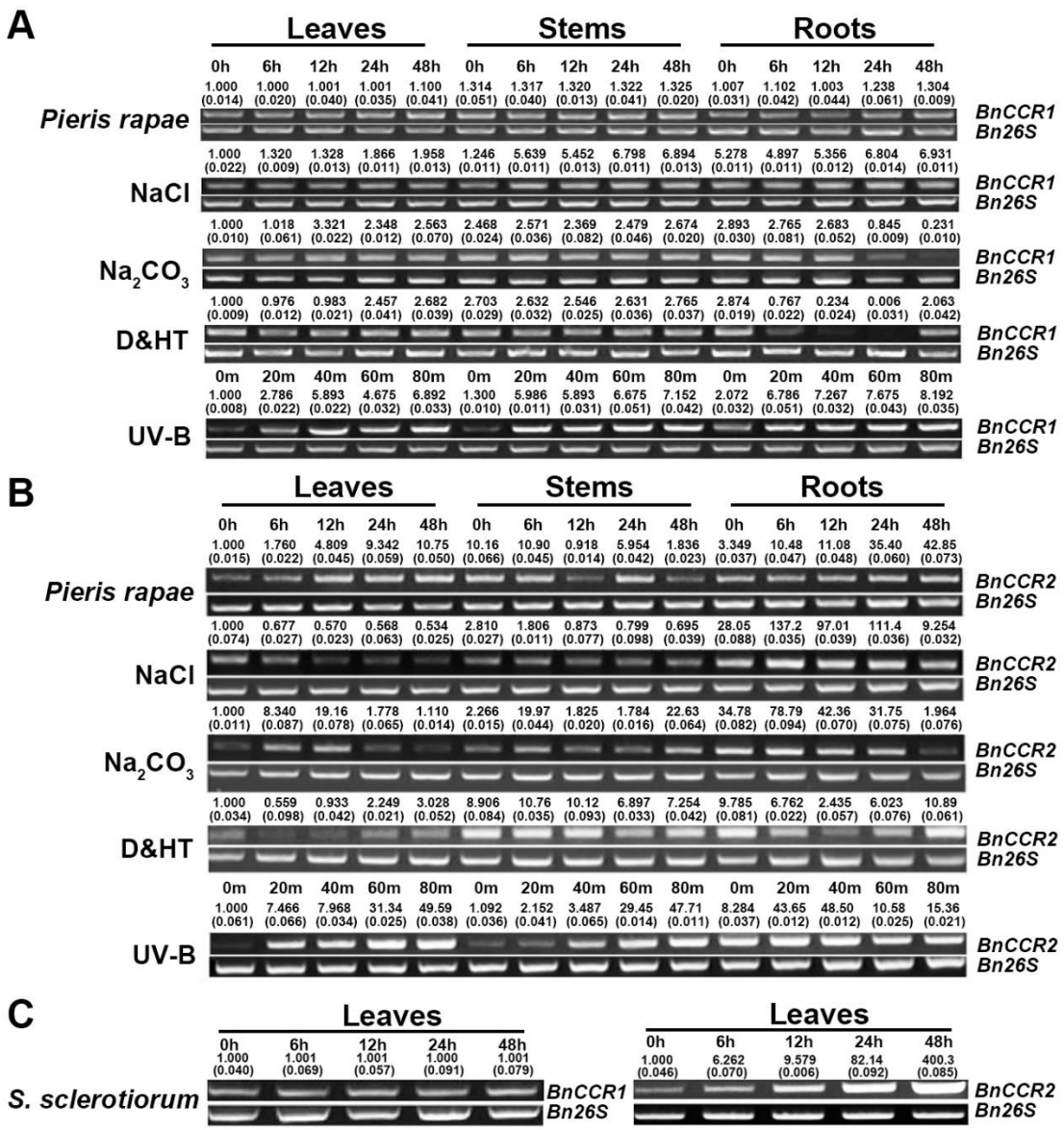

Figure 3. Overall expression of *BnCCR1*-subfamily and *BnCCR2*-subfamily distinctly respond to various stresses in *B. napus* seedlings.

The value (SEM in brackets) above the sRT-PCR band represents the relative expression level of qRT-PCR result. The expression level in the first sample is set as 1.000 for quantification of other samples. m, minutes; D&HT, drought & high temperature.

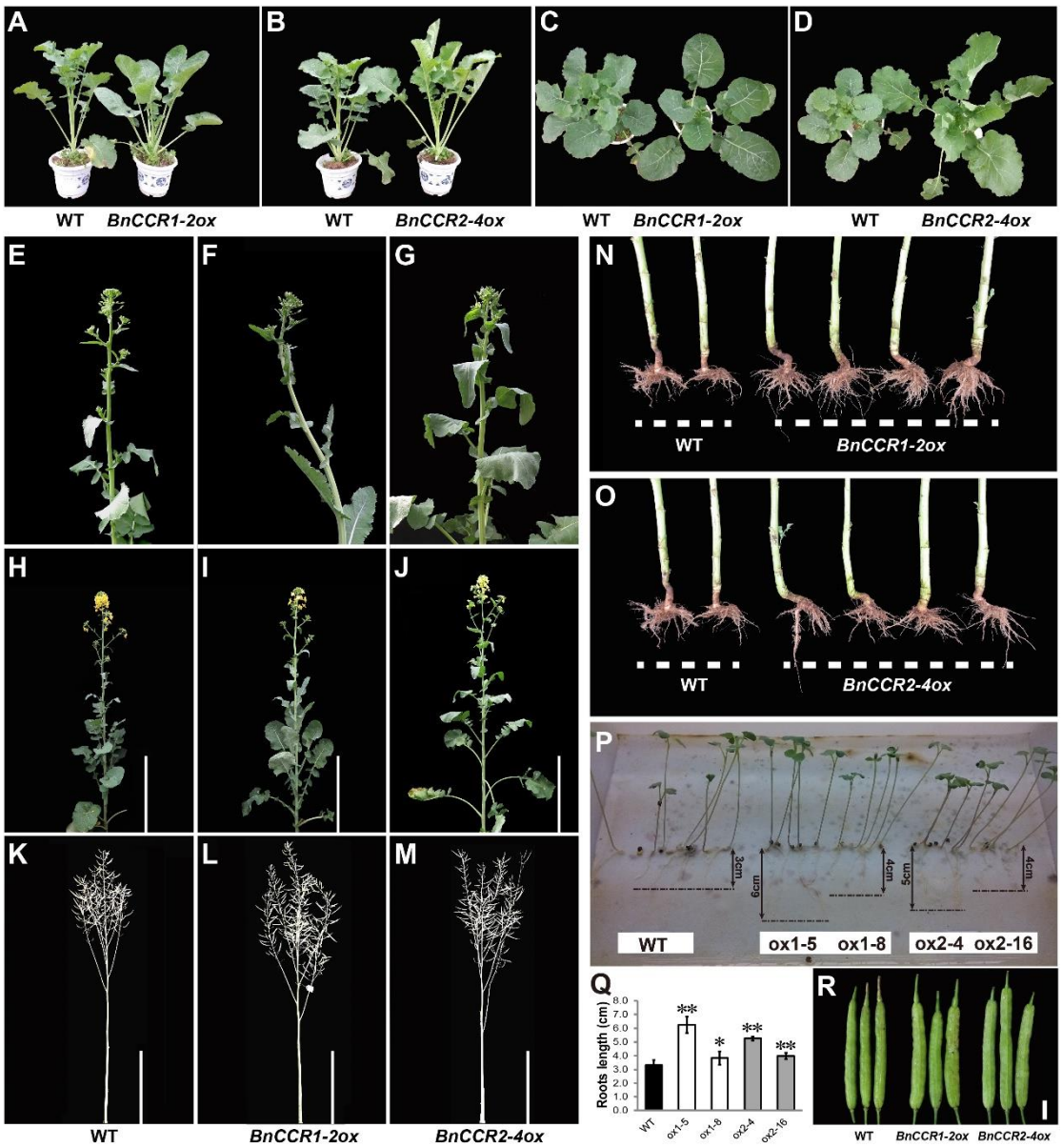

Figure 4. Different phenotypic modifications in *BnCCR1-2ox* and *BnCCR2-4ox* plants.

(A) to **(M)** Plant phenotypes of different stages. Vegetative stage (**[A]** to **[D]**), middle-later bolting stage (**[E]** to **[G]**), flowering stage (**[H]** to **[J]**), harvest stage (**[K]** to **[M]**). Bending phenomenon of the upper stem of *BnCCR1-2ox* plants at late bolting stage **(F)** will disappear after flowering **(I)**.

(N) and **(O)** Root system at mature stage.

(P) and **(Q)** Root system of one-week old seedlings, and the investigated values with statistical significance. Data represent means **±** SD of at least 5 biological replicates. Asterisks indicate that means differed significantly from WT values (*P < 0.05; **P < 0.01, Student's *t* tests).

(R) Siliques at mature stage, indicating the wider siliques of *BnCCR1-2ox* and *BnCCRR2-4ox* compared with WT. Bar = 1cm.

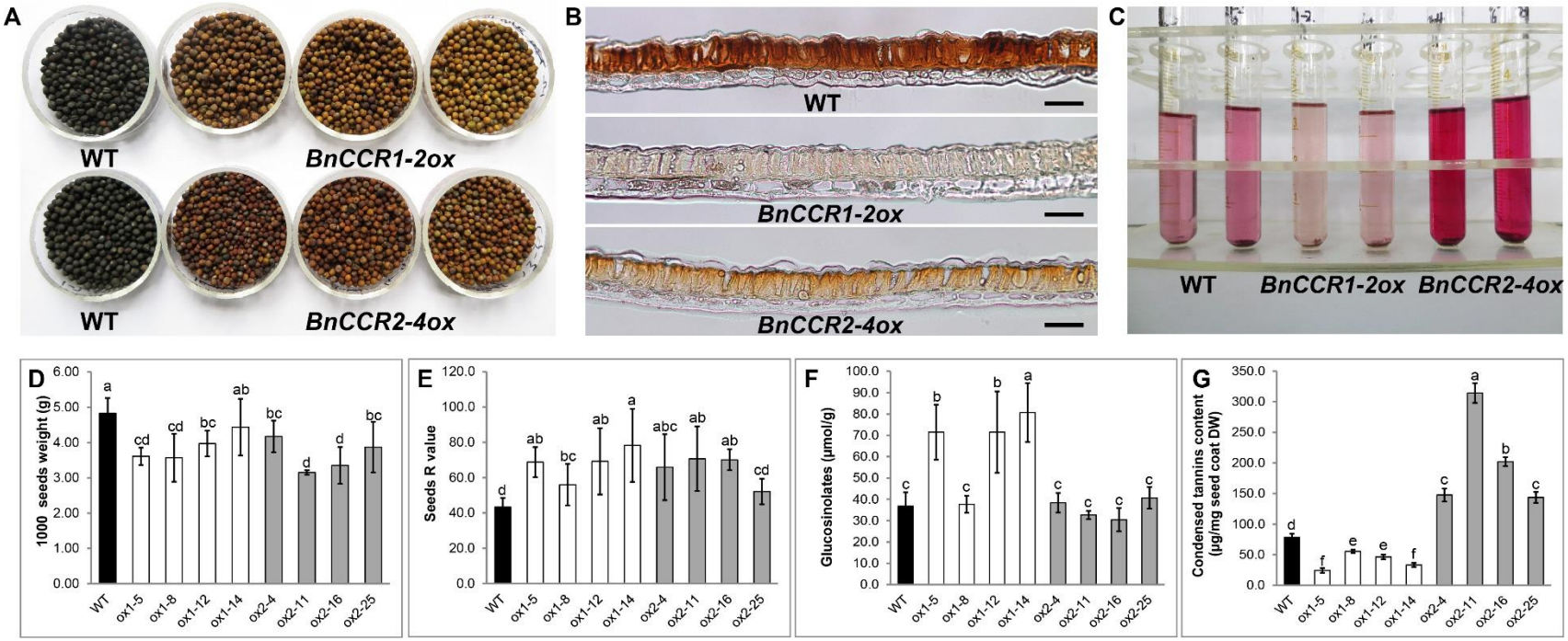

Figure 5. Yellow seeds from T3 plants of *BnCCR1-2ox* and *BnCCR2-4ox* in contrast with black seeds from WT plants.

(A) and **(B)** Seeds and seed coat cross-sections, highlighting the yellow-seed trait caused by seed color lightening by *CCR* overexpression. Bar = 50µm.

(C) Extractable insoluble condensed tannins from seed coat, showing deeper color of *BnCCR2-4ox* as compared with *BnCCR1-2ox* and WT which implies easier extraction.

(D) 1000 seeds weight; **(E)** Seeds R value (higher value means deeper yellow color of the seeds coat); **(F)** Glucosinolates content (µmol/g); **(G)** Insoluble condensed tannins content of the seed coat. Data represent means ± SD of at least three biological replicates. Values are means ± SD of three biological replicates. Different letters behind the SD indicate statistically significant differences (one-way ANOVA, $P < 0.05$, Duncan's test).

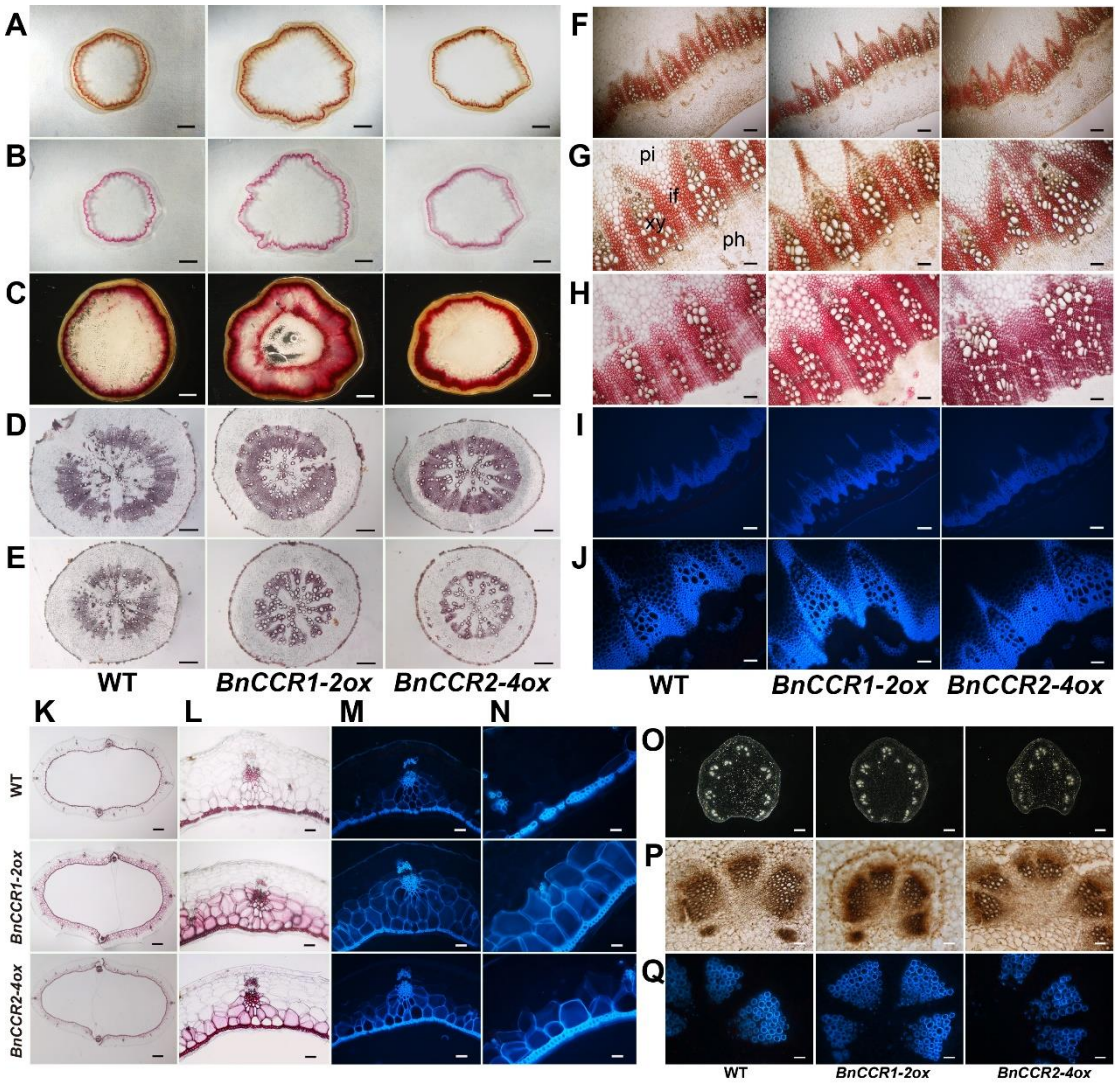

Figure 6. *BnCCR1-2ox* and *BnCCR2-4ox* plants show differently fortified lignification patterns in various organs.

(A) to **(C)** Whole cross frozen stem-sections at early flowering stage (**[A]** and **[B]**), and whole cross free hand stem-section at harvesting stage **(C)**. **(A)** Mäule staning; **(B)** and **(C)** phloroglucinol-HCl staining. Bar = 2mm.
(D) to **(E)** Cross-sections at mature stage of roots with more interfascicular fibers **(D)** and less interfascicular fibers **(E)**, stained with phloroglucinol-HCl method. Bar = 500μm.
(F) to **(J)** Cross-sections of different parts of the stem at different developing stages. Middle-lower part of the stem at early flowering stage using Mäule staining with different amplification folds (**[F]** and **[G]**). Middle-lower part of the stem at mature stage with phloroglucinol-HCl staining **(H).** Autofluorescence of the middle stem at early flowering stage under UV light with different amplification folds (**[I]** and **[J]**)**.** if, interfascicular fiber; ph, phloem; pi, pith; xy, xylem. **(F)** and **(I)**, bar = 200μm; **(G)**, **(H)** and **(J)**, bar = 80μm.
(K) to **(N)** Silique wall cross-sections at mature stage. Whole sections **(K)**; Local sections (**[L]** to **[N]**)**. (K)** to **(L)** Phloroglucinol-HCl staining; **(M)** and **(N)** Autofluorescence viewed under UV light. **(K)**, bar = 500μm; **(L)** and **(M)**, bar = 100μm; **(N)**, bar = 50μm.
(O) to **(Q)** Cross sections of the middle petiole with different methods. The whole cross-sections without any treatment **(I)**; The vascular bundle with Mäule staining **(P)**; The autofluorescence of the vascular bundle under UV light **(Q)**; bar = 50μm. **(I)**, bar = 1000μm; **(P)**, bar = 100μm; **(Q)**, bar = 50μm.

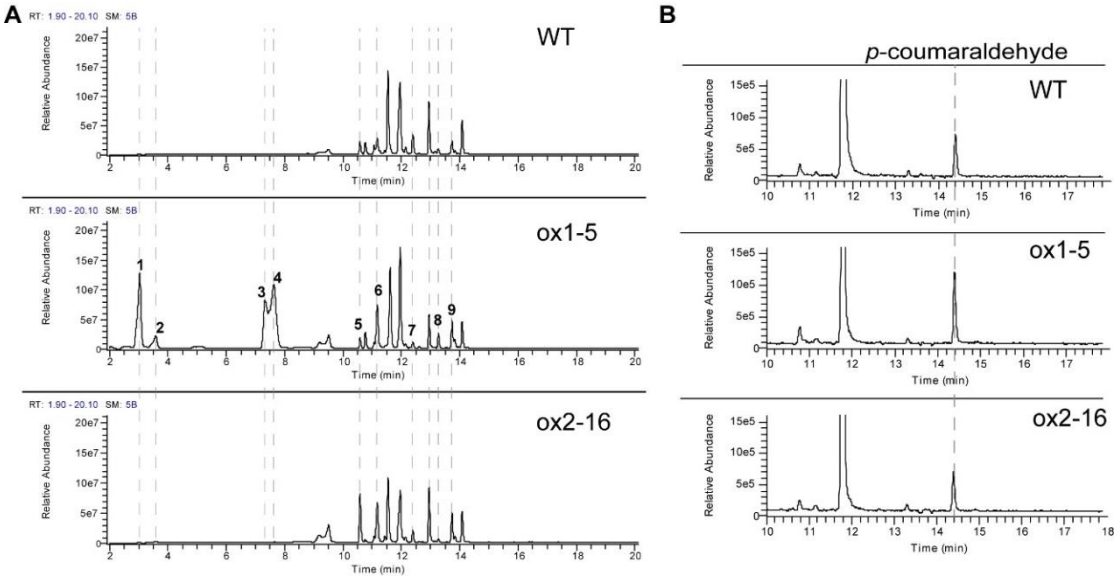

Figure 7. Secondary metabolites are distinctly modified in stems of *BnCCR1-2ox* and *BnCCR2-4ox* plants.

Secondary metabolites were determined by UPLC-HESI-MS/MS. 1, 1-S-[(3S)-3-Hydroxy-N-(sulfooxy)-5-hexenimidoyl]-1-thio-beta-D-glucopyranose; 2, 3-butenyl glucosinolate; 3, 4-pentenyl glucosinolate-1; 4, 4-pentenyl glucosinolate-2; 5, km-3-O-sophoroside-7-O-glucoside; 6, 3-O-caffeoylquinic acid; 7, qn-3-O-sophoroside; 8, sinapoylhexose; 9, sinapoyl malate.

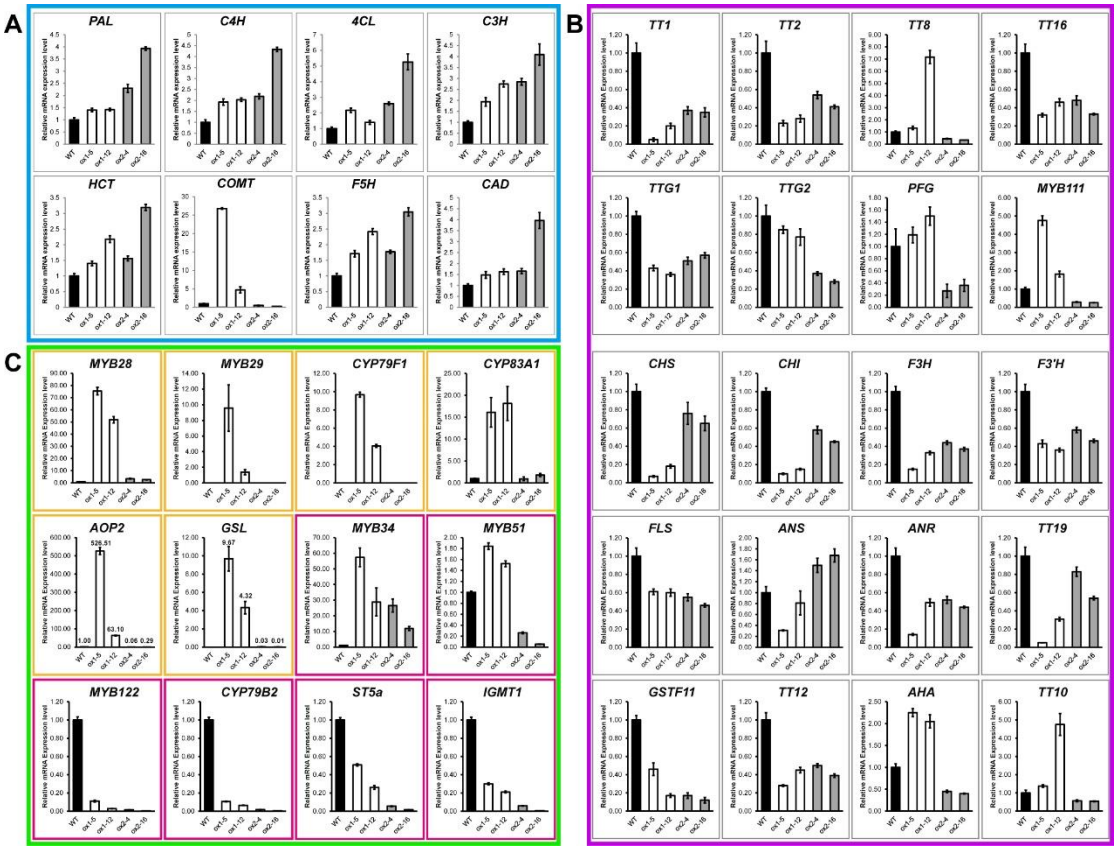

Figure 8. Gene expression patterns of lignin, flavonoid and glucosinolate pathways are tremendously and differentially influenced in *BnCCR1-2ox* and *BnCCR2-4ox* plants.

(A) Transcript levels of the genes related to lignin biosynthesis in stems.

(B) Transcript levels of the genes related to flavonoid biosynthesis in seeds.

(C) Transcript levels of the genes related to glucosinolate biosynthesis in leaves. The *MYB29*, *CYP79F1* and *GSL* have no expression in WT, hence their expression level in *BnCCRox* is set relative to zero. The expression levels of other genes are set relative to WT. The yellow frame marks the genes involved in the synthesis of aliphatic glucosinolates. The red frame marks the genes involved in the synthesis of indole glucosinolates.

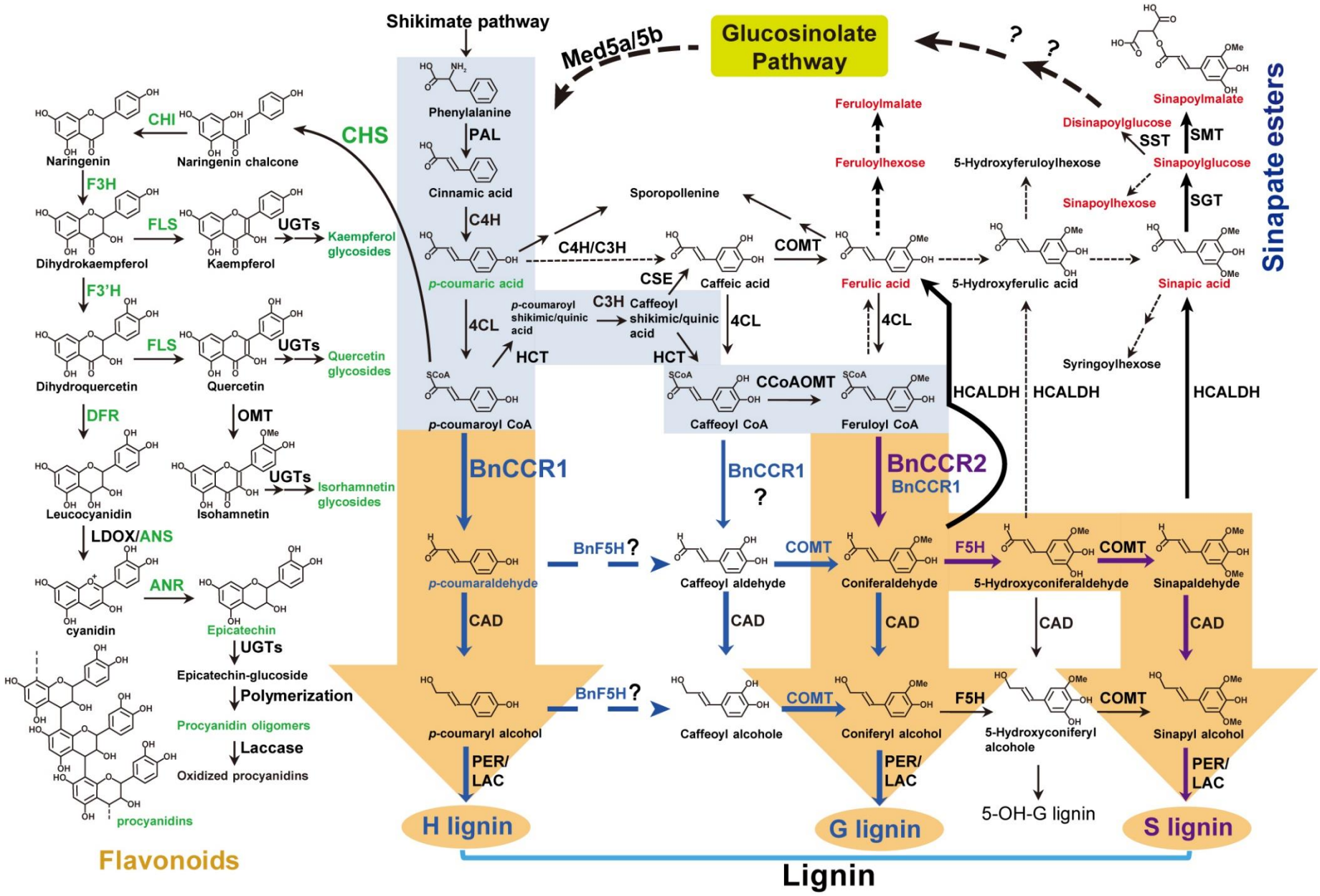
Shikimate pathway
Med5a/5b
Glucosinolate Pathway
Phenylalanine
PAL
Cinnamic acid
C4H
p-coumaric acid
C4H/C3H
Sporopollenine
CSE
Caffeic acid
COMT
Ferulic acid
4CL
p-coumaroyl shikimic/quinic acid
C3H
Caffeoyl shikimic/quinic acid
HCT
p-coumaroyl CoA
Caffeoyl CoA
CCoAOMT
Feruloyl CoA
Feruloylmalate
Feruloylhexose
5-Hydroxyferuloylhexose
5-Hydroxyferulic acid
Sinapic acid
Sinapoylmalate
Disinapoylglucose
SST
SMT
Sinapoylglucose
Sinapoylhexose
SGT
Syringoylhexose
Sinapate esters
HCALDH
CHS
CHI
Naringenin
Naringenin chalcone
F3H
Dihydrokaempferol
FLS
Kaempferol
UGTs
Kaempferol glycosides
F3'H
Dihydroquercetin
Quercetin
Quercetin glycosides
DFR
OMT
Leucocyanidin
Isohamnetin
Isorhamnetin glycosides
LDOX/ANS
cyanidin
ANR
Epicatechin
Epicatechin-glucoside
Polymerization
Procyanidin oligomers
Laccase
Oxidized procyanidins
procyanidins
Flavonoids
BnCCR1
BnCCR2
BnF5H?
p-coumaraldehyde
Caffeoyl aldehyde
Coniferaldehyde
F5H
5-Hydroxyconiferaldehyde
Sinapaldehyde
CAD
p-coumaryl alcohol
Caffeoyl alcohole
Coniferyl alcohol
5-Hydroxyconiferyl alcohole
Sinapyl alcohol
PER/LAC
H lignin
G lignin
5-OH-G lignin
S lignin
Lignin

Figure 9. BnCCR1 and BnCCR2 play different roles in phenylpropanoid pathway.

The metabolic flux shifts in *BnCCR1-2ox* and *BnCCR2-4ox* plants are displayed in this map. The main route, which is conserved in angiosperms, is marked with the big background arrows (the general phenylpropanoid pathway is marked in light blue, while lignin-specific pathway is marked in brown). The blue arrows and names represent flux enhancement related to *BnCCR1-2ox*. Metabolites accumulation and related gene expression are increased in the stem of *BnCCR1-2ox*, indicating that overexpression of *BnCCR1* subfamily will significantly promote the biosynthesis of G and H lignin units. The purple arrows and names represent flux enhancement related to *BnCCR2-4ox*. Metabolites accumulation and related genes expression are increased in the stem of *BnCCR2-4ox*, indicating that overexpression of *BnCCR2* subfamily will significantly promote the biosynthesis of S lignin unit. The metabolites and the enzymes downregulated in both *BnCCR1-2ox* and *BnCCR2-4ox* plants are marked in green, whereas those with upregulation are in red. Unexpectedly, glucosinolates deposition and pathway gene expression are significantly and differently remodeled in *BnCCR1-2ox* and *BnCCR2-4ox* plants. Dashed arrows represent unknown or unauthenticated routes. Arrows with a question mark are suggested pathways in this study. Two successive arrows represent two or more metabolic conversions.

The enzymes and their abbreviations are as follows: ANR, anthocyanidin reductase; ANS, anthocyanidin synthase; CAD, cinnamyl alcohol dehydrogenase; 4CL, 4-coumarate:CoA ligase; C3H, *p*-coumarate 3-hydroxylase; C4H, cinnamate 4-hydroxylase; CCoAOMT, caffeoyl-CoA O-methyltransferase; CCR, cinnamoyl-CoA reductase; CHI, chalcone isomerase; CHS, chalcone synthase; COMT, caffeic acid *O*-methyltransferase; CSE, caffeoyl shikimate esterase; DFR, dihydroflavonol 4-reductase; F3H, flavanone 3-hydroxylase; F3'H, flavonoid 3'-hydroxylase; F5H, ferulate 5-hydroxylase; FLS, flavonol synthase; HCALDH, hydroxycinnamaldehyde dehydrogenase; HCT, hydroxycinnamoyl-CoA:shikimate/quinic hydroxycinnamoyl transferase; LAC, laccase; LDOX, leucoanthocyanidin dioxygenase; Med: mediator; PAL, phenylalanine ammonia-lyase; PER, peroxidase; SGT, sinapate 1-glucosyltransferase; SMT, sinapoylglucose:malate sinapoyltransferase; SST, sinapoylglucose:sinapoylglucose sinapoylglucosetransferase; UGT, uridine diphosphate glycosyltransferase.

Parsed Citations

Abdulrazzak, N., Pollet, B., Ehlting, J., Larsen, K., Asnaghi, C., Ronseau, S., Proux, C., Erhardt, M., Seltzer, V., Renou, J.P., Ullmann, P., Pauly, M., Lapierre, C., and Werck-Reichhart, D. (2006). A coumaroyl-ester-3-hydroxylase insertion mutant reveals the existence of nonredundant meta-hydroxylation pathways and essential roles for phenolic precursors in cell expansion and plant growth. Plant Physiol. 140, 30-48.
Google Scholar: Author Only Title Only Author and Title

Acreche, M.M., and Slafer, G.A. (2011). Lodging yield penalties as affected by breeding in Mediterranean wheats. Field Crop Res. 122, 40-48.
Google Scholar: Author Only Title Only Author and Title

Anderson, N.A., Tobimatsu, Y., Ciesielski, P.N., Ximenes, E., Ralph, J., Donohoe, B.S., Ladisch, M., and Chapple, C. (2015). Manipulation of guaiacyl and syringyl monomer biosynthesis in an arabidopsis cinnamyl alcohol dehydrogenase mutant results in atypical lignin biosynthesis and modified cell wall structure. Plant Cell 27, 2195-2209.
Google Scholar: Author Only Title Only Author and Title

Auger, B., Marnet, N., Gautier, V., Maia-Grondard, A., Leprince, F., Renard, M., Guyot, S., Nesi, N., and Routaboul, J.M. (2010). A detailed survey of seed coat flavonoids in developing seeds of Brassica napus L. J. Agr. Food Chem. 58, 6246-6256.
Google Scholar: Author Only Title Only Author and Title

Bart, R.S., Chern, M., Vega-Sanchez, M.E., Canlas, P., and Ronald, P.C. (2010). Rice Snl6, a cinnamoyl-CoA reductase-like gene family member, is required for nh1-mediated immunity to Xanthomonas oryzae pv. oryzae. Plos Genet. 6. e1001123.
Google Scholar: Author Only Title Only Author and Title

Baucher, M., Monties, B., Van Montagu, M., and Boerjan, W. (1998). Biosynthesis and genetic engineering of lignin. Crit. Rev. Plant Sci. 17, 125-197.
Google Scholar: Author Only Title Only Author and Title

Baucher, M., Halpin, C., Petit-Conil, M., and Boerjan, W. (2003). Lignin: Genetic engineering and impact on pulping. Crit. Rev. Biochem. Mol. 38, 305-350.
Google Scholar: Author Only Title Only Author and Title

Berry, P.M. (2018). Lodging resistance in cereals. In: Meyers R. (eds) Encyclopedia of Sustainability Science and Technology. Springer New York, NY. https://doi.org/10.1007/1978-1001-4939-2493-1006_1228-1003.
Google Scholar: Author Only Title Only Author and Title

Berry, P.M., and Spink, J. (2012). Predicting yield losses caused by lodging in wheat. Field Crop Res. 137, 19-26.
Google Scholar: Author Only Title Only Author and Title

Berthet, S., Demont-Caulet, N., Pollet, B., Bidzinski, P., Cezard, L., Le Bris, P., Borrega, N., Herve, J., Blondet, E., Balzergue, S., Lapierre, C., and Jouanin, L. (2011). Disruption of laccase4 and 17 results in tissue-specific alterations to lignification of Arabidopsis thaliana stems. Plant Cell 23, 1124-1137.
Google Scholar: Author Only Title Only Author and Title

Besseau, S., Hoffmann, L., Geoffroy, P., Lapierre, C., Pollet, B., and Legrand, M. (2007). Flavonoid accumulation in Arabidopsis repressed in lignin synthesis affects auxin transport and plant growth. Plant Cell 19, 148-162.
Google Scholar: Author Only Title Only Author and Title

Boerjan, W., Ralph, J., and Baucher, M. (2003). Lignin biosynthesis. Annu. Rev. Plant Biol. 54, 519-546.
Google Scholar: Author Only Title Only Author and Title

Caño-Delgado, A., Penfield, S., Smith, C., Catley, M., and Bevan, M. (2003). Reduced cellulose synthesis invokes lignification and defense responses in Arabidopsis thaliana. Plant J. 34, 351-362.
Google Scholar: Author Only Title Only Author and Title

Cardoza, V., and Stewart, C.N. (2003). Increased agrobacterium-mediated transformation and rooting efficiencies in canola (Brassica napus L.) from hypocotyl segment explants. Plant Cell Rep. 21, 599-604.
Google Scholar: Author Only Title Only Author and Title

Chabannes, M., Barakate, A., Lapierre, C., Marita, J.M., Ralph, J., Pean, M., Danoun, S., Halpin, C., Grima-Pettenati, J., and Boudet, A.M. (2001). Strong decrease in lignin content without significant alteration of plant development is induced by simultaneous down-regulation of cinnamoyl CoA reductase (CCR) and cinnamyl alcohol dehydrogenase (CAD) in tobacco plants. Plant J. 28, 257-270.
Google Scholar: Author Only Title Only Author and Title

Chang, X.F., Chandra, R., Berleth, T., and Beatson, R.P. (2008). Rapid, microscale, acetyl bromide-based method for high-throughput determination of lignin content in Arabidopsis thaliana. J. Agr. Food Chem. 56, 6825-6834.
Google Scholar: Author Only Title Only Author and Title

Chantreau, M., Portelette, A., Dauwe, R., Kiyoto, S., Cronier, D., Morreel, K., Arribat, S., Neutelings, G., Chabi, M., Boerjan, W., Yoshinaga, A., Mesnard, F., Grec, S., Chabbert, B., and Hawkins, S. (2014). Ectopic lignification in the flax lignified bast fiber1 mutant stem is associated with tissue-specific modifications in gene expression and cell wall composition. Plant Cell 26, 4462-4482.

Google Scholar: Author Only Title Only Author and Title

Chao, N., Jiang, W.T., Wang, X.C., Jiang, X.N., and Gai, Y. (2019). Novel motif is capable of determining CCR and CCR-like proteins based on the divergence of CCRs in plants. Tree Physiol. 39, 2019-2026.
Google Scholar: Author Only Title Only Author and Title

Chao, N., Li, N., Qi, Q., Li, S., Lv, T., Jiang, X.N., and Gai, Y. (2017). Characterization of the cinnamoyl-CoA reductase (CCR) gene family in Populus tomentosa reveals the enzymatic active sites and evolution of CCR. Planta 245, 61-75.
Google Scholar: Author Only Title Only Author and Title

Chapple, C.C.S., Vogt, T., Ellis, B.E., and Somerville, C.R. (1992). An Arabidopsis mutant defective in the general phenylpropanoid pathway. Plant Cell 4, 1413-1424.
Google Scholar: Author Only Title Only Author and Title

Chen, H., Nelson, R.S., and Sherwood, J.L. (1994). Enhanced recovery of transformants of agrobacterium-tumefaciens after freeze-thaw transformation and drug selection. Biotechniques 16, 664-&.
Google Scholar: Author Only Title Only Author and Title

Chen, L., Auh, C., Chen, F., Cheng, X.F., Aljoe, H., Dixon, R.A., and Wang, Z.Y. (2002). Lignin deposition and associated changes in anatomy, enzyme activity, gene expression, and ruminal degradability in stems of tall fescue at different developmental stages. J. Agr. Food Chem. 50, 5558-5565.
Google Scholar: Author Only Title Only Author and Title

Costa, S., and Dolan, L. (2003). Epidermal patterning genes are active during embryogenesis in Arabidopsis. Development 130, 2893-2901.
Google Scholar: Author Only Title Only Author and Title

Cutler, S.R., Rodriguez, P.L., Finkelstein, R.R., and Abrams, S.R. (2010). Abscisic acid: emergence of a core signaling network. Annu. Rev. Plant Biol., 61, 651-679.
Google Scholar: Author Only Title Only Author and Title

Dauwe, R., Morreel, K., Goeminne, G., Gielen, B., Rohde, A., Van Beeumen, J., Ralph, J., Boudet, A.M., Kopka, J., Rochange, S.F., Halpin, C., Messens, E., and Boerjan, W. (2007). Molecular phenotyping of lignin-modified tobacco reveals associated changes in cell-wall metabolism, primary metabolism, stress metabolism and photorespiration. Plant J. 52, 263-285.
Google Scholar: Author Only Title Only Author and Title

De Meester, B., Calderón, B.M., de Vries, L., Pollier, J., Goeminne, G., Van Doorsselaere, J., Chen, M., Ralph, J., Vanholme, R., and Boerjan, W. (2020). Tailoring poplar lignin without yield penalty by combining a null and haploinsufficient CINNAMOYL-CoA REDUCTASE2 allele. Nat. Commun. 11, 1-13.
Google Scholar: Author Only Title Only Author and Title

De Meester, B., de Vries, L., Ozparpucu, M., Gierlinger, N., Corneillie, S., Pallidis, A., Goeminne, G., Morreel, K., De Bruyne, M., De Rycke, R., Vanholme, R., and Boerjan, W. (2018). Vessel-specific reintroduction of CINNAMOYL-COA REDUCTASE1 (CCR1) in dwarfed ccr1 mutants restores vessel and xylary fiber integrity and increases biomass. Plant Physiol. 176, 611-633.
Google Scholar: Author Only Title Only Author and Title

del Río, L.E., Bradley, C.A., Henson, R.A., Endres, G.J., Hanson, B.K., Mckay, K., Halvorson, M., Porter, P.M., Le Gare, D.G., and Lamey, H.A. (2007). Impact of Sclerotinia stem rot on yield of canola. Plant Dis. 91, 191-194.
Google Scholar: Author Only Title Only Author and Title

Derikvand, M.M., Sierra, J.B., Ruel, K., Pollet, B., Do, C.T., Thevenin, J., Buffard, D., Jouanin, L., and Lapierre, C. (2008). Redirection of the phenylpropanoid pathway to feruloyl malate in Arabidopsis mutants deficient for cinnamoyl-CoA reductase 1. Planta 227, 943-956.
Google Scholar: Author Only Title Only Author and Title

Ding, Y.J., Mei, J.Q., Liu, Y., Wang, L., Li, Y.H., Wan, H.F., Li, J.N., and Qian, W. (2015). Transfer of sclerotinia stem rot resistance from wild Brassica oleracea into B. rapa. Mol. Breeding 35.
Google Scholar: Author Only Title Only Author and Title

Do, C.T., Pollet, B., Thevenin, J., Sibout, R., Denoue, D., Barriere, Y., Lapierre, C., and Jouanin, L. (2007). Both caffeoyl Coenzyme A 3-O-methyltransferase 1 and caffeic acid O-methyltransferase 1 are involved in redundant functions for lignin, flavonoids and sinapoyl malate biosynthesis in Arabidopsis. Planta 226, 1117-1129.
Google Scholar: Author Only Title Only Author and Title

Escamilla-Treviño, L.L., Shen, H., Uppalapati, S.R., Ray, T., Tang, Y.H., Hernandez, T., Yin, Y.B., Xu, Y., and Dixon, R.A. (2010). Switchgrass (Panicum virgatum) possesses a divergent family of cinnamoyl CoA reductases with distinct biochemical properties. New Phytol. 185, 143-155.
Google Scholar: Author Only Title Only Author and Title

Fan, B., Hu, S., Lu, H., and Jiang, X. (2006). Soluble prokaryotic expression of 4-coumarate: coenzyme A ligase from Populus tomentosa and enzyme activity of recombinant 4CL1. Journal-Beijing Forestry University-Chinese Edition- 28, 1-8.
Google Scholar: Author Only Title Only Author and Title

Fornalé, S., Rencoret, J., Garcia-Calvo, L., Capellades, M., Encina, A., Santiago, R., Rigau, J., Gutierrez, A., del Rio, J.C., and Caparros-

Ruiz, D. (2015). Cell wall modifications triggered by the down-regulation of Coumarate 3-hydroxylase-1 in maize. Plant Sci. 236, 272-282.
Google Scholar: Author Only Title Only Author and Title

Franke, R., Hemm, M.R., Denault, J.W., Ruegger, M.O., Humphreys, J.M., and Chapple, C. (2002). Changes in secondary metabolism and deposition of an unusual lignin in the ref8 mutant of Arabidopsis. Plant J. 30, 47-59.
Google Scholar: Author Only Title Only Author and Title

Fraser, C.M., and Chapple, C. (2011). The phenylpropanoid pathway in Arabidopsis. The Arabidopsis book / American Society of Plant Biologists 9, e0152.
Google Scholar: Author Only Title Only Author and Title

Friedt, W., and Snowdon, R. (2009). Oilseed rape. In Oil crops (Springer), pp. 91-126.
Google Scholar: Author Only Title Only Author and Title

Fu, C., Chai, Y.R., Ma, L.J., Wang, R., Hu, K., Wu, J.Y., Li, J.N., Liu, X., and Lu, J.X. (2017). Evening primrose (Oenothera biennis) Δ6 fatty acid desaturase gene family: cloning, characterization, and engineered GLA and SDA production in a staple oil crop. Mol Breeding 37(6), 83.
Google Scholar: Author Only Title Only Author and Title

Fukushima, R.S., and Hatfield, R.D. (2001). Extraction and isolation of lignin for utilization as a standard to determine lignin concentration using the acetyl bromide spectrophotometric method. J. Agr. Food Chem. 49, 3133-3139.
Google Scholar: Author Only Title Only Author and Title

Giordano, A., Liu, Z.Q., Panter, S.N., Dimech, A.M., Shang, Y.J., Wijesinghe, H., Fulgueras, K., Ran, Y.D., Mouradov, A., Rochfort, S., Patron, N.J., and Spangenberg, G.C. (2014). Reduced lignin content and altered lignin composition in the warm season forage grass Paspalum dilatatum by down-regulation of a Cinnamoyl CoA Reductase Gene. Transgenic Res. 23, 503-517.
Google Scholar: Author Only Title Only Author and Title

Goujon, T., Ferret, V., Mila, I., Pollet, B., Ruel, K., Burlat, V., Joseleau, J.P., Barriere, Y., Lapierre, C., and Jouanin, L. (2003). Down-regulation of the AtCCR1 gene in Arabidopsis thaliana: effects on phenotype, lignins and cell wall degradability. Planta 217, 218-228.
Google Scholar: Author Only Title Only Author and Title

Gui, J.S., Luo, L.F., Zhong, Y., Sun, J.Y., Umezawa, T., and Li, L.G. (2019). Phosphorylation of LTF1, an MYB transcription factor in Populus, acts as a sensory switch regulating lignin biosynthesis in wood cells. Mol. Plant 12, 1325-1337.
Google Scholar: Author Only Title Only Author and Title

Hemm, M.R., Ruegger, M.O., and Chapple, C. (2003). The Arabidopsis ref2 mutant is defective in the gene encoding CYP83A1 and shows both phenylpropanoid and glucosinolate phenotypes. Plant Cell 15, 179-194.
Google Scholar: Author Only Title Only Author and Title

Hoffmann, L., Besseau, S., Geoffroy, P., Ritzenthaler, C., Meyer, D., Lapierre, C., Pollet, B., and Legrand, M. (2004). Silencing of hydroxycinnamoyl-coenzyme A shikimate/quinate hydroxycinnamoyltransferase affects phenylpropanoid biosynthesis. Plant Cell 16, 1446-1465.
Google Scholar: Author Only Title Only Author and Title

Huang, H.H., Xu, L.L., Tong, Z.K., Lin, E.P., Liu, Q.P., Cheng, L.J., and Zhu, M.Y. (2012). De novo characterization of the Chinese fir (Cunninghamia lanceolata) transcriptome and analysis of candidate genes involved in cellulose and lignin biosynthesis. BMC Genomics 13, 648.
Google Scholar: Author Only Title Only Author and Title

Huang, J.L., Gu, M., Lai, Z.B., Fan, B.F., Shi, K., Zhou, Y.H., Yu, J.Q., and Chen, Z.X. (2010). Functional analysis of the Arabidopsis PAL gene family in plant growth, development, and response to environmental stress. Plant Physiol. 153, 1526-1538.
Google Scholar: Author Only Title Only Author and Title

Jensen, L.M., Jepsen, H.S.K., Halkier, B.A., Kliebenstein, D.J., and Burow, M. (2015). Natural variation in cross-talk between glucosinolates and onset of flowering in Arabidopsis. Front Plant Sci 6, 697.
Google Scholar: Author Only Title Only Author and Title

Jones, L., Ennos, A.R., and Turner, S.R. (2001). Cloning and characterization of irregular xylem4 (irx4): a severely lignin-deficient mutant of Arabidopsis. Plant J. 26, 205-216.
Google Scholar: Author Only Title Only Author and Title

Kaur, H., Shaker, K., Heinzel, N., Ralph, J., Galis, I., and Baldwin, I.T. (2012). Environmental stresses of field growth allow cinnamyl alcohol dehydrogenase-deficient Nicotiana attenuata plants to compensate for their structural deficiencies. Plant Physiol. 159, 1545-1570.
Google Scholar: Author Only Title Only Author and Title

Kawasaki, T., Koita, H., Nakatsubo, T., Hasegawa, K., Wakabayashi, K., Takahashi, H., Urnemura, K., Urnezawa, T., and Shimamoto, K. (2006). Cinnamoyl-CoA reductase, a key enzyme in lignin biosynthesis, is an effector of small GTPase Rac in defense signaling in rice. P. Natl. Acad. Sci. USA 103, 230-235.
Google Scholar: Author Only Title Only Author and Title

Kendall, S.L., Holmes, H., White, C.A., Clarke, S.M., and Berry, P.M. (2017). Quantifying lodging-induced yield losses in oilseed rape.

Field Crop Res. 211, 106-113.
Google Scholar: Author Only Title Only Author and Title

Kim, J.I., Dolan, W.L., Anderson, N.A., and Chapple, C. (2015). Indole glucosinolate biosynthesis limits phenylpropanoid accumulation in Arabidopsis thaliana. Plant Cell 27, 1529-1546.
Google Scholar: Author Only Title Only Author and Title

Kim, J.I., Zhang, X., Pascuzzi, P.E., Liu, C.J., and Chapple, C. (2020). Glucosinolate and phenylpropanoid biosynthesis are linked by proteasome-dependent degradation of PAL. New Phytol. 225, 154-168.
Google Scholar: Author Only Title Only Author and Title

Ko, J.K., Ximenes, E., Kim, Y., and Ladisch, M.R. (2015). Adsorption of enzyme onto lignins of liquid hot water pretreated hardwoods. Biotechnol Bioeng. 112, 447-456.
Google Scholar: Author Only Title Only Author and Title

Koch, S., Dunker, S., Kleinhenz, B., Rohrig, M., and von Tiedemann, A. (2007). Crop loss-related forecasting model for Sclerotinia stem rot in winter oilseed rape. Phytopathology 97, 1186-1194.
Google Scholar: Author Only Title Only Author and Title

Labeeuw, L., Martone, P.T., Boucher, Y., and Case, R.J. (2015). Ancient origin of the biosynthesis of lignin precursors. Biol. Direct 10, 23.
Google Scholar: Author Only Title Only Author and Title

Lacombe, E., Hawkins, S., VanDoorsselaere, J., Piquemal, J., Goffner, D., Poeydomenge, O., Boudet, A.M., and GrimaPettenati, J. (1997). Cinnamoyl CoA reductase, the first committed enzyme of the lignin branch biosynthetic pathway: Cloning, expression and phylogenetic relationships. Plant J. 11, 429-441.
Google Scholar: Author Only Title Only Author and Title

Lapierre, C., Pollet, B., and Rolando, C. (1995). New insights into the molecular architecture of hardwood lignins by chemical degradative methods. Res. Chem. Intermediat. 21, 397-412.
Google Scholar: Author Only Title Only Author and Title

Lauvergeat, V., Lacomme, C., Lacombe, E., Lasserre, E., Roby, D., and Grima-Pettenati, J. (2001). Two cinnamoyl-CoA reductase (CCR) genes from Arabidopsis thaliana are differentially expressed during development and in response to infection with pathogenic bacteria. Phytochemistry 57, 1187-1195.
Google Scholar: Author Only Title Only Author and Title

Lee, M.H., Jeon, H.S., Kim, S.H., Chung, J.H., Roppolo, D., Lee, H.J., Cho, H.J., Tobimatsu, Y., Ralph, J., and Park, O.K. (2019). Lignin-based barrier restricts pathogens to the infection site and confers resistance in plants. Embo J. 38, e101948.
Google Scholar: Author Only Title Only Author and Title

Leplé, J.C., Dauwe, R., Morreel, K., Storme, V., Lapierre, C., Pollet, B., Naumann, A., Kang, K.Y., Kim, H., Ruel, K., Lefebvre, A., Joseleau, J.P., Grima-Pettenati, J., De Rycke, R., Andersson-Gunneras, S., Erban, A., Fehrle, I., Petit-Conil, M., Kopka, J., Polle, A., Messens, E., Sundberg, B., Mansfield, S.D., Ralph, J., Pilate, G., and Boerjan, W. (2007). Downregulation of cinnamoyl-coenzyme a reductase in poplar: Multiple-level phenotyping reveals effects on cell wall polymer metabolism and structure. Plant Cell 19, 3669-3691.
Google Scholar: Author Only Title Only Author and Title

Li, J.Q., Fan, F.F., Wang, L.H., Zhan, Q.W., Wu, P.J., Du, J.L., Yang, X.C., and Liu, Y.L. (2016). Cloning and expression analysis of cinnamoyl-CoA reductase (CCR) genes in sorghum. PeerJ 4, e2005.
Google Scholar: Author Only Title Only Author and Title

Li, X., Weng, J.K., and Chapple, C. (2008). Improvement of biomass through lignin modification. Plant J. 54, 569-581.
Google Scholar: Author Only Title Only Author and Title

Li, X., Bonawitz, N.D., Weng, J.K., and Chapple, C. (2010). The growth reduction associated with repressed lignin biosynthesis in Arabidopsis thaliana is independent of flavonoids. Plant Cell 22, 1620-1632.
Google Scholar: Author Only Title Only Author and Title

Lin, L.Z., Sun, J.H., Chen, P., and Harnly, J. (2011). UHPLC-PDA-ESI/HRMS/MSn analysis of anthocyanins, flavonol glycosides, and hydroxycinnamic acid derivatives in red mustard greens (Brassica juncea Coss Variety). J. Agr. Food Chem. 59, 12059-12072.
Google Scholar: Author Only Title Only Author and Title

Liu, C., Wang, J.L., Huang, T.D., Wang, F., Yuan, F., Cheng, X.M., Zhang, Y., Shi, S.W., Wu, J.S., and Liu, K.D. (2010). A missense mutation in the VHYNP motif of a DELLA protein causes a semi-dwarf mutant phenotype in Brassica napus. Theor. Appl. Genet. 121, 249-258.
Google Scholar: Author Only Title Only Author and Title

Liu, H., Yang, Q.Y., Fan, C.C., Zhao, X.Q., Wang, X.M., and Zhou, Y.M. (2015). Transcriptomic basis of functional difference and coordination between seeds and the silique wall of Brassica napus during the seed-filling stage. Plant Sci. 233, 186-199.
Google Scholar: Author Only Title Only Author and Title

Liu, L.Z., Stein, A., Wittkop, B., Sarvari, P., Li, J.N., Yan, X.Y., Dreyer, F., Frauen, M., Friedt, W., and Snowdon, R.J. (2012). A knockout mutation in the lignin biosynthesis gene CCR1 explains a major QTL for acid detergent lignin content in Brassica napus seeds. Theor. Appl. Genet. 124, 1573-1586.

Google Scholar: Author Only Title Only Author and Title

Lomascolo, A., Uzan-Boukhris, E., Sigoillot, J.C., and Fine, F. (2012). Rapeseed and sunflower meal: a review on biotechnology status and challenges. Appl. Microbiol. Biot. 95, 1105-1114.
Google Scholar: Author Only Title Only Author and Title

Ma, Q.H. (2009). The expression of caffeic acid 3-O-methyltransferase in two wheat genotypes differing in lodging resistance. J. Exp. Bot. 60, 2763-2771.
Google Scholar: Author Only Title Only Author and Title

Mei, J., Qian, L., Disi, J.O., Yang, X., Li, Q., Li, J., Frauen, M., Cai, D., and Qian, W. (2011). Identification of resistant sources against Sclerotinia sclerotiorum in Brassica species with emphasis on B. oleracea. Euphytica 177, 393-399.
Google Scholar: Author Only Title Only Author and Title

Mohammadin, S., Nguyen, T.P., van Weij, M.S., Reichelt, M., and Schranz, M.E. (2017). Flowering locus C (FLC) is a potential major regulator of glucosinolate content across developmental stages of Aethionema arabicum (Brassicaceae). Front Plant Sci. 8, 876.
Google Scholar: Author Only Title Only Author and Title

Moura, J.C.M.S., Bonine, C.A.V., Viana, J.D.F., Dornelas, M.C., and Mazzafera, P. (2010). Abiotic and biotic stresses and changes in the lignin content and composition in plants. J. Integr. Plant Biol. 52, 360-376.
Google Scholar: Author Only Title Only Author and Title

Naczk, M., Amarowicz, R., Pink, D., and Shahidi, F. (2000). Insoluble condensed tannins of canola/rapeseed. J. Agr. Food Chem. 48, 1758-1762.
Google Scholar: Author Only Title Only Author and Title

Nakashima, J., Chen, F., Jackson, L., Shadle, G., and Dixon, R.A. (2008). Multi-site genetic modification of monolignol biosynthesis in alfalfa (Medicago sativa): effects on lignin composition in specific cell types. New Phytol. 179, 738-750.
Google Scholar: Author Only Title Only Author and Title

Pan, L.G., Assirelli, A., Suardi, A., Civitarese, V., Del Giudice, A., Costa, C., and Santangelo, E. (2012). The harvest of oilseed rape (Brassica napus L.): The effective yield losses at on-farm scale in the Italian area. Biomass Bioenerg. 46, 453-458.
Google Scholar: Author Only Title Only Author and Title

Patten, A.M., Cardenas, C.L., Cochrane, F.C., Laskar, D.D., Bedgar, D.L., Davin, L.B., and Lewis, N.G. (2005). Reassessment of effects on lignification and vascular development in the irx4 Arabidopsis mutant. Phytochemistry 66, 2092-2107.
Google Scholar: Author Only Title Only Author and Title

Peng, D.L., Chen, X.G., Yin, Y.P., Lu, K.L., Yang, W.B., Tang, Y.H., and Wang, Z.L. (2014). Lodging resistance of winter wheat (Triticum aestivum L.): Lignin accumulation and its related enzymes activities due to the application of paclobutrazol or gibberellin acid. Field Crop Res. 157, 1-7.
Google Scholar: Author Only Title Only Author and Title

Piquemal, J., Lapierre, C., Myton, K., O'Connell, A., Schuch, W., Grima-Pettenati, J., and Boudet, A.M. (1998). Down-regulation of cinnamoyl-CoA reductase induces significant changes of lignin profiles in transgenic tobacco plants. Plant J. 13, 71-83.
Google Scholar: Author Only Title Only Author and Title

Porebski, S., Bailey, L.G., and Baum, B.R. (1997). Modification of a CTAB DNA extraction protocol for plants containing high polysaccharide and polyphenol components. Plant Mol. Biol. Rep. 15, 8-15.
Google Scholar: Author Only Title Only Author and Title

Prashant, S., Sunita, M.S., Pramod, S., Gupta, R.K., Kumar, S.A., Karumanchi, S.R., Rawal, S.K., and Kishor, P.B.K. (2011). Down-regulation of Leucaena leucocephala cinnamoyl CoA reductase (LlCCR) gene induces significant changes in phenotype, soluble phenolic pools and lignin in transgenic tobacco. Plant Cell Rep. 30, 2215-2231.
Google Scholar: Author Only Title Only Author and Title

Qu, C.M., Fu, F.Y., Lu, K., Zhang, K., Wang, R., Xu, X.F., Wang, M., Lu, J.X., Wan, H.F., Tang, Z.L., and Li, J.N. (2013). Differential accumulation of phenolic compounds and expression of related genes in black- and yellow-seeded Brassica napus. J. Exp. Bot. 64, 2885-2898.
Google Scholar: Author Only Title Only Author and Title

Ragauskas, A.J., Williams, C.K., Davison, B.H., Britovsek, G., Cairney, J., Eckert, C.A., Frederick, W.J., Hallett, J.P., Leak, D.J., Liotta, C.L., Mielenz, J.R., Murphy, R., Templer, R., and Tschaplinski, T. (2006). The path forward for biofuels and biomaterials. Science 311, 484-489.
Google Scholar: Author Only Title Only Author and Title

Ralph, J., Kim, H., Lu, F., Grabber, J.H., Leple, J.C., Berrio-Sierra, J., Derikvand, M.M., Jouanin, L., Boerjan, W., and Lapierre, C. (2008). Identification of the structure and origin of a thioacidolysis marker compound for ferulic acid incorporation into angiosperm lignins (and an indicator for cinnamoyl CoA reductase deficiency). Plant J. 53, 368-379.
Google Scholar: Author Only Title Only Author and Title

Robinson, A.R., and Mansfield, S.D. (2009). Rapid analysis of poplar lignin monomer composition by a streamlined thioacidolysis procedure and near-infrared reflectance-based prediction modeling. Plant J. 58, 706-714.

Google Scholar: Author Only Title Only Author and Title

Rochfort, S.J., Imsic, M., Jones, R., Trenerry, V.C., and Tomkins, B. (2006). Characterization of flavonol conjugates in immature leaves of pak choi [Brassica rapa L. ssp chinensis L. (Hanelt.)] by HPLC-DAD and LC-MS/MS. J. Agr. Food Chem. 54, 4855-4860.
Google Scholar: Author Only Title Only Author and Title

Ruel, K., Berrio-Sierra, J., Derikvand, M.M., Pollet, B., Thevenin, J., Lapierre, C., Jouanin, L., and Joseleau, J.P. (2009). Impact of CCR1 silencing on the assembly of lignified secondary walls in Arabidopsis thaliana. New Phytol. 184, 99-113.
Google Scholar: Author Only Title Only Author and Title

Saghaimaroof, M.A., Soliman, K.M., Jorgensen, R.A., and Allard, R.W. (1984). Ribosomal DNA spacer-length polymorphisms in barley: Mendelian inheritance, chromosomal location, and population-dynamics. P. Natl. Acad. Sci-Biol. 81, 8014-8018.
Google Scholar: Author Only Title Only Author and Title

Schilmiller, A.L., Stout, J., Weng, J.K., Humphreys, J., Ruegger, M.O., and Chapple, C. (2009). Mutations in the cinnamate 4-hydroxylase gene impact metabolism, growth and development in Arabidopsis. Plant J. 60, 771-782.
Google Scholar: Author Only Title Only Author and Title

Shao, Y.L., Jiang, J.J., Ran, L.P., Lu, C.L., Wei, C.X., and Wang, Y.P. (2014). Analysis of flavonoids and hydroxycinnamic acid derivatives in rapeseeds (Brassica napus L. var. napus) by HPLC-PDA-ESI(-)-MSn/HRMS. J. Agr. Food Chem. 62, 2935-2945.
Google Scholar: Author Only Title Only Author and Title

Sibout, R., Eudes, A., Mouille, G., Pollet, B., Lapierre, C., Jouanin, L., and Seguin, A. (2005). CINNAMYL ALCOHOL DEHYDROGENASE-C and -D are the primary genes involved in lignin biosynthesis in the floral stem of Arabidopsis. Plant Cell 17, 2059-2076.
Google Scholar: Author Only Title Only Author and Title

Tamasloukht, B., Lam, M.S.J.W.Q., Martinez, Y., Tozo, K., Barbier, O., Jourda, C., Jauneau, A., Borderies, G., Balzergue, S., Renou, J.P., Huguet, S., Martinant, J.P., Tatout, C., Lapierre, C., Barriere, Y., Goffner, D., and Pichon, M. (2011). Characterization of a cinnamoyl-CoA reductase 1 (CCR1) mutant in maize: effects on lignification, fibre development, and global gene expression. J. Exp. Bot. 62, 3837-3848.
Google Scholar: Author Only Title Only Author and Title

Thévenin, J., Pollet, B., Letarnec, B., Saulnier, L., Gissot, L., Maia-Grondard, A., Lapierre, C., and Jouanin, L. (2011). The simultaneous repression of CCR and CAD, two enzymes of the lignin biosynthetic pathway, results in sterility and dwarfism in Arabidopsis thaliana. Mol. Plant 4, 70-82.
Google Scholar: Author Only Title Only Author and Title

Tian, X.M., Xie, J., Zhao, Y.L., Lu, H., Liu, S.C., Qu, L., Li, J.M., Gai, Y., and Jiang, X.N. (2013). Sense-, antisense- and RNAi-4CL1 regulate soluble phenolic acids, cell wall components and growth in transgenic Populus tomentosa Carr. Plant Physiol. Bioch. 65, 111-119.
Google Scholar: Author Only Title Only Author and Title

Tohge, T., Nishiyama, Y., Hirai, M.Y., Yano, M., Nakajima, J., Awazuhara, M., Inoue, E., Takahashi, H., Goodenowe, D.B., Kitayama, M., Noji, M., Yamazaki, M., and Saito, K. (2005). Functional genomics by integrated analysis of metabolome and transcriptome of Arabidopsis plants over-expressing an MYB transcription factor. Plant J. 42, 218-235.
Google Scholar: Author Only Title Only Author and Title

Tongyan, W., Lingqin, X., and Xueju, Y. (2002). Study on the correlations between the components of the plant height and the yield and other traits of wheat. Journal of Agricultural University of Hebei (China), 25, 10-12,18.
Google Scholar: Author Only Title Only Author and Title

Tu, Y., Rochfort, S., Liu, Z.Q., Ran, Y.D., Griffith, M., Badenhorst, P., Louie, G.V., Bowman, M.E., Smith, K.F., Noel, J.P., Mouradov, A., and Spangenberg, G. (2010). Functional analyses of caffeic acid O-methyltransferase and cinnamoyl-CoA-reductase genes from perennial ryegrass (Lolium perenne). Plant Cell 22, 3357-3373.
Google Scholar: Author Only Title Only Author and Title

Van Acker, R., Leple, J.C., Aerts, D., Storme, V., Goeminne, G., Ivens, B., Legee, F., Lapierre, C., Piens, K., Van Montagu, M.C.E., Santoro, N., Foster, C.E., Ralph, J., Soetaert, W., Pilate, G., and Boerjan, W. (2014). Improved saccharification and ethanol yield from field-grown transgenic poplar deficient in cinnamoyl-CoA reductase. P. Natl. Acad. Sci. USA 111, 845-850.
Google Scholar: Author Only Title Only Author and Title

van der Rest, B., Danoun, S., Boudet, A.M., and Rochange, S.F. (2006). Down-regulation of cinnamoyl-CoA reductase in tomato (Solanum lycopersicum L.) induces dramatic changes in soluble phenolic pools. J. Exp. Bot. 57, 1399-1411.
Google Scholar: Author Only Title Only Author and Title

Vanholme, R., Demedts, B., Morreel, K., Ralph, J., and Boerjan, W. (2010). Lignin biosynthesis and structure. Plant Physiol. 153, 895-905.
Google Scholar: Author Only Title Only Author and Title

Vanholme, R., Storme, V., Vanholme, B., Sundin, L., Christensen, J.H., Goeminne, G., Halpin, C., Rohde, A., Morreel, K., and Boerjan, W. (2012). A systems biology view of responses to lignin biosynthesis perturbations in Arabidopsis. Plant Cell 24, 3506-3529.
Google Scholar: Author Only Title Only Author and Title

Vanholme, R., Cesarino, I., Rataj, K., Xiao, Y.G., Sundin, L., Goeminne, G., Kim, H., Cross, J., Morreel, K., Araujo, P., Welsh, L., Haustraete, J., McClellan, C., Vanholme, B., Ralph, J., Simpson, G.G., Halpin, C., and Boerjan, W. (2013). Caffeoyl shikimate esterase (CSE) is an enzyme in the lignin biosynthetic pathway in Arabidopsis. Science 341, 1103-1106.

Google Scholar: Author Only Title Only Author and Title

Vermerris, W., Thompson, K.J., McIntyre, L.M., and Axtell, J.D. (2002). Evidence for an evolutionarily conserved interaction between cell wall biosynthesis and flowering in maize and sorghum. BMC Evol. Biol. 2, 1-8.
Google Scholar: Author Only Title Only Author and Title

Voelker, S.L., Lachenbruch, B., Meinzer, F.C., Jourdes, M., Ki, C.Y., Patten, A.M., Davin, L.B., Lewis, N.G., Tuskan, G.A., Gunter, L., Decker, S.R., Selig, M.J., Sykes, R., Himmel, M.E., Kitin, P., Shevchenko, O., and Strauss, S.H. (2010). Antisense down-regulation of 4CL expression alters lignification, tree growth, and saccharification potential of field-grown poplar. Plant Physiol. 154, 874-886.
Google Scholar: Author Only Title Only Author and Title

Vogt, T. (2010). Phenylpropanoid biosynthesis. Mol. Plant 3, 2-20.
Google Scholar: Author Only Title Only Author and Title

Wagner, A., Tobimatsu, Y., Goeminne, G., Phillips, L., Flint, H., Steward, D., Torr, K., Donaldson, L., Boerjan, W., and Ralph, J. (2013). Suppression of CCR impacts metabolite profile and cell wall composition in Pinus radiata tracheary elements. Plant Mol. Biol. 81, 105-117.
Google Scholar: Author Only Title Only Author and Title

Weng, J.K., and Chapple, C. (2010). The origin and evolution of lignin biosynthesis. New Phytol. 187, 273-285.
Google Scholar: Author Only Title Only Author and Title

Weng, J.K., Mo, H.P., and Chapple, C. (2010). Over-expression of F5H in COMT-deficient Arabidopsis leads to enrichment of an unusual lignin and disruption of pollen wall formation. Plant J. 64, 898-911.
Google Scholar: Author Only Title Only Author and Title

Weng, J.K., Akiyama, T., Ralph, J., and Chapple, C. (2011). Independent recruitment of an O-methyltransferase for syringyl lignin biosynthesis in Selaginella moellendorffii. Plant Cell 23, 2708-2724.
Google Scholar: Author Only Title Only Author and Title

Xue, J.S., Luo, D.X., Xu, D.Y., Zeng, M.H., Cui, X.F., Li, L.G., and Huang, H. (2015). CCR1, an enzyme required for lignin biosynthesis in Arabidopsis, mediates cell proliferation exit for leaf development. Plant J. 83, 375-387.
Google Scholar: Author Only Title Only Author and Title

Yang, H., Li, J.W., Yang, J.P., Wang, H., Zou, J.L., and He, J.J. (2014). Effects of nitrogen application rate and leaf age on the distribution pattern of leaf SPAD readings in the rice canopy. Plos One 9, e88421.
Google Scholar: Author Only Title Only Author and Title

Yosef, E., and Ben-Ghedalia, D. (1999). Changes in thioacidolysis products of lignin in wheat straw as affected by SO2 treatment and passage through the gastro-intestine of sheep. Anim. Feed Sci. Tech. 80, 55-65.
Google Scholar: Author Only Title Only Author and Title

Zhang, G.P., Chen, J.X., and Bull, D.A. (2001). The effects of timing of N application and plant growth regulators on morphogenesis and yield formation in wheat. Plant Growth Regul. 35, 239-245.
Google Scholar: Author Only Title Only Author and Title

Zhang, K., Lu, K., Qu, C.M., Liang, Y., Wang, R., Chai, Y.R., and Li, J.N. (2013). Gene silencing of BnTT10 family genes causes retarded pigmentation and lignin reduction in the seed coat of Brassica napus. Plos One 8, e61247.
Google Scholar: Author Only Title Only Author and Title

Zhang, W.B., Wei, R., Chen, S., Jiang, J., Li, H.Y., Huang, H.J., Yang, G., Wang, S., Wei, H.R., and Liu, G.F. (2015). Functional characterization of CCR in birch (Betula platyphylla x Betula pendula) through overexpression and suppression analysis. Physiol. Plantarum 154, 283-296.
Google Scholar: Author Only Title Only Author and Title

Zhao, J., Wang, J., An, L., Doerge, R., Chen, Z.J., Grau, C.R., Meng, J., and Osborn, T.C. (2007a). Analysis of gene expression profiles in response to Sclerotinia sclerotiorum in Brassica napus. Planta 227, 13-24.
Google Scholar: Author Only Title Only Author and Title

Zhao, Q., Tobimatsu, Y., Zhou, R., Pattathil, S., Gallego-Giraldo, L., Fu, C., Jackson, L.A., Hahn, M.G., Kim, H., Chen, F., Ralph, J., and Dixon, R.A. (2013). Loss of function of cinnamyl alcohol dehydrogenase 1 leads to unconventional lignin and a temperature-sensitive growth defect in Medicago truncatula. P. Natl. Acad. Sci. USA 110, 13660-13665.
Google Scholar: Author Only Title Only Author and Title

Zhao, X.Y., Yu, X.H., Foo, E., Symons, G.M., Lopez, J., Bendehakkalu, K.T., Xiang, J., Weller, J.L., Liu, X.M., Reid, J.B., and Lin, C.T. (2007b). A study of gibberellin homeostasis and cryptochrome-mediated blue light inhibition of hypocotyl elongation. Plant Physiol. 145, 106-118.
Google Scholar: Author Only Title Only Author and Title

Zhou, R., Jackson, L., Shadle, G., Nakashima, J., Temple, S., Chen, F., and Dixon, R.A. (2010). Distinct cinnamoyl CoA reductases involved in parallel routes to lignin in Medicago truncatula. P. Natl. Acad. Sci. USA 107, 17803-17808.
Google Scholar: Author Only Title Only Author and Title

Zuber, U., Winzeler, H., Messmer, M.M., Keller, M., Keller, B., Schmid, J.E., and Stamp, P. (1999). Morphological traits associated with

lodging resistance of spring wheat (Triticum aestivum L.). J. Agron. Crop. Sci. 182, 17-24.
Google Scholar: Author Only Title Only Author and Title